



TECHNISCHE
UNIVERSITÄT
WIEN

Vienna University of Technology

INSTITUT FÜR
MECHANIK UND
MECHATRONIK
Mechanics & Mechatronics



DISSERTATION

Hybrid model predictive control for building energy supply systems

ausgeführt zum Zwecke der Erlangung des akademischen Grades
eines Doktors der technischen Wissenschaften
unter der Leitung von

Ao.Univ.Prof. Dipl.-Ing. Dr.techn. Martin Kozek

am Institut für Mechanik und Mechatronik
Abteilung für Regelungstechnik und Prozessautomatisierung

eingereicht an der Technischen Universität Wien,
Fakultät für Maschinenwesen und Betriebswissenschaften

von

Dipl.-Ing. Barbara Mayer
Schörgelgasse 68F
8010 Graz

Geboren am 11.04.1980
Matr.Nr.: 9830826

Graz, am 20. März 2017

Danksagung

Mein Dank gilt zuallererst Prof. Dr. Stefan Jakubek und Ao. Prof. Dr. Martin Kozek für die Möglichkeit der externen Dissertation am Institut. Meinem Mentor Martin Kozek danke ich darüber hinaus ganz besonders für die wissenschaftliche Betreuung, vor allem aber auch für die menschliche Komponente, die angenehme Arbeitsatmosphäre trotz räumlicher Distanz und das Teilen der Begeisterung für das Thema. Ausserdem danke ich Michaela für die gemeinsame Arbeit am Projekt – die Diskussionen, das Arbeiten an unseren Ansprüchen und Zielen, die Freude an gemeinsamen Ergebnissen und das Wiederaufrichten bei Mißerfolgen.

Besonderer Dank gebührt meiner Familie, meinem Netz, in dem mich jeder nach seinen Möglichkeiten in dieser Zeit liebevoll unterstützt hat. Ich danke meinen Jungs, die mir eine wichtige Distanz und Perspektive zur Arbeit verschafft haben. Von ganzem Herzen danke ich meinem Ma, der in vielerlei Hinsicht Stütze und Unterstützer war und mir viel Zeit, Energie und Motivation für mein Vorhaben geschenkt hat.

Eidesstattliche Erklärung

Ich erkläre eidesstattlich, dass ich die Arbeit selbständig angefertigt, keine anderen als die angegebenen Hilfsmittel benutzt und alle aus ungedruckten Quellen, gedruckter Literatur oder aus dem Internet im Wortlaut oder im wesentlichen Inhalt übernommenen Formulierungen und Konzepte gemäß den Richtlinien wissenschaftlicher Arbeiten zitiert, durch Fußnoten gekennzeichnet bzw. mit genauer Quellenangabe kenntlich gemacht habe.

Graz, am 20. März 2017

Barbara Mayer

Kurzfassung

Der Gebäudesektor ist heute zu einem hohen Ausmaß verantwortlich für den Verbrauch von Primärenergie. Ziel ist es daher Energie in vorwiegend großen Gebäuden einzusparen und gleichzeitig mehr Energie aus erneuerbaren Quellen zu nutzen. Neben diesen umwelttechnischen Anforderungen gibt es jedoch noch Vorgaben anderer Interessensgruppen. Für Benützer darf dabei der Komfort (gesetzlich) nicht eingeschränkt werden, für Gebäudebetreiber hingegen ist eine kostenminimierte Fahrweise wünschenswert. Modellbasierte prädiktive Regelung (MPC) ist das ideale Werkzeug für diese divergenten Zielvorstellungen unter Berücksichtigung technischer Einschränkungen und externer (Stör-)Größen.

Basierend auf einem modularen, hierarchischen MPC Konzept für Mehrzonen-Gebäude liegt der Kern dieser Arbeit in der Modellierung, der Reglerauslegung sowie -optimierung für die Ebene der Energiebereitstellung. Komplexe Stränge beinhalten schaltende Aggregate wie Wärmepumpen oder Kältemaschinen mit nachfolgenden Schichtspeichern. Die nichtlineare Dynamik dieser kontinuierlichen Systeme wird von den diskreten Aggregatzuständen beeinflusst. Analytisch hergeleitete nichtlineare hybride Modelle beschreiben das Gesamtsystem, das mit stückweise linearen Modellen mathematisch approximiert wird. Ein dafür ausgelegter hybrider, gemischt-ganzzahliger MPC (MI-MPC) optimiert nicht nur die Speicherbewirtschaftung sondern gleichzeitig auch die Aggregatschaltungen unter Einhaltung von Ein- und Ausschaltzeiten. Die Implementierung des MI-MPCs beinhaltet einen auf das System zugeschnittenen Branch and Bound Algorithmus, der technische Einschränkungen zur Reduktion der Suchräume nutzt.

Das Ziel einer industriellen (Wieder-)Verwendbarkeit des Regelungskonzeptes kann-

te mit einem modularen Design von individuell für die einzelnen Energieversorgungsstränge zugeordneten MPCs erreicht werden. Das resultierende modulare MPC-Schema (MPCC) bevorzugt die Verwendung von erneuerbaren Energien wie freie Kühlung oder Geothermie und gewährleistet die Bereitstellung eines vorgegebenen Energiebedarfs der Nutzungsebene zu minimalen Kosten unter Berücksichtigung technischer Restriktionen sowie Einbeziehung der Wettervorhersagen. Darüber hinaus können zeitlich variierende Kosten pro Energiequelle in die Zielfunktion eingehen, was eine Integration in ein intelligentes Netz ermöglicht. Das MPCC ist daher wesentlicher Baustein für eine nachhaltige Gebäudeautomatisierung.

Die vorliegende Dissertation und die darin enthaltenen Veröffentlichungen sind im Laufe eines Forschungsprojektes am Institut für Mechanik und Mechatronik (Abteilung für Regelungstechnik und Prozessautomatisierung) in Kooperation mit dem Forschungspartner FH Joanneum, Institut für Industrielwirtschaft, und dem Industriepartner evon GmbH entstanden. Das Projekt wurde von der Österreichischen Forschungsförderungsgesellschaft (FFG Nr. 832103) gefördert.

Abstract

Buildings are responsible for a large proportion of primary energy consumption. Thus, the aim is to reduce the energy demand of buildings and to increase the amount of energy taken from renewable sources. However, these environmental demands are supplemented with (legal) requirements regarding user comfort or a cost-efficient building operation. Model predictive control (MPC) is an effective means to gain optimal solutions for these conflicting goals with respect to technical constraints and external disturbances.

Based on a modular hierarchic MPC concept for multi-zone buildings main part of this work is modeling, control design and optimization for the energy supply system. Complex supply circuits include switching aggregates such as heat pumps or chillers with stratified storage tanks. The nonlinear dynamics of the continuous process are influenced by the state of the corresponding aggregate. The resulting analytically derived nonlinear hybrid model is approximated by a piecewise affine system. The dedicated hybrid mixed-integer MPC (MI-MPC) is simultaneously capable to optimize the stratified storage management and the switching states of the aggregate considering minimum up and down times by solving a mixed-integer problem. The implementation of the MI-MPC includes a branch and bound algorithm using technical constraints to reduce the remaining search space.

The aim to develop an industrially (re)utilizable MPC-concept has been achieved by modularizing the control scheme such that each energy supply circuit is individually controlled by a dedicated MPC. The resulting modular predictive control concept (MPCC) prefers the usage of renewable energy sources such as free cooling or geothermal source. It is further capable to accurately provide the energy demanded

by the user (energy consumption) level while minimizing the costs with respect to technical constraints incorporating weather forecasts. Additionally, the concept can cope with time-varying energy costs allowing an integration into smart grids. Thus, the MPCC is an ideal tool for sustainable building automation.

The present thesis and the papers within this work have originated in a course of a research project at the Institute of Mechanics und Mechatronics (Division of Control and Process Automation) in cooperation with the research partner FH Joanneum, Institute of Industrial Management, and the industrial partner evon GmbH. The project has been funded by the Austrian Research Promotion Agency (FFG Nr. 832103).

Contents

1	Introduction	1
1.1	Motivation	1
1.2	Project SmartMSR	2
1.3	Goals	4
1.4	Methodology	5
1.4.1	Modeling	5
1.4.2	Hybrid model predictive control	8
1.4.3	Modular model predictive control concept	10
1.5	Summary of Scientific Approaches	13
1.6	Scientific Contribution	14
	Bibliography	16
2	Publications	18
2.1	Publication A	18
2.2	Publication B	33
2.3	Publication C	48
2.4	Publication D	69
	Curriculum Vitae	81
	List Of Scientific Publications	83

List of Figures

1.1	Schematic closed-loop system for energy efficient building heating and cooling control.	2
1.2	Hierarchical control structure with the user level (UL) MPC and the energy supply level (ESL) MPC. Green blocks show the subject of the present thesis.	4
1.3	Basic supply circuit.	6
1.4	Complex supply circuit.	6
1.5	The three operation modes of the stratified storage tank depending on the state of the switching aggregate and the mass flows to and from the storage.	6
1.6	The binary tree for the hybrid system optimization with branch and bound.	10
1.7	Modular control structure for FC and TABS embedded into a hierarchical building control structure. Blue feedback loops indicate the cooling, red loops the heating circuits.	11

Chapter 1

Introduction

1.1 Motivation

Buildings are responsible for about 40 % of the total energy consumption in Europe, [1]. Various approaches in the fields of building architecture, physics, and development of new materials have improved the building construction and provided the basis for more sustainable building operation, [2]. Nevertheless, building automation plays a central role in the operation phase since it is responsible for controlling all thermal comfort influencing subsystems such as heating, cooling, or air conditioning systems. Operating buildings energy efficiently thus means an optimization of closed-loop control systems such that the energy demand is minimized without compromising the user comfort. However, modern large buildings are complex systems not only because of their thermodynamic principles but also due to various energy sources and supply systems. Furthermore, several external parameters such as ambient temperature, radiance, or occupancy influence the thermal condition of the individual building zones to different extends, [3, 4]. However, conventional building control systems based on proportional -integral -deviation- and rule based controllers are more difficult to integrate in an optimization scheme and lack the integrability of weather or occupancy forecasts into their control decisions.

Model based predictive control (MPC) though is ideal for the application in building automation system since it is capable of solving predefined optimization tasks in real time. The MPC uses an underlying building model, the technical constraints, and

the overall objective function, [5]. Furthermore, its predictive character incorporates disturbances such as ambient temperature, radiance, and occupancy. However, due to basic thermodynamical principles the system model is highly nonlinear with couplings between manipulated variables and system states resulting in veritable challenges for the corresponding modeling and control task. Figure 1.1 shows the overall schematic closed loop system. The desired thermal user comfort, $\vartheta_{\text{indoor}}^{\text{ref}}$, is the reference for the nonlinear MPC (NMPC) structure which is computing an optimal strategy in order to guarantee user comfort with as little energy demand as possible.

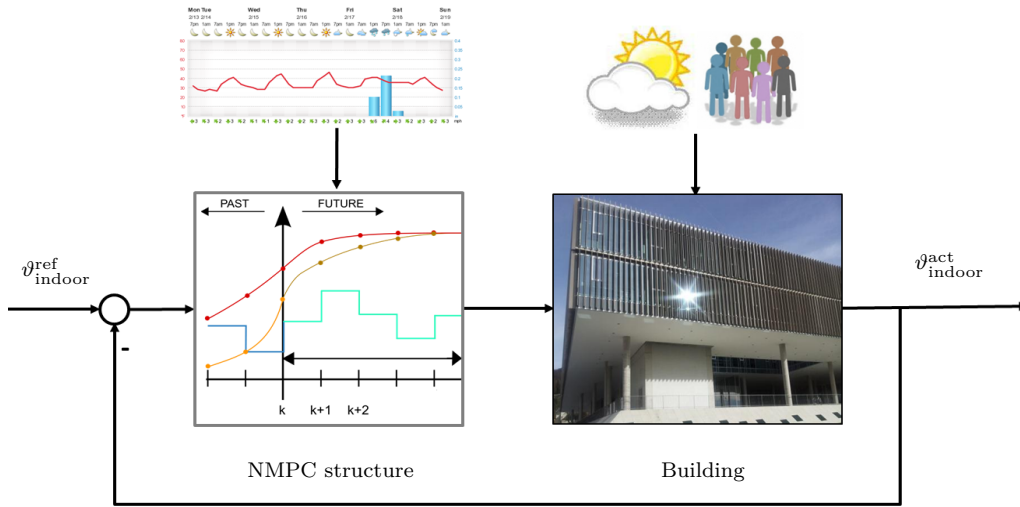


Figure 1.1: Schematic closed-loop system for energy efficient building heating and cooling control.

The NMPC structure consists of two hierarchically coupled NMPCs - one cooperative fuzzy MPC and one modular MPC concept including an mixed-integer MPC, see 1.2. The focus of this thesis lies on the mixed-integer MPC and the modular MPC concept for the control of the building energy supply system.

1.2 Project SmartMSR

The content of the present thesis has been developed within the project 'SmartMSR' which was conducted by the research partners Vienna University of Technology and the FH Joanneum University of Applied Sciences and the industry partner even

GmbH. The three and a half years project (November 2011 - June 2015) funded by the Austrian Research Promotion Agency FFG was basis for two doctoral theses. Scope of the project was the development of a tool chain enabling an industrial application of model based predictive control in buildings. Thus, the tool chain consists of three major links: modeling and system identification, integration of disturbances, nonlinear MPC design and control optimization. The concept was planned to be developed and tested on a large modern demonstration building, the University Salzburg Nonntal.

The overall building control task including the maximization of the user comfort, the minimization of energy demand and respective costs can be seen as the optimization of two underlying systems with different time constants, disturbances, and mathematical demands: the user level where energy is consumed and the energy supply level connecting the energy sources with the supply systems. Although most approaches have considered the entire building for modeling and control, [6, 7], decoupling of these two levels has turned out to be an advantageous approach. In [8] a distributed MPC was presented distinguishing these two levels. However, a hierarchical control concept further naturally splits the overall optimization task into two smaller subjects, allowing independent identification of the two differently characterized systems, with customized dedicated control designs. Figure 1.2 shows the overall hierarchical control concept consisting of two predictive controllers for the energy supply system and the building, as well as the underlying systems. The energy demand of the user (energy consumption) level couples the two controllers.

Hence, the focus of the two doctoral theses has naturally been put on the two almost independent, hierarchically connected control tasks. Dr. Michaela Killian has been working on the tool chain for the user level whereas the content for the present thesis is modeling, control design and optimization for the energy supply level such as marked with green frames in Figure 1.2. The coupling and testing phase has been conducted together.

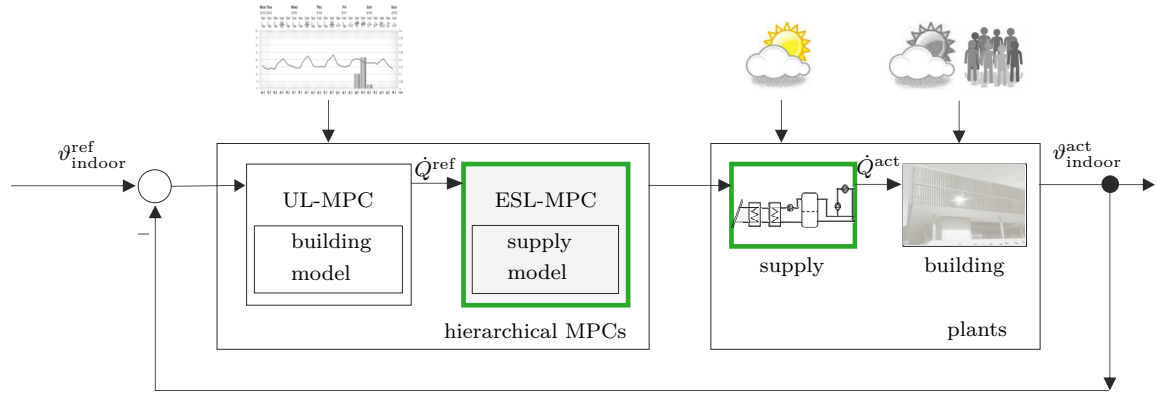


Figure 1.2: Hierarchical control structure with the user level (UL) MPC and the energy supply level (ESL) MPC. Green blocks show the subject of the present thesis.

1.3 Goals

The main goal for the corresponding project was the development of a tool chain incorporating model based predictive control techniques for an industrial application in building automation. Since the overall task could be split into two subjects, see green marked frames in Figure 1.2, the goals for the present thesis have been broken down to i) modeling of the underlying heating and cooling supplies and storages and ii) development, implementation, and optimization of a dedicated nonlinear MPC taking disturbances into account. As a result the controller has been designed to minimize the energy costs and to maximize the use of renewable energies while accurately delivering the (already minimized) energy demand of the user level.

The controlled process is the energy supply circuits connecting the energy sources with the corresponding energy supply systems. Each circuit consists of a specific set of aggregates such as heat exchangers, free cooling towers, chillers, heat pumps and stratified storage tanks determining different characteristics. Chillers and heat pumps are aggregates either switched on or off usually connected with stratified storage tanks which are operated in a charging or discharging mode depending on the state of the aggregate and the mass flows to and from the storage tank. The aim was to optimize the continuous mass flows of pumps and supply temperatures with

respect to discrete states (on and off times) of the switching aggregates. For that reason a mixed-integer MPC based on the hybrid model approximating the heating and cooling process in all storage modes has been developed.

1.4 Methodology

In this work focus is firstly put on appropriately combining existing modeling and system identification techniques for the application in MPC, see Sections 2.1 and 2.2. Secondly, the design and development of a dedicated nonlinear MPC (NMPC) structure for the building heating and cooling supply is presented, see 2.1 and 2.2. Furthermore, potential analyzes are conducted, see Sections 2.2 and 2.3.

1.4.1 Modeling

Modeling the heating and cooling energy supply process for the industrial tool chain faces the challenge of finding an appropriate balance of model detail, depth, and accuracy in order to operate a powerful MPC with a manageable effort for modeling respective system identification. It is thus a crucial part for building predictive control, [9]. The common base for all models are energy balance equations (1.1), resulting in a set of first order differential equations.

$$\dot{Q} = \Delta T \cdot \dot{m} \cdot cp = (T_s - T_r) \cdot \dot{m} \cdot cp \quad (1.1)$$

The first principle models therefore cover the most important variables: the control variable heating respective cooling powers \dot{Q} , the manipulated variables mass flow \dot{m} , supply temperature T_s , and the disturbance return temperature T_r .

In order to reutilize the models a modular control concept has been developed where each supply circuit is initially considered separately, see Section 1.4.3. Thus, complex circuits incorporating switching aggregates and storage are distinguished from basic circuits with heat exchangers and pumps only.

Basic circuits, see Figure 1.3, for e.g. district heat are approximated by static models using (1.1), where $\dot{m}_s = \dot{m}$. In contrast, those supply circuits with switching aggregates such as chillers or heat pumps and a stratified storage tank, see Figure 1.4, require a dynamic model depicting the energy state of the system. These are the

temperature of the hot or cold water in the storage tank, T_{st} , and the position of the thermocline, z , which are respected in the nonlinear dynamic state space model.

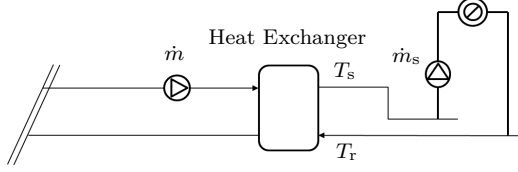


Figure 1.3: Basic supply circuit.

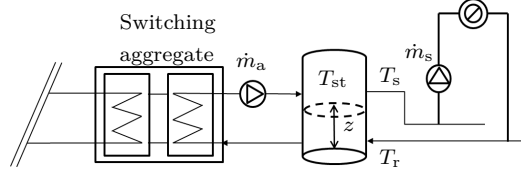


Figure 1.4: Complex supply circuit.

The stratified storage can be operated in three distinct modes which is illustrated by Figure 1.5: (a) charging, if the aggregate is switched on ($\delta_a = 1$) and the mass flow from the aggregate to the storage, \dot{m}_a , is higher than the one from the storage to the supply system, \dot{m}_s ; (b) discharging, if the aggregate is switched on ($\delta_a = 1$) and the mass flow from the aggregate to the storage, \dot{m}_a , is lower than the one from the storage to the supply system, \dot{m}_s ; (c) discharging, if the aggregate is switched off ($\delta_a = 0$), hence the mass flow from the aggregate to the storage, \dot{m}_a , is zero and consequently lower than \dot{m}_s . δ_i for $i = 1, 2, 3$ indicate whether the corresponding mode is active. Note that only one mode is active at each time; hence $\sum_{i=1}^3 \delta_i = 1$.

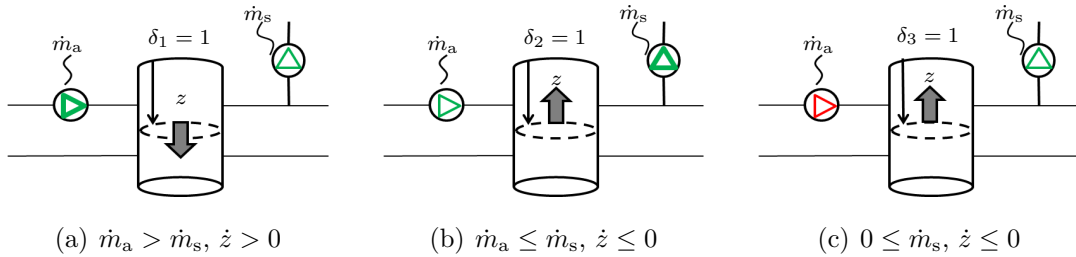


Figure 1.5: The three operation modes of the stratified storage tank depending on the state of the switching aggregate and the mass flows to and from the storage.

Depending on the operation mode of the stratified storage tank the water supply temperature, T_s , is differently defined, see Equation (1.2). The state z , the height of the water in the stratified storage below (in case of cooling) or above (in case of

heating) the thermocline, is denoted by Equation (1.3), where r denotes the radius of the tank and ρ the density of the water inside the tank.

$$T_s = \begin{cases} T_a & \text{if } \dot{m}_a > \dot{m}_s, \delta_a = 1 \Leftrightarrow \delta_1 = 1 \\ \frac{T_a \dot{m}_a - T_{st} \dot{m}_{st}}{\dot{m}_s} & \text{if } \dot{m}_a \leq \dot{m}_s, \delta_a = 1 \Leftrightarrow \delta_2 = 1 \\ T_{st} & \text{if } \dot{m}_a \leq \dot{m}_s, \delta_a = 0 \Leftrightarrow \delta_3 = 1 \end{cases} \quad (1.2)$$

$$z = \frac{m_a - m_s}{r^2 \pi \rho} \quad (1.3)$$

The derivative of state T_{st} is derived from the heat flow balance

$$\dot{Q} = \dot{Q}^{\text{in}} - \dot{Q}^{\text{out}}$$

and the respective case of Equation (1.2).

The set of equations can be rewritten as a compact representation by a mixed logical dynamical (MLD) System, [10], of the form:

$$x(t+1) = A_t x(t) + B_{1t} u(t) + B_{2t} \delta(t) + B_{3t} z(t), \quad (1.4a)$$

$$y(t) = C_t x(t) + D_{1t} u(t) + D_{2t} \delta(t) + D_{3t} z(t), \quad (1.4b)$$

$$E_{2t} \delta(t) + E_{3t} z(t) \leq E_{1t} u(t) + E_{4t} x(t) + E_{5t}, \quad (1.4c)$$

using the states x , the continuous and discrete manipulated variables $u = \{u_c, u_d\}$ and the control variable y . z -variables are auxiliary continuous representatives of the state modes and the δ variables are auxiliary discrete variables representing the hybrid modes at each time step t . The inequality system in (1.4c) is a compact form of the logical conditions arising due to the discrete modes and possible switches between them. This modeling approach has been applied on the heating circuits, see Publication A, Section 2.1.

For the cooling circuits an additional system identification routine has become necessary, since it includes a cooling tower which is a complex energy supply aggregate with discrete stages of fan speed. Modeling it analytically aims at detailed complex models with nonlinear dynamics of high order impractical for MPC. Thus, linear regression models have been used, [11], to identify a linear model for each stage based on the historic measured data of the automation system of the University in Salzburg. For more detail see Publication B, Section 2.2.

1.4.2 Hybrid model predictive control

Optimizing the hybrid system with continuous as well as discrete manipulated variables results in a nonlinear mixed-integer problem which has to be solved in each optimization step by the MPC. The control of such a hybrid system has been solved with different approaches. In [12] a dual stage optimization is used where firstly the tank operation mode is chosen and secondly, the problem is recast to a nonlinear program with a fixed tank operation mode profile, whereas in [13] a suboptimal iterative approach has been applied by varying operating points. Within this work a dedicated branch and bound algorithm is presented. For the development of the mixed-integer MPC (MI-MPC) four steps have been crucial:

1. Dealing with the non-linearity of the hybrid model.
2. Formulating the objective function.
3. Identifying and quantifying all relevant technical constraints.
4. Inclusion of an appropriate algorithm to cope with the mixed-integer problem.

Linearization

The hybrid model, first formulated as a nonlinear piecewise affine system such as denoted in a simplified form in equation (1.2) has firstly been linearized around the operating point and has secondly been reformulated resulting in a closed MLD state space system, (1.4), with an inequality system which covers the possible conditions for the transitions from one affine system to another. Hence, outcome of step one is a linear approximation of the nonlinear hybrid model, see Publication A, Section 2.1.

Objective function

The objective target, minimizing the energy costs while minimizing the deviation of the delivered power \dot{Q}_i^{act} of supply system $i \in \{\text{TABS}, \text{FC}\}$ from the respective energy demand of the user level \dot{Q}_i^{ref} , has been formulated as a quadratic function including all future time instances $t + k$ within the prediction horizon N_p resulting in a mixed-integer quadratic problem (MIQP) to be solved each step:

$$J^* = \min_{\Delta u \in U} \sum_{k=0}^{Np-1} (1 - \alpha) \left\| \Delta \dot{Q}_i^{\text{ref}}(t+k) - \Delta \dot{Q}_i^{\text{act}}(t+k) \right\|_{Q_y}^2 + \alpha \left\| \Delta u(t+k) \right\|_{Q_u}^2 \quad (1.5)$$

Note that the Δ -formulation does denote the deviation from the actual value to the respective operation point and $u = \{u_c, u_d\}$ are continuous as well as discrete manipulated variables. The parameter $\alpha \in [0, 1]$ allows to put more weight on the minimization of the energy costs or on the deviation of the delivered power to the given reference. In Publication A, see Section 2.1, the effect of a variation of α is given. Further weighting factors respective matrices are Q_y and Q_u .

Constraints

The constraints include technical limitations of pumps, aggregates, and stratified storage tanks given by minima and maxima of the corresponding manipulated variables and states.

$$\begin{aligned} u_{i,\min} &\leq u_i \leq u_{i,\max} \\ x_{i,\min} &\leq x_i \leq x_{i,\max} \end{aligned} \quad (1.6)$$

For the storage tank management the maximal volume of the tank is important. Whereas pumps are respected with minimal and maximal mass flows, aggregates such as chillers and heat pumps require minimal up and down times and a certain interval for the supply temperature.

Branch and Bound Algorithm

In the first controller design the mixed-integer problem has been solved by an external solver called Gurobi [14], see Publication A, Section 2.1. However, for an industrial application a more cost-effective solution is frequently desired. Therefore, a dedicated branch and bound algorithm, generally motivated and presented e.g. in [15], has been designed and implemented resulting in a suboptimal but very effective method to solve the mixed-integer problem by relaxing the integrality constraints of the discrete variables. This means that they are allowed to span over the whole continuous interval. The respective problem is therefore represented by a specific

tree structure, see Figure 1.6, where each theoretical solution of the optimization problem is represented by a branch (path from the root to one leaf). In order to reduce the search space to accelerate the optimization routine a preprocessing step has been developed eliminating those branches which would violate constraints over the optimization horizon Np given at the respective optimization step t (see branch ending with x in Figure 1.6). Especially the limitation of storage volume, the corresponding stored energy, and the minimal up and down times of the chiller or the heat pump are key parameters for the preprocessing step. For more detail see Publication B, Section 2.2.

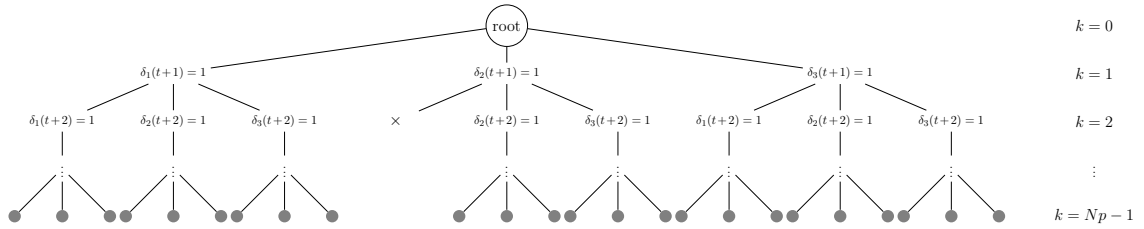


Figure 1.6: The binary tree for the hybrid system optimization with branch and bound.

1.4.3 Modular model predictive control concept

Given the MI-MPC, the overall control concept has been redesigned by assigning one MPC to one energy supply circuit in order to use the best suited MPC. The advantage of the gained modularity lies firstly in the industrial usage, since the modeling, implementation, parametrization and commissioning can be done independently. Secondly, the task for each MPC is less complex, because each hybrid system (circuits with switching aggregates and connected storage) is controlled by a MI-MPC, while for each simple circuit an LMPC is chosen using a static, linearized form of Equation (1.1).

The overall resulting control system for the heating and cooling supply of the demonstration building is depicted in Figure 1.7.

Since the hierarchic control task had been split into the two layers, for the user level any predictive controller is assumed delivering a trajectory for the energy demand of

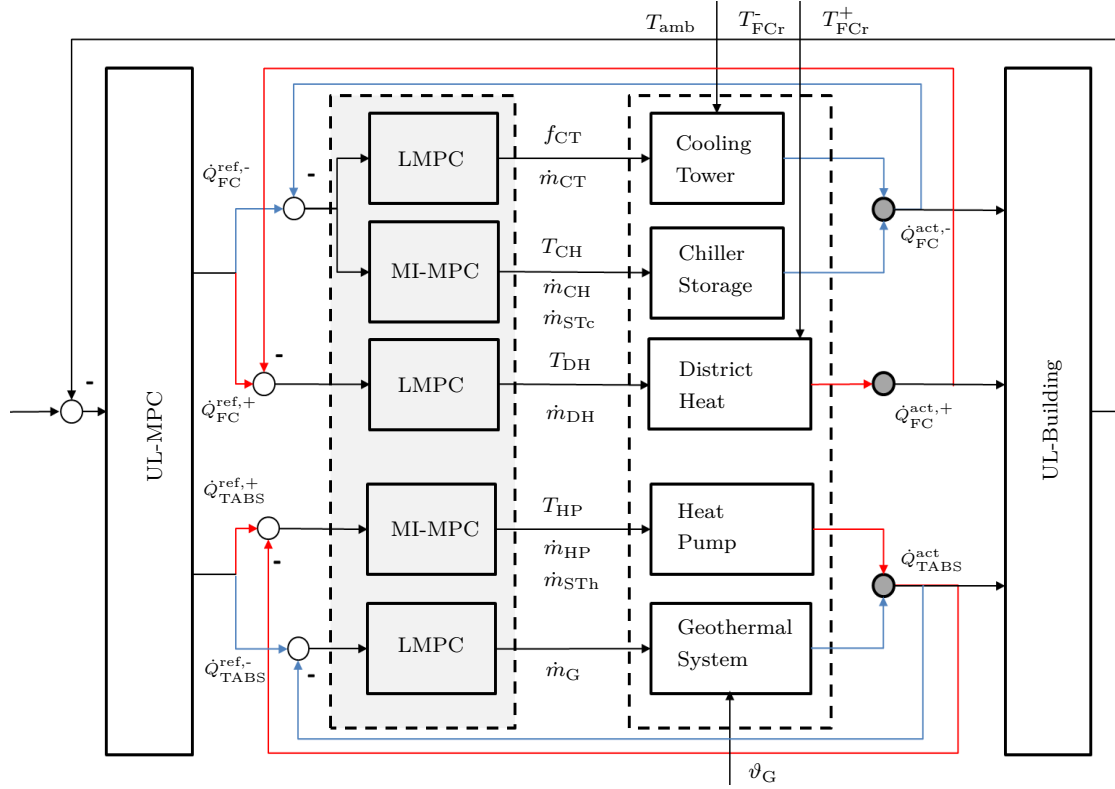


Figure 1.7: Modular control structure for FC and TABS embedded into a hierarchical building control structure. Blue feedback loops indicate the cooling, red loops the heating circuits.

each energy supply system of building. However, the overall NMPC building control structure proposes an CFMPC for the multizone user level given in Publication D, Section 2.4. Regarding the supply system a distinction is made for heating and cooling supply for the fan coil (FC), $\dot{Q}_{\text{FCref},+}$ and $\dot{Q}_{\text{FCref},-}$ respectively, as well as for the thermally activated building system (TABS). This becomes important because the user level controller optimizes the energy demand with respect to different time constants of the energy supply systems which is an information the energy supply level does not have. Hence, it plays an important role whether the heating or cooling energy is provided for the system with the slow dynamics (TABS) or the system with the fast dynamics (FC).

In this particular case, the cooling circuits of the free cooling tower and the chiller are connected since the free cooling tower is cooling down the water of the secondary circuit of the chiller. Hence, if the chiller is switched on free cooling is exclusively used for this purpose meaning that either the one or the other cooling circuit is active for the supply of the FC system. Nevertheless, two controllers are working simultaneously - one for each circuit, but the supply of the free cooling is forced whenever technically possible. The restrictions are the ambient temperature T_{amb} , since free cooling is only active if $T_{\text{amb}} < 18^\circ\text{C}$ and the chiller has not to be activated for charging the stratified storage tank. However, given these rules and the MI-MPC which is managing the storage efficiently, the MPCC is capable of maximizing the usage of the free cooling tower for direct cooling supply. The corresponding simulation results given in Publication B, Section 2.2, and [16] show promising figures in terms of active free cooling hours and the amount of cooling power supplied within this time compared to a rule-based controller.

Further potential analyzes of the developed MPCC are conducted in Publication C, Section 2.3. Closed loop simulations of the overall hierarchic control structure including the CFMC as well as the MPCC show promising results in terms of user satisfaction, energy efficiency, and minimization of costs in comparison to the conventional control concept implemented in the demonstration building. The NMPC structure thus enables sustainable building automation.

1.5 Summary of Scientific Approaches

The Publications A-C, see Section 2.1-2.3, show the results chronologically. Publication A, Section 2.1, covers the first principle modeling of the hybrid system on the example of the heating supply of the demonstration building and the basic control design of the mixed-integer MPC (MI-MPC). An appropriate objective function and corresponding constraints including minimal up and down times for the heat pump are given. Furthermore, it contains the results of a robustness analysis of the MI-MPC regarding disturbances of the heat load prediction. Therefore an approximated Pareto front has been computed for a fixed set of weights and varying parameter α , putting more emphasis either on the mean error or on the energy costs for different lengths of Np .

Publication B, see Section 2.2, demonstrates the methodology of modeling the cooling circuits in a modular way combining analytical hybrid modeling for the chiller circuit and system identification routine for the cooling tower circuit and shows the results of the validation for each model. Furthermore, the optimized control design based on the developed branch and bound approach is explained in detail. Simulation results show the performance of the new MI-MPC separately for the transition and the cooling period in terms of estimated monetary savings, number of active free cooling hours, and number of switching cycles of the chiller. The figures are compared to a conventional proportional –integral –derivative (PID) controller with additional rules. The proposed MPC structure reduces the costs by about 50 %, increases the usage of renewable energy source by at least 50 %, and manages the chiller and storage tank in a way that the transitions of the chiller from state off to on are reduces by about 70 %.

Publication C, see Section 2.3, focuses the effect of MPC on the sustainability of buildings. Therefore, the interaction of building automation, including MPC in general and hybrid MPC in special, with users, operators, the environment, and the smart grid are discussed. Each group is affected by building automation influencing cost, energy, and user comfort aspects. Simulation results show that MPC is an ideal tool to enable sustainable building automation.

Publication D, see 2.4, presents the CFMPC developed for multizone heating and cooling control using TS-fuzzy models. The concept is developed for the user level of a specific demonstration building within a hierarchical control scheme. The CFMPC achieves significantly higher control performance with slightly less energy consumption in contrast to state-of-the-art controllers and MPCs in building.

1.6 Scientific Contribution

The hierarchic control concept consisting of two nonlinear MPCs leads to two optimization problems with different time constants. The developed control concept for the energy supply level is flexible towards more energy supply circuits and sources since the basic modeling approach can be used and the control structure easily extended according to the distinction in basic and complex circuits. The mixed-integer MPC is the core development within the modular predictive control concept. It is capable to manage the stratified storage tank operation depending on the switching sequences while guaranteeing the energy demand of the user level and minimizing the energy costs. The capability of maximal usage of renewable energy sources is only one indicator that the developed control concept can make a contribution for sustainable building automation. The scientific contributions of this work are all applicable in industry.

The scientific contributions of this work and can be summarized:

- Hierarchical control concept
 - Decoupling of conflicting optimization problems.
 - Easy to implement and the possibility to use individual MPCs, instead of the overall hierarchy.
 - For the specific building the flexibility for adding new building zones or supply sources is given.
 - The preparation for future integration in Smart Grids and for flexible pricing is given and can be easily added in the specific MPCs.

-
- Modeling and system identification
 - Development of analytically derived hybrid model based on energy balance equation.
 - Linearization of first order differential equation.
 - Black box model identification for cooling tower.
 - Model validation is given.
 - Development of hybrid mixed-integer MPC (MI-MPC)
 - Design, formulation, and implementation of dedicated MI-MPC using hybrid model.
 - Respecting latency times for minimal up and down times for switching aggregates (unit commitment problem).
 - Managing the stratified storage tank operation depending on the switching sequences.
 - Capability to cope with time-variant prices of (electric) energy.
 - Robustness analysis is given.
 - Development of dedicated branch and bound algorithm solving MIQP on-line with search space reduction to accelerate optimization.
 - Design of flexible modular predictive control concept
 - Combining LMPCs and MI-MPCs for flexible control of varying amount of energy supply circuits and sources of basic or complex type.
 - Perfect for industrial application due to modularity.
 - Potential analyzes comparing MPCC to a PID and rule-based control concept in simulation.

Bibliography

- [1] European Commission. Buildings, 2016.
- [2] Oscar Ortiz, Francesc Castells, and Guido Sonnemann. Sustainability in the construction industry: A review of recent developments based on lca. *Construction and Building Materials*, 23(1):28–39, 2009.
- [3] Frauke Oldewurtel, Alessandra Parisio, Colin N Jones, Dimitrios Gyalistras, Markus Gwerder, Vanessa Stauch, Beat Lehmann, and Manfred Morari. Use of model predictive control and weather forecasts for energy efficient building climate control. *Energy and Buildings*, 45:15–27, 2012.
- [4] Frauke Oldewurtel, David Sturzenegger, and Manfred Morari. Importance of occupancy information for building climate control. *Applied Energy*, 101:521–532, 2013.
- [5] Eduardo F Camacho and Carlos Bordons Alba. *Model predictive control*. Springer Science & Business Media, 2013.
- [6] Jan Sirokỳ, Frauke Oldewurtel, Jirí Cigler, and Samuel Prívara. Experimental analysis of model predictive control for an energy efficient building heating system. *Applied Energy*, 88(9):3079–3087, 2011.
- [7] David Sturzenegger, Dimitrios Gyalistras, Manfred Morari, and Roy S Smith. Model predictive climate control of a swiss office building: Implementation, results, and cost–benefit analysis. *IEEE Transactions on Control Systems Technology*, 24(1):1–12, 2016.
- [8] Yudong Ma, Francesco Borrelli, Brandon Hancey, Brian Coffey, Sorin Bengea, and Philip Haves. Model predictive control for the operation of building cooling

- systems. *Control Systems Technology, IEEE Transactions on*, 20(3):796–803, 2012.
- [9] Samuel Privara, Jirí Cigler, Zdeněk Vána, Frauke Oldewurtel, Carina Sagerschnig, and Eva Záčeková. Building modeling as a crucial part for building predictive control. *Energy and Buildings*, 56:8–22, 2013.
- [10] Alberto Bemporad and Manfred Morari. Control of systems integrating logic, dynamics, and constraints. *Automatica*, 35(3):407–427, 1999.
- [11] Lennart Ljung. System identification—theory for the user, 2nd edition ptr prentice hall. *Upper Saddle River, NJ*, 1999.
- [12] Yudong Ma, Anthony Kelman, Allan Daly, and Francesco Borrelli. Predictive control for energy efficient buildings with thermal storage. *IEEE Control System Magazine*, 32(1):44–64, 2012.
- [13] Felix Berkenkamp and Markus Gwerder. Hybrid model predictive control of stratified thermal storages in buildings. *Energy and Buildings*, 84:233–240, 2014.
- [14] Inc Gurobi Optimization. Gurobi optimizer reference manual, 2014.
- [15] Christodoulos A Floudas. *Nonlinear and mixed-integer optimization: fundamentals and applications*. Oxford University Press, 1995.
- [16] Barbara Mayer, Michaela Killian, and Martin Kozek. Modular model predictive control concept for building energy supply systems: Simulation results for a large office building. In *Modelling and Simulation (EUROSIM), 2016 9th EUROSIM Congress on*, pages 271–275. IEEE, 2016.

Chapter 2

Publications

2.1 Publication A

Barbara Mayer, Michaela Killian, and Martin Kozek.

Management of hybrid energy supply systems in buildings using mixed-integer model predictive control.

Energy Conversion and Management, Volume 98, 2015, pages 470-483, ISSN: 0196-8904.

DOI: 10.1016/j.enconman.2015.02.076

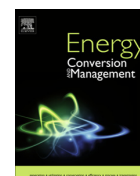
Own Contribution

Problem statement, selection of methods and algorithms for modeling, control design, implementation and simulation, as well as structuring, writing and editing the paper was done by the applicant under the supervision of the third author and mentor. Discussion of methodology and results as well as editing and proof read was done by second author.



Contents lists available at ScienceDirect

Energy Conversion and Management

journal homepage: www.elsevier.com/locate/enconman

Management of hybrid energy supply systems in buildings using mixed-integer model predictive control

Barbara Mayer^{a,*}, Michaela Killian^b, Martin Kozek^b^a FH Joanneum, Institute of Industrial Management, Werk-VI-Strasse 46, 8605 Kapfenberg, Austria^b Vienna University of Technology, Institute of Mechanics and Mechatronics, Getreidemarkt 9, 1060 Vienna, Austria

ARTICLE INFO

Article history:

Received 3 December 2014

Accepted 25 February 2015

Available online 18 April 2015

Keywords:

Mixed-integer model predictive control (MI-MPC)

Hybrid energy supply system

Building control

Unit commitment

Stratified storage tank management

ABSTRACT

In this paper a mixed-integer model predictive controller for hybrid energy supply systems in buildings is presented. This approach is based on a hierarchical building control concept where the energy supply level is coupled to the energy consumption level only by the heat load. The supply level is characterized by non-linear dynamics due to a stratified water storage tank and a switched heat pump with minimum on/off times. The mixed-integer model predictive controller optimizes the unit commitment problem at minimum costs while satisfying the consumption level's predicted heat load. The hybrid system is formulated as a piecewise affine model comprising continuous and discrete system inputs. Moreover, the proposed controller is able to manage the stratified storage tank including switching sequences of the heat pump with respect to energy price forecasts. The effectiveness of this approach is shown by a comparison to a model predictive controller with an a priori fixed operation mode profile, where the heat pump is only operating at night, and discussing the effect of the variation of the stratified storage tank size. The proposed concept is able to flexibly manage all sizes of stratified storage tanks with better performance than the reference control strategy, which is only effective for larger tanks. Additionally, a robustness analyses demonstrates that the mixed-integer model predictive controller can handle errors in the heat load prediction from the consumption level. Both analyses show promising results for the practical use of the proposed controller within the hierarchical control concept or as a control module in a similar but more general application.

© 2015 Elsevier Ltd. All rights reserved.

1. Introduction

According to the statistics of the International Energy Agency the building sector consumes up to 40% of the total final energy consumption, [1]. In order to achieve significant reductions in primary energy consumption passive measures like improved insulation are taken, but also renewable energy sources are being considered, which are highly dependent on weather conditions. Therefore, the periods of efficient energy production do usually not coincide with the energy demand of buildings. That is why appropriate thermal energy storages become necessary, [2]. They are realized either by thermally activated building systems (TABS), where massive concrete structures are thermally activated, or by dedicated thermal storage such as stratified tanks. The usage of an increasing number of energy sources, the combination of continuous and switching heat sources, together with the

management of storage requires new control strategies. Regarding management of the energy production level, the points of view differ considerably and range from peak load shifting approaches, [3], to integrated storage management with building automation systems, [4].

Model-based predictive control (MPC) has been proven as a promising technology for building control, [5]. Most of the presented approaches of recent years focus on the control of the entire building comprising the buildings' zone control as well as the energy supply optimization within one model and controller. In [6] building modeling approaches are discussed, whereas [7] presents how to include forecasts into the MPC strategy. However, a building can be seen as a two-layer structure, the High Level (HiLe) energy-consuming layer and the Low Level (LoLe) energy providing layer, [8]. This paper is based on the fundamental concept presented in [8]: (i) A HiLe-MPC optimizes the heat load for maximum comfort and minimum energy consumption, (ii) the LoLe-MPC provides the requested heat load with minimum monetary costs. As the two layers exhibit different non-linear system dynamics and optimization targets an hierarchical

* Corresponding author. Tel.: +43 386233600 6347.

E-mail addresses: barbara.mayer@fh-joanneum.at (B. Mayer), michaela.killian@tuwien.ac.at (M. Killian), martin.kozek@tuwien.ac.at (M. Kozek).

approach is reasonable, splitting one modeling and control problem into two optimization tasks. The resulting modularity in implementation and operation is an important advantage for industrial implementation.

Focusing on the LoLe, the presence of possibly numerous switching aggregates such as heat pumps requires the management of on/off times which consequently influences the operation modes of the stratified storage tanks at each time step. Furthermore, this unit commitment problem involves constraints on the minimum on/off times, which are considered due to constraints on the aggregates' actuators and the aim to reduce maintenance costs over the whole lifecycle. The resulting system is a hybrid system, [9], where each operation mode requires a dedicated, generally non-linear, model. The combination of continuous and discrete decision variables leads to a mixed-integer non-linear optimization problem (MINP), for which there is no exact solution technique. However, by approximating the dedicated models by piecewise linear models, mixed-integer linear programming (MILP) can be used to solve the optimization problem, yielding suboptimal solutions.

Summarizing, the main challenges for the LoLe control are (i) the hybrid energy supply system including continuous as well as discrete control variables for switching aggregates with minimum on/off times, (ii) the mixed-integer MPC formulation (with time variant cost structure) and (iii) the coupling to the HiLe controller with uncertain load prediction.

Using MPC requires accurate but rather simple models. Therefore, appropriate assumptions on the system have to be made. Refs. [10,11] have presented hybrid system formulations for cooling systems including different operation modes. In [10] a two-layered stratified storage tank was considered with constant tank temperatures as well as fixed return temperatures from the building. Ref. [11] generalizes the stratified storage tank management for an arbitrary number of stratification layers, energy sources and consumers. Nevertheless, both [10,11] assume two tank operation modes, charging and discharging, specified by an a priori fixed operation plan. Subsequently, chillers are only switched on at night, in order to charge the stratified storage tank, and switched off during day, when the tank is discharged. In contrast to the aforementioned building control references, this paper focuses on the model-based predictive control of the buildings' heating supply (LoLe) covering the unit commitment problem and introduces the hybrid mixed-integer MPC (MI-MPC) approach; a method which has not yet been applied to building heating control. The energy supply system includes a geothermal heat pump, a stratified two-layered water storage tank, and a TABS system. District heat supply is considered as an additional heating circuit providing energy for the Fan Coils (FC) in the indoor rooms. While [12] shows first experimental results on MPC for building heating control, in [7] focus is put on the comparison of different MPC concepts. However, both use bi-linear models to describe the overall system, whereas this paper introduces a hybrid mixed-integer formulation including discrete decision variables for aggregate switching times as well as constraints on minimum on/off times. The resulting unit commitment and MILP problem has also been theoretically introduced in the field of microgrid operation optimization, [13]. The feasibility and effectiveness of this approach has been experimentally proven in [14], where the method was applied to a microgrid in Athens, Greece. Although the fundamental problem formulation is similar, the model depth for the microgrid is lower than needed for building energy supply, where pumps must be controlled individually. In contrast to [13,14], the modeling approach utilized here is based on analytically derived first order non-linear differential equations, approximated by piecewise linear models. The hybrid mixed-integer problem formulation is carried out as introduced in [9] resulting in a piecewise affine (PWA) system.

The simulation results of the proposed decoupled LoLe mixed-integer MPC are compared to those with an a priori fixed tank operation mode profile in terms of mean error, (monetary) costs and coefficient of performance (COP) of the energy supply of the TABS system. Additionally, the effect of varying the tank size on the controller's decision and the resulting costs are discussed. Since recent work show that the impact of forecasting accuracy on the predictive control strategy is high, [15], an analysis of the MI-MPCs robustness is given with respect to the uncertainty of the heat load prediction from the HiLe. For simulating this error the deterministic reference trajectory is disturbed with a fixed bias and a randomly generated white noise over the entire simulation period.

The paper is structured as follows: The problem is formulated in Section 2, followed by introduction of the model of the energy supply hybrid system, Section 3. The mixed-integer MPC formulation is given in Section 4 and the simulation results discussed in Section 5. Finally, conclusions are drawn in Section 6.

2. Building control

In this Section the fundamental approach, the concept of hierarchical building control, the energy supply system, and the problem formulation are given.

2.1. Fundamental approach

Large building heating control necessarily includes the whole building, the High Level (HiLe), where the building indoor rooms are conditioned, as well as the Low Level (LoLe), where heating is provided. In recent years, most of the MPC approaches have focused on the control of both layers in one controller, [7,6]. Therefore, one model including both systems' dynamics has to be taken into account. The complexity for modeling and control is high as both systems are inherently non-linear and the time constants and optimization targets are completely different. The approach presented in [8] splits this optimization problem by defining a dedicated MPC for each of the two levels, which interact via the predicted heat load from the HiLe \dot{Q}_i^{ref} and the actual delivered heat from the LoLe \dot{Q}_i , where i denotes different heating supply circuits. The maximization of the users' comfort is the central objective for the HiLe-MPC, considering stochastic disturbances ambient temperature, radiance and occupancy. In contrast, the LoLe controller optimizes the operation of the switching aggregate and consequently the number of available energy sources used to meet the HiLe requirement by minimizing the costs. This is a classical unit commitment problem (when to optimally switch an aggregate on/off), but additionally the stratified storage tank's operation and the usage of electric energy with time-varying pricing is optimized. Note that the relevant dynamics in the higher level is comparatively slow (from hours to several days), whereas in the lower level it is faster (from minutes to several hours). In [8], this hierarchically decoupled approach was presented, which is briefly explained in Section 2.2 since it defines the requirement for control of the energy supply system Section 2.3 and in [16] the HiLe-MPC was further developed.

2.2. Hierarchic building control

Fig. 1 shows a schematic diagram of the two building layers and the single coupling point between the controllers. The HiLe optimizes the user comfort by minimizing the deviation of the indoor temperature from the consumer preference. \dot{Q}_i^{ref} , for $i = \{\text{TABS}, \text{FC}\}$, depicts the energy demand of the HiLe to fulfill the optimization target, which constitutes the control variables

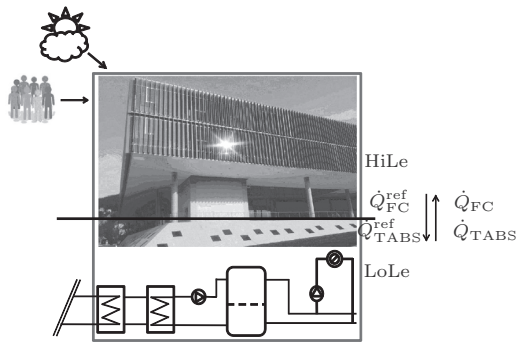


Fig. 1. Concept of hierarchic building control.

of the HiLe-MPC at the same time. As each building zone j can be controlled individually by a separate MPC, the sum of these control variables $\sum_j \dot{Q}_{ij}^{ref}$ is the reference value for the energy supply of the LoLe-MPC. However, the important fact is the decoupling of the optimization problems. Stochastic disturbances such as weather and occupancy information only affect the HiLe-MPC, [7], Fig. 1. Decoupling is useful due to the fact that (i) the dynamic behavior is significantly different in HiLe-MPC and LoLe-MPC, (ii) the modeling and optimization problem is split into two tasks, and (iii) the possibility of modular application is given. Minimum up- and down-times and operation modes of the stratified storage tank are the reason for the dynamics in LoLe, whereas the dynamics in the HiLe differ not least due to large time constants. Global optimal solutions may not be reached with a decoupled method, but two local optimal solutions are more likely to be feasible and easier in operation due to the resulting real time capability. Industrially motivated, system identification of the HiLe may be data-driven, [17], while LoLe can be modeled by an analytical approach. Additionally, the optimization targets of the two layers differ fundamentally, so that large benefits arise with an hierarchically decoupled approach that allows modular application in industry.

2.3. Energy supply system

In the following the variables, parameters and subscriptions given in Tables 1 and 2, respectively, will be used.

Due to the different temperature levels, the heating supply system consists of two separated supply circuits, see Fig. 2, one responsible for the Fan Coil (FC) system in the indoor rooms and the other one for the TABS system implemented as activated concrete in two office floors.

District heating is the source of the first circuit, directly fed through to the distributor for the office floors, whereas the TABS system is provided by a geothermal-based heat pump and a

Table 2

Definition of subscripts.

Subscripts	Description
'h'	Hot water above thermocline
'c'	Cold water below thermocline
's'	Supply water to the building
'r'	Return water from the building
'TABS'	TABS system
'FC'	Fan Coils system
'HP'	Heat pump
'DH'	District heat
'amb'	Ambient
'in'	Indoor

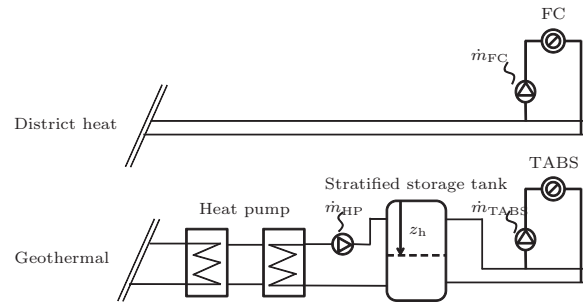


Fig. 2. Heating circuits for FC and TABS.

subsequent stratified water storage tank. The water-glycol mixture fed by the geothermal pipes varies between 12 °C and 16 °C depending on the season and ambient temperature. The TABS system has a minimum supply temperature constraint which depends on the insulation of the pipe system. Therefore, it is reasonable to operate a stratified storage tank in order to compensate the temperature gap. This also enables an energy saving management since the heat pump can be switched off regularly. As in [11,10], the assumption is that the warm water enters the storage tank at the top and is also drawn from there, whereas the cold return water from the building is supplied to the bottom. The storage tank can operate in two basic operation modes: charging and discharging. These operation modes depend on the status of the heat pump (on/off) and on the difference of the mass flows to, \dot{m}_{HP} , and from, \dot{m}_{TABS} the storage tank. As the supply systems are located in the basement of the building, the ambient temperature T_{amb} is assumed to be constant with 20 °C. The water return temperatures $T_{TABS,r}$ and $T_{FC,r}$ are also assumed to have a constant level of 22 °C and 30 °C. This assumption is plausible, because the HiLe-MPC optimizes the energy amount needed to guarantee user comfort. Since the LoLe controller is designed to meet these requirements, the resulting return temperatures are almost constant.

Table 1

Definition of variables and parameters.

Variables	Description
z	Height of stratified water storage tank [m]
T	Temperature of the water [°C]
\dot{m}	Mass flow rate [kg/s]
\dot{Q}	Heat flow from LoLe to HiLe [W]
cp	Specific heat capacity of water [J/kg K]
ρ	Density of water [g/cm ³]
r	Radius of tank [m]
k	Coefficient of thermal conductivity of the storage tank [W/m °C]
v	Volume of the stratified water storage tank [m ³]
δ	Discrete variable

2.4. Control problem statement

For the energy supply system outlined in Section 2.3 a control design should be performed which guarantees that the actual heat supply \dot{Q}_i tracks the desired heat load \dot{Q}_i^{ref} with optimal performance (meaning both minimum error and minimum costs). Available variables for that task are heat pump, supply pumps, and supply temperature. Moreover, the management of the stratified storage tank should utilize the storage capacity as effectively as possible. As a model based control scheme is to be used, the following Section focuses on the modeling of the energy supply system.

3. Energy supply system model

In this Section the models for both heating circuits are derived analytically. The non-linear equations are given and the linearization is outlined.

3.1. FC supply model

The FC supply model is determined as a static first order non-linear differential equation with the control output \dot{Q}_{FC} and the manipulated variables \dot{m}_{FC} and $T_{FC,s}$:

$$\dot{Q}_{FC} = \dot{m}_{FC} \cdot (T_{FC,s} - T_{FC,r}) \cdot cp, \quad (1)$$

with $T_{FC,s} = T_{DH}$ and \dot{m}_{FC} as the system's inputs. Linearizing the model at the operating point $O = \{T_{FC,s}^0, \dot{m}_{FC}^0\}$, results in:

$$\Delta \dot{Q}_{FC} = c_1 \cdot cp \cdot \Delta T_{FC,s} + c_2 \cdot cp \cdot \Delta \dot{m}_{FC}, \quad (2)$$

with $\Delta T_{FC,s} = T_{FC,s} - T_{FC,s}^0$ and $\Delta \dot{m}_{FC} = \dot{m}_{FC} - \dot{m}_{FC}^0$. The coefficients c_1 and c_2 are provided in [Appendix A](#).

3.2. TABS supply model

For the TABS supply model, the water storage tank is modeled as a two-layer stratified storage tank with one perfectly separating thermocline as in [\[10\]](#). As the tank is within a closed hydraulic system, the water level in the storage tank is assumed to be constant with $z = z_h + z_c$ at each time. Nevertheless, as the focus of this work is placed on heating control, only the height and volume of water above the thermocline z_h and v_h , respectively, are of importance in the following. On the hot generation side, the tank is supplied by the mass inflow \dot{m}_{HP} with water from the heat pump, whereas on the consumption side, the mass outflow \dot{m}_{TABS} determines the amount of hot water provided for the TABS system, see [Fig. 2](#). Consequently, the status of the heat pump determines the mass flow rate \dot{m}_{HP} . In order to make the controller decide whether the heat pump is switched on or off, the discrete variable $\delta_{HP} \in \{0, 1\}$ is introduced, which affects the mass flow rate \dot{m}_{HP} and its constraints, see [Section 4.2](#). If the heat pump is switched on, it operates between 30% and 70% of its nominal power, whereas there is no mass flow at all if the pump is switched off. Therefore, the stratified storage tank's operation mode depends on the controller's decision, on the difference of the two mass flows, and on the status of the heat pump, see [Fig. 3](#).

The water supply temperature $T_{TABS,s}$ depends on the active operation mode. Each mode is represented by one dedicated model. The hybrid system's dynamics are given by the change in z_h and the temperature of the hot water in the stratified storage tank T_h over time. Thus, these two variables form the states of the system. The manipulated variables are given by the mass flows \dot{m}_{HP} and \dot{m}_{TABS} and by the temperature of the water supply from the heat pump T_{HP} to the stratified storage tank. The control outputs \dot{Q}_{TABS} and T_{TABS} are expressed by the two states and the manipulated variables in each case.

3.2.1. Continuous non-linear model

The TABS supply model is determined as a set of non-stationary first order non-linear differential equations based on heat and mass flow balances:

$$\frac{dQ_h(m_h, T_h)}{dt} = \dot{Q}_h^{in} - \dot{Q}_h^{out}, \quad (3)$$

$$\dot{m}_h = \dot{m}_h^{in} - \dot{m}_h^{out} = \dot{m}_{HP} - \dot{m}_{TABS}. \quad (4)$$

For all operation modes, m_h is the mass of hot water in the stratified storage tank above the thermocline, r denotes the radius of the tank and ρ the density of the hot water:

$$m_h = z_h \cdot r^2 \pi \rho. \quad (5)$$

Hence, the derivative of the height of stratified water storage tank above the thermocline \dot{z}_h can be derived from Eqs. (4) and (5) independently from the operation mode:

$$\frac{dz_h}{dt} = g(\dot{m}_{HP}, \dot{m}_{TABS}) = \frac{\dot{m}_{HP} - \dot{m}_{TABS}}{r^2 \pi \rho}. \quad (6)$$

The heat flow based on the heat balance Eq. (3) is expressed by the following total differential, where the derivative of the temperature \dot{T}_h is denoted by the losses to the ambience:

$$\frac{dQ_h(m_h, T_h)}{dt} = \dot{m}_h \cdot T_h \cdot cp + m_h \cdot \dot{T}_h \cdot cp = (\dot{m}_{HP} - \dot{m}_{TABS}) \cdot T_h \cdot cp - 2r\pi \cdot k \cdot z_h \cdot (T_h - T_{amb}). \quad (7)$$

Charging: $\dot{m}_{HP} > \dot{m}_{TABS}$ and $\delta_{HP} = 1$

The mass flow rate of the heat pump is higher than the mass flow needed for the TABS system. Therefore, the energy content rises and z_h increases as the thermocline lowers, see [Fig. 3\(a\)](#). This operation mode is only feasible if the heat pump is active. In this case the temperature T_h can be approximated by T_{HP} and Eq. (7) can be written as:

$$\dot{m}_h \cdot T_h \cdot cp + m_h \cdot \dot{T}_h \cdot cp = (\dot{m}_{HP} - \dot{m}_{TABS}) \cdot T_{HP} \cdot cp - 2r\pi \cdot k \cdot z_h \cdot (T_h - T_{amb}) \quad (8)$$

The time derivative of the temperature of the hot water in the stratified storage tank \dot{T}_h can therefore be expressed by utilizing Eq. (8) where m_h is substituted by Eq. (5) and \dot{m}_h is substituted by Eq. (4):

$$\dot{T}_h = \frac{(\dot{m}_{HP} - \dot{m}_{TABS}) \cdot (T_{HP} - T_h) \cdot cp - 2r\pi \cdot k \cdot z_h \cdot (T_h - T_{amb})}{z_h \cdot r^2 \pi \rho \cdot cp}. \quad (9)$$

As the mass flow to the storage tank is higher than the mass flow to the TABS system, the temperature of the water supply for the TABS system, $T_{TABS,s}$, is assumed to be the temperature of the water supply from the heat pump (direct feed through). Hence, the heat flow to the TABS system is derived from this assumption and the non-stationary heat balance (3):

$$T_{TABS,s} = T_{HP}, \quad (10a)$$

$$\dot{Q}_{TABS} = \dot{m}_{TABS} \cdot (T_{HP} - T_{TABS,r}) \cdot cp. \quad (10b)$$

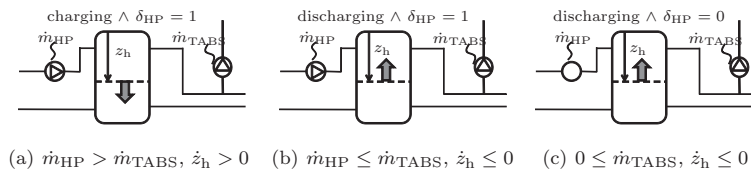


Fig. 3. The three operation modes of the stratified storage tank.

Discharging: $\dot{m}_{HP} \leq \dot{m}_{TABS}$ and $\delta_{HP} = 1$

If the mass flow rate produced by the heat pump is lower than the mass flow needed for the TABS system, the stratified storage tank is discharged, see Fig. 3(b). The time derivative of the temperature of the hot water in the stratified storage tank \dot{T}_h can be directly expressed from Eq. (7):

$$\frac{dT_h}{dt} = \frac{-2r\pi \cdot k \cdot z_h \cdot (T_h - T_{amb})}{z_h \cdot r^2 \pi \rho \cdot cp}. \quad (11)$$

If the heat pump is active the water supply temperature to the TABS system, $T_{TABS,s}$, is a mixture of the water supply temperature from the heat pump and temperature of the hot water in the stratified storage tank weighted by the corresponding mass flows. This also causes a different formulation of the heat flow to the TABS system than in the charging mode:

$$T_{TABS,s} = \frac{\dot{m}_{HP} \cdot T_{HP} - (\dot{m}_{HP} - \dot{m}_{TABS}) \cdot T_h}{\dot{m}_{TABS}}, \quad (12a)$$

$$\dot{Q}_{TABS} = \dot{m}_{HP} \cdot (T_{HP} - T_h) \cdot cp + \dot{m}_{TABS} \cdot (T_h - T_{TABS,r}) \cdot cp. \quad (12b)$$

Discharging: $0 \leq \dot{m}_{TABS}$ and $\delta_{HP} = 0$

If the mass flow rate produced by the heat pump is zero the stratified storage tank is discharged, see Fig. 3(c). The deviation of the temperature of the hot water in the stratified storage tank \dot{T}_h is equal to the corresponding formulation for charging while the heat pump is on. The water supply temperature to the TABS system $T_{TABS,s}$ is then equal to the temperature of the hot water in the stratified storage tank:

$$T_{TABS,s} = T_h, \quad (13a)$$

$$\dot{Q}_{TABS} = \dot{m}_{TABS} \cdot (T_h - T_{TABS,r}) \cdot cp. \quad (13b)$$

3.2.2. Continuous linearized model

In order to use the MI-MPC a piecewise linear model is required to formally describe the hybrid system. For the linear approximation, operating points for both states and all manipulated variables are fixed, $O = \{z_h^o, T_h^o, T_{HP}^o, \dot{m}_{HP}^o, \dot{m}_{TABS}^o\}$. The linearized, continuous system is given by the three sets of linear Eqs. (17)–(19) derived from the respective non-linear part of the model (9)–(13). The coefficients $c_3 - c_{19}$ are provided in Appendix A.

The method to derive the following linearized equations for each operation mode is exemplarily demonstrated for one specific model equation. For all operation modes z_h is given by Eq. (6).

The following Δ -variables define the deviation from the operating point: $\Delta z_h = z_h - z_h^o$, $\Delta \dot{m}_{HP} = \dot{m}_{HP} - \dot{m}_{HP}^o$ and $\Delta \dot{m}_{TABS} = \dot{m}_{TABS} - \dot{m}_{TABS}^o$. Consequently, Eq. (6) can be rewritten:

$$\Delta z_h = g(\dot{m}_{HP}^o, \dot{m}_{TABS}^o, \Delta \dot{m}_{HP}, \Delta \dot{m}_{TABS}). \quad (14)$$

Developing Eq. (14) in a first-order Taylor series at the operating point results in:

$$\begin{aligned} \Delta z_h = & g(\dot{m}_{HP}^o, \dot{m}_{TABS}^o) + \frac{\partial g(\dot{m}_{HP}, \dot{m}_{TABS})}{\partial \dot{m}_{HP}} \Big|_o \Delta \dot{m}_{HP} \\ & + \frac{\partial g(\dot{m}_{HP}, \dot{m}_{TABS})}{\partial \dot{m}_{TABS}} \Big|_o \Delta \dot{m}_{TABS}. \end{aligned} \quad (15)$$

With $g(\dot{m}_{HP}^o, \dot{m}_{TABS}^o) = 0$ the linearized equation for Δz_h is given by:

$$\Delta z_h = \frac{1}{r^2 \pi \rho} \Delta \dot{m}_{HP} - \frac{1}{r^2 \pi \rho} \Delta \dot{m}_{TABS}. \quad (16)$$

Charging: $\dot{m}_{HP} > \dot{m}_{TABS}$ and $\delta_{HP} = 1$

$$\Delta \dot{T}_h = c_3 \cdot \Delta T_{HP} + c_4 \cdot \Delta \dot{m}_{HP} + c_5 \cdot \Delta \dot{m}_{TABS} + c_6 \cdot \Delta z_h + c_7 \cdot \Delta T_h$$

$$\Delta T_{TABS,s} = \Delta T_{HP}$$

$$\Delta \dot{Q}_{TABS} = c_8 \cdot cp \cdot \Delta T_{HP} + c_9 \cdot cp \cdot \Delta \dot{m}_{TABS} \quad (17)$$

Discharging: $\dot{m}_{HP} \leq \dot{m}_{TABS}$ and $\delta_{HP} = 1$

$$\Delta \dot{T}_h = \frac{-2k}{r\rho \cdot cp} \Delta T_h$$

$$\Delta T_{TABS,s} = c_{10} \cdot \Delta T_{HP} + c_{11} \cdot \Delta \dot{m}_{HP} + c_{12} \cdot \Delta \dot{m}_{TABS} + c_{13} \cdot \Delta T_h$$

$$\begin{aligned} \Delta \dot{Q}_{TABS} = & c_{14} \cdot cp \cdot \Delta T_{HP} + c_{15} \cdot cp \cdot \Delta \dot{m}_{HP} \\ & + c_{16} \cdot cp \cdot \Delta \dot{m}_{TABS} + c_{17} \cdot cp \cdot \Delta T_h \end{aligned} \quad (18)$$

Discharging: $0 \leq \dot{m}_{TABS}$ and $\delta_{HP} = 0$

$$\Delta \dot{T}_h = \frac{-2k}{r\rho \cdot cp} \Delta T_h$$

$$\Delta T_{TABS,s} = \Delta T_h$$

$$\Delta \dot{Q}_{TABS} = c_{18} \cdot cp \cdot \Delta T_h + c_{19} \cdot cp \cdot \Delta \dot{m}_{TABS} \quad (19)$$

Summarized, the system manipulated Δ -variables, the state Δ -variables, and the system output Δ -variables are given by:

$$\Delta u = [\Delta T_{HP}, \Delta \dot{m}_{HP}, \Delta \dot{m}_{TABS}, \Delta T_{FC}, \Delta \dot{m}_{FC}]^T,$$

$$\Delta x = [\Delta z_h, \Delta T_h]^T,$$

$$\Delta y = [\Delta \dot{Q}_{TABS}, \Delta T_{TABS,s}, \Delta \dot{Q}_{FC}]^T. \quad (20)$$

3.3. Piecewise affine (PWA) model

The MI-MPC requires a model formulation in a linear state space form. Therefore, the overall hybrid system introduced in Sections 3.1 and 3.2 is transformed into a piecewise affine (PWA) model. As motivated in Section 3 the hybrid system consists of two continuous states, $X = X_c = \{z_h, T_h\} \in \mathbb{R}^2$, five continuous manipulated variables, $U_c = \{T_{HP}, \dot{m}_{HP}, \dot{m}_{TABS}, T_{FC}, \dot{m}_{FC}\} \in \mathbb{R}^5$, one discrete input $U_d = \delta_{HP}$ with $U = \begin{Bmatrix} U_c \\ U_d \end{Bmatrix} \in \mathbb{R}^5 \times \{0, 1\}$ and three

continuous outputs, $Y = Y_c = \{\dot{Q}_{TABS}, T_{TABS,s}, \dot{Q}_{FC}\} \in \mathbb{R}^3$.

The auxiliary logical variables $\delta_m(t) \in \{0, 1\}, \forall m = 1, \dots, 3$ are introduced to denote the operation mode of the stratified storage tank. As the system can only be in one mode at each time they are satisfying

$$\sum_{m=1}^3 \delta_m(t) = 1 \quad (21)$$

as an additional constraint. In the following, the overall discrete-time PWA system is considered, which is derived from (2), (17)–(19) with a sampling time of $t_s = 1$ h:

$$\begin{aligned} x(t+1) = & \begin{cases} A_1 x(t) + B_1 u(t), & \text{if } \delta_1(t) = 1 \\ A_2 x(t) + B_2 u(t), & \text{if } \delta_2(t) = 1 \\ A_3 x(t) + B_3 u(t), & \text{if } \delta_3(t) = 1, \end{cases} \\ y(t) = & \begin{cases} C_1 x(t) + D_1 u(t), & \text{if } \delta_1(t) = 1 \\ C_2 x(t) + D_2 u(t), & \text{if } \delta_2(t) = 1 \\ C_3 x(t) + D_3 u(t), & \text{if } \delta_3(t) = 1, \end{cases} \end{aligned} \quad (22)$$

where the matrices $A_m \in \mathbb{R}^{2 \times 2}$, $B_m \in \mathbb{R}^{2 \times 5}$, $C_m \in \mathbb{R}^{3 \times 2}$ and $D_m \in \mathbb{R}^{3 \times 5}$ are given in the Appendix. The auxiliary variables δ_m for $m = 1, 2, 3$ can be expressed by:

$$\begin{aligned} \delta_1(t) &= \delta_{\text{charge}}(t) \delta_{HP}(t) \\ \delta_2(t) &= (1 - \delta_{\text{charge}}(t)) \delta_{HP}(t) \\ \delta_3(t) &= (1 - \delta_{\text{charge}}(t)) (1 - \delta_{HP}(t)), \end{aligned} \quad (23)$$

with

$$\delta_{\text{charge}} = \begin{cases} 1 & \text{if } \dot{m}_{HP} - \dot{m}_{TABS} > 0 \\ 0 & \text{if } \dot{m}_{HP} - \dot{m}_{TABS} \leq 0. \end{cases}$$

The non-linear model (22) and the logical expressions in (23) can be transformed to a set of mixed integer linear inequalities as presented in [9].

4. Mixed-integer MPC formulation

The MI-MPC formulation consists of its objective function and a set of constraints. In this section both parts are motivated and formally described. The objective of the MI-MPC is to minimize both the deviation to the head load prediction from the HiLe and the costs while respecting constraints on control inputs, states and minimum on/off times of the heat pump. The optimization procedure is carried out as a moving horizon control strategy [18], at time t an optimal solution for the manipulated variables $U^* = \{u_{t|t}^*, \dots, u_{t+Np-1|t}^*\}$ is calculated for the complete horizon. Only the first element $u_{t|t}^*$ is actually applied to the plant (22), then the optimization problem is repeated at time $t+1$ with the updated states x_{t+1} .

4.1. Objective function

For the LoLe optimization problem, minimum deviation to the head load prediction from the HiLe, the minimum costs, and sustainable management of the stratified tank are relevant.

Note that each Δ -variable in (24) denotes the respective deviation from the fixed operating point: $v = v^0 + \Delta v$. The corresponding Δ -vectors used are given in (20). The MI-MPC optimization function is formulated over the prediction horizon Np as follows:

$$J^* = \min_{\Delta u \in U} \sum_{k=0}^{Np-1} [(1-\alpha) \cdot (|Q(\Delta y_{\text{ref}}(t+k) - \Delta y_{\text{act}}(t+k))| + |S(\Delta x_{\text{ref}} - \Delta x_{\text{act}}(t+k))|) + \alpha \cdot (R(t+k)(\Delta u(t+k) + u^0) + |T(\Delta u(t+k) - \Delta u(t+k-1))|)], \quad (24)$$

where Δy_{ref} denotes the shifted reference output vector and Δx_{ref} the shifted reference state vector. The objective function (24) consists of four additive terms covering the four objectives. The first addresses the three continuous outputs, whereas the second term refers to the continuous states of the stratified storage tank. The third covers the costs occurring due to the manipulated variables and the fourth is limiting the change in control increments. Each of these terms is penalized individually. The weights on the output deviation to the reference heat load Q , the weights on the state deviation S and the weights on control increments T are time-invariant. The weight on control inputs $R(t+k)$ depends on the fluctuating, possibly predicted energy prices and is therefore time-variant. Since the linearized model is formulated in Δ -values (see (2), (17)–(19)), all variables in the objective function (24) are deviations to the operating point, e.g. $\Delta u_{\text{act}} = u_{\text{act}} - u^0$. However, in order to penalize the absolute costs, in the third term the manipulated variables $\Delta u(t+k)$ are re-shifted by their operating points u^0 .

Apart from the primary weights Q, S, T and $R(t+k)$, $\alpha \in \{0, 1\}$ is an additional weight of the minimization criterion, which allows a global balance between performance and cost variables, respectively.

4.2. Constraints

The MI-MPC has to cope with several types of constraints, for the overall optimization problem defined in Section 4.3. Firstly, constraints on operation and capacities for control inputs and states:

$$x_{i,\min} \leq x_i \leq x_{i,\max}, \quad (25a)$$

$$u_{i,\min} \leq u_i \leq u_{i,\max}. \quad (25b)$$

As the heat pump is a switching aggregate operating either between 30% and 70% of its nominal power or at zero level if it is switched off, the constraint set for \dot{m}_{HP} is disconnected. Therefore, the corresponding constraint (25b) is modified:

$$\dot{m}_{\text{HP},\min} \delta_{\text{HP}} \leq \dot{m}_{\text{HP}} \leq \dot{m}_{\text{HP},\max} \delta_{\text{HP}}. \quad (26)$$

Constraints for minimum on/off times in each sampling time $t+k$ for which the heat pump has to be kept on/off can be expressed by the following mixed integer linear inequalities, as demonstrated in [13]:

$$\delta_{\text{HP}}(t+k) - \delta_{\text{HP}}(t+k-1) \leq \delta_{\text{HP}}(\omega_{\text{up}}), \quad (27a)$$

$$\delta_{\text{HP}}(t+k-1) - \delta_{\text{HP}}(t+k) \leq 1 - \delta_{\text{HP}}(\omega_{\text{down}}), \quad (27b)$$

with $\omega_{\text{up}} = t+k, t+k+1, \dots, \min(t+Np, t+k+T_{\text{HP}}^{\text{up}}-1)$ and $\omega_{\text{down}} = t+k, t+k+1, \dots, \min(t+Np, t+k+T_{\text{HP}}^{\text{down}}-1)$.

4.3. MPC optimization target by MILP

According to the predictive control theory with moving horizon strategy, [18], the MPC is solving an MILP at each time step $t+k$, given initial storage states z_h and T_h and a prediction horizon Np , but only the first sample of the input sequence is implemented. The MPC solves an optimal finite-horizon control problem given in (24).

subject to

- The PWA model (21) and (22) in terms of linear inequalities,
- the input and state constraints on operation and capacity (25) and (26) with (30),
- the constraints for minimum on- and off times (27).

The controller for the comparison analysis is set up with the same structure, substituting the discrete manipulative variable δ_{HP} by the predefined operation mode profile.

5. Simulation results

In this Section the simulation results for the comparison of the MI-MPC and the MPC with fixed operation mode profile are given. Therefore the comparison metrics will be defined. For this analysis, the volume of the stratified tank v_h is varied in the simulation, see Section 5.3. Hence, its maximum ranges from 30 m³ to 50 m³. In a second analysis, the robustness of the MI-MPC with respect to uncertain heat load predictions and depending on the length of the prediction horizon is shown in Section 5.4 based on an approximated Pareto front.

5.1. Comparison metrics

The mean error (ME) is a critical value as the LoLe MI-MPC has to provide the energy demanded by the HiLe. The costs are caused by the electric costs to generate the mass flow rates and temperatures and by the penalties on control increments:

$$\text{ME} = \frac{1}{Np} \sum_{i=1}^{Np} (|Q(y_{\text{ref}}(i) - y_{\text{act}}(i))| + |S(x_{\text{ref}} - x_{\text{act}}(i))|), \quad (28)$$

$$\text{costs} = \sum_{i=1}^{Np} (R(i)(u(i) + u_o) + |T(u(i) - u(i-1))|). \quad (29)$$

For the comparison analysis of the two controllers the coefficient of performance (COP) of the TABS system is additionally defined as the

ratio of the thermally generated energy $E_{t.g.}$ (for the usage in the building) and the amount of electrical energy consumed $E_{e.c.}$ by the energy supply systems, [10]:

$$COP = E_{t.g.} / E_{e.c.},$$

with

$$E_{t.g.} = \sum_{i=0}^{Np-1} \dot{m}_{TABS}^i \cdot (T_{TABS,s}^i - T_{TABS,r}) \cdot \Delta t,$$

$$E_{e.c.} = \sum_{i=0}^{Np-1} k_1 \cdot \dot{m}_{HP}^i + k_2 \cdot \dot{m}_{TABS,s}^i + \frac{\dot{m}_{HP}^i \cdot (T_{HP,s}^i - T_{c,s}) \cdot cp}{COP_{HP}}.$$

The COP_{HP} is approximated by a linear equation, as discussed in [19]:

$$COP_{HP} = c_0 + c_1 \cdot T_{c,s} + c_2 \cdot T_{h,s}$$

with $c_0 = 5.593$, $c_1 = 0.0569 \text{ K}^{-1}$ and $c_2 = -0.0661 \text{ K}^{-1}$ constant. $T_{h,s}$ denotes the temperature of the heat pump on the hot side which is $T_{HP,s}^0 = 35$, and the cold supply to the heat pump $T_{c,s}$ is assumed to be constant with 16°C as the water is taken from the geothermal pipes. The comparison of the ME, the costs, and the COP for the two different control strategies is shown in SubSection 5.3.

5.2. Simulation setup

The MI-MPC is implemented in the Matlab framework using Yalmip, [20]. For the MILP task the Gurobi solver, [21], was added. The hybrid system is formulated as a PWA system. The MPC for comparison analysis is run with the same Yalmip implementation exchanging the discrete manipulated variable δ_{HP} with the a priori fixed storage tank operation mode profile.

The University of Salzburg, representing the demonstration building, contains the energy heat supply circuits such as shown in Fig. 2.

The only important coupling point between the HiLe and the LoLe is the heat demand of the HiLe and the effectively realized amount of energy provided by the LoLe, as depicted in Fig. 1. The corresponding picture of the building shows the modern 27.000 m² building in the center of Salzburg, Austria. It has five floors above ground containing several large and numerous smaller meeting rooms, offices and lecture rooms. There are six atrium within the modern building complex. For this study, the second and third floor of the building is considered, comprised of about 500 rooms, almost all used as offices, and about 13.000 m². The corresponding characteristics of the heat supply circuit as admissible ranges, see (30), for pumps and the heat pump are derived from the characteristic curves and technical data sheets. The operation constraints and admissible ranges for this work are therefore given by:

$$\begin{aligned} T_{HP} &\in [20, 60][^\circ\text{C}] \\ \dot{m}_{HP} &\in \{0\} \cup [6, 15][\text{kg/s}] \\ \dot{m}_{TABS} &\in [6, 15][\text{kg/s}] \\ T_{FC} &\in [20, 70][^\circ\text{C}] \\ \dot{m}_{FC} &\in [7, 18][\text{kg/s}] \\ T_h &\in [0, 60][^\circ\text{C}] \\ z_h &\in [0.1, 2][\text{m}]. \end{aligned} \quad (30)$$

The operating points are chosen as given in Table 3 for linearizing the non-linear models:

Table 3
Operating points of input and state variables.

Variables	Operating point	Unit
z_h^0	1	[m]
T_h^0	30	[°C]
T_{HP}^0	35	[°C]
\dot{m}_{HP}^0	9	[kg/s]
\dot{m}_{TABS}^0	7	[kg/s]
T_{FC}^0	70	[°C]
\dot{m}_{FC}^0	12	[kg/s]

The radius of the stratified storage tank r is varied from 2.03 m to 2.8 m in order to study the effects on an increase in volume v_h . The coefficient of thermal conductivity k amounts $0.01 \text{ W/m}^2 \cdot ^\circ\text{C}$ and the ambient temperature in the basement, T_{amb} , is assumed to be constant with 20°C . The minimum on/off-times for the heat pump for this work are given by $T_{HP}^{up} = T_{HP}^{down} = 1 \text{ h}$.

The energy costs used for the simulation runs are given in Table 4. The assumption comprises a low night rate and a high day rate in the morning for electric energy. In the afternoon, the costs change every two hours between the low night and the high day tariff. The costs for the district heat are assumed to be constant.

The prediction horizon is 24 h, and the simulation is presented for three days, the sampling time is one hour. The desired energy from the HiLe for the TABS as well as for the FC system, \dot{Q}_i^{ef} , is a snapshot of historic data from the demonstration building. This output reference is firstly interpreted deterministically. In a further simulation study, robustness is shown. The desired heat demand trajectory is overlaid by a low pass filtered sinus as a bias and a random white noise in order to simulate error of the heat load prediction from the HiLe.

5.3. Analysis of simulation results

For the comparison analysis, the weighting parameter α is kept constant with 0.1 and the initial states $v_h(0)$ and $T_h(0)$ are chosen at their operating points, such that the stratified storage tank is half full with hot water. The stratified storage tank is assumed to have a volume of 30 m³ for the first comparison analysis. Figs. 4 and 5 show the simulation results of the MI-MPC and the MPC with fixed operation mode profile, respectively. The first subplots (a) show the output and the reference trajectories for both circuits. In subplot (b) one can see the manipulated temperatures from the heat pump, the district heat and the temperature of the hot water in the stratified storage tank. The third subplot (c) depicts the manipulated mass flows to and from the tank to the building for the TABS system as well as the mass flow to the fan coil system, whereas subplot (d) shows the trajectories of the states v_h and T_h . The last subplot (e) in Fig. 4 shows the decision on δ_{HP} , whereas in Fig. 5 the corresponding line represents the fixed operating mode

Table 4
Energy costs [€/kW h].

Time slots	Electric energy	District heat
08:00–12:00	€0.12	€0.09
12:00–14:00	€0.06	€0.09
14:00–16:00	€0.12	€0.09
16:00–18:00	€0.06	€0.09
18:00–20:00	€0.12	€0.09
20:00–08:00	€0.06	€0.09

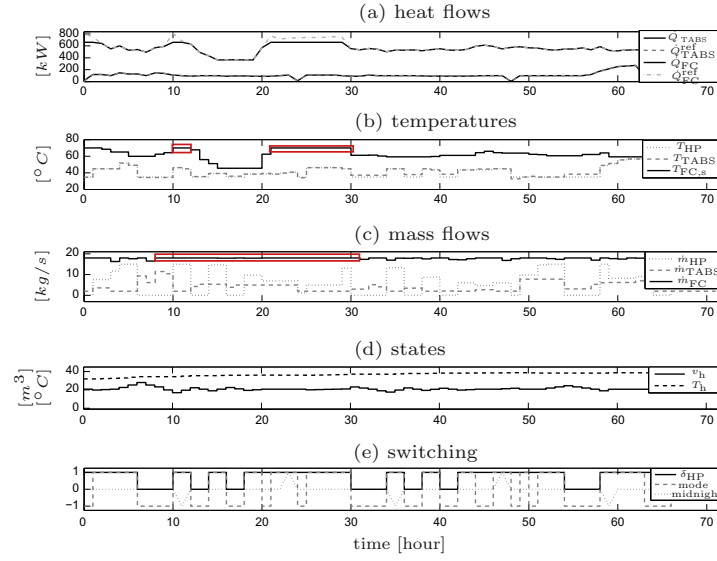


Fig. 4. MI-MPC with optimized operation mode. Bold rectangles mark sections where manipulated variables are limited by constraints and control errors result. (For interpretation of the references to colour in this figure legend, the reader is referred to the web version of this article.)

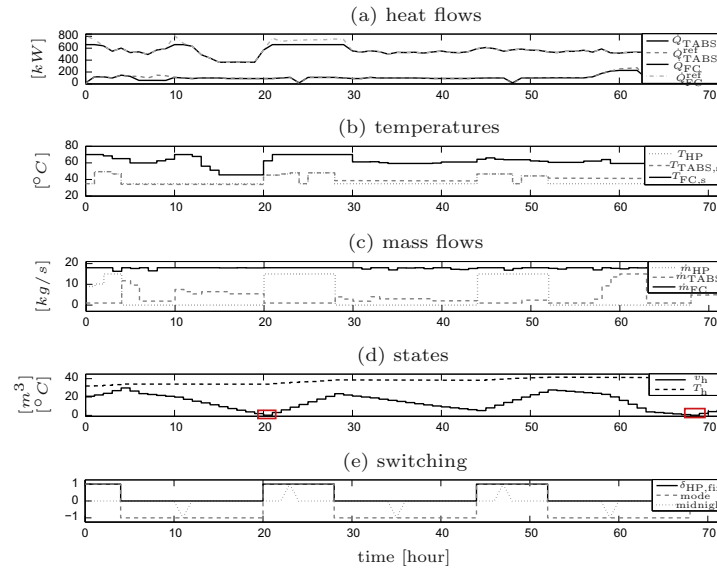


Fig. 5. MPC with fixed operation mode profile. Bold rectangles mark sections where the output of hot water volume in the tank remains in its lower constraint. (For interpretation of the references to colour in this figure legend, the reader is referred to the web version of this article.)

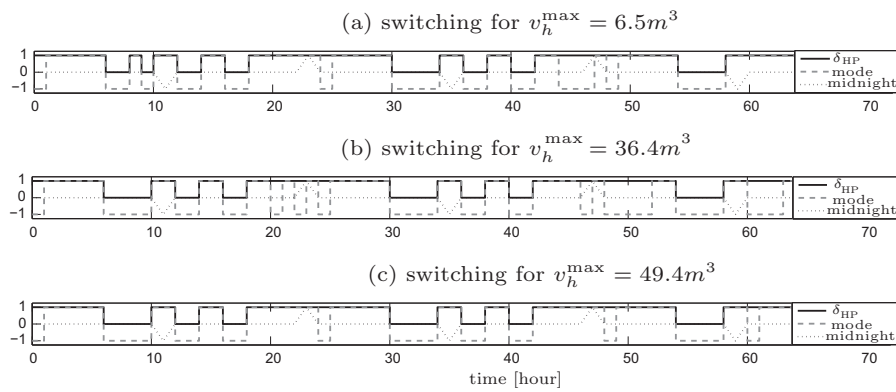
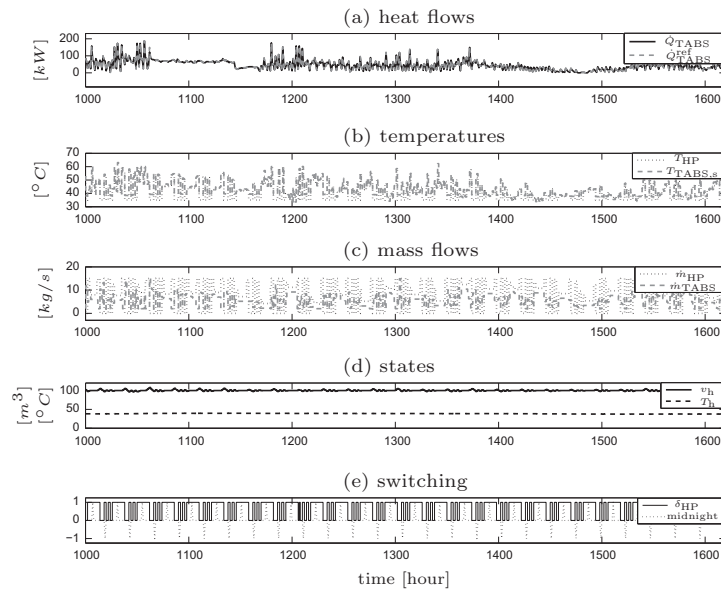
profile. It should be noted, that both controllers are not able to provide the heat load demanded for the FC at all times, because both manipulated variables \dot{m}_{FC} and $T_{FC,s}$ are at their upper bounds and the saturation level is reached, see Figs. 4 and 5 at simulation time 10–12 h and 22–30 h, respectively. In Fig. 5 (d) the volume reaches the lower constraint at the end of the first and third discharging period, whereas the MI-MPC is able to operate the stratified storage tank more efficiently. The actual storage tank volume used by the two controllers differs considerably. The MI-MPC uses an actual volume of 11.22 m³ for its optimal management strategy,

whereas the MPC with fixed operation mode profile needs an actual volume of 27.22 m³.

The comparison according to the metrics introduced in Section 5.1 is given in Table 5. For this analysis the radius of the stratified storage tank r is increased from 2.03 m to 2.8 m, so that the maximum volume is increased from 26 m³ up to 49.4 m³. The simulation results show that for a stratified storage tank volume below 32.5 m³ there is no feasible solution for the MPC with fixed operation mode profile, as long as the stratified storage tank is supposed to be half full with hot water at the start of the simulation.

Table 5Performance comparison for different levels of the storage tank volume v_h^{\max} .

Metrics	$v_h^{\max} = 26 \text{ m}^3$		$v_h^{\max} = 36.4 \text{ m}^3$		$v_h^{\max} = 49.4 \text{ m}^3$	
	MI-MPC	MPC	MI-MPC	MPC	MI-MPC	MPC
ME	60.93	–	55.64	82.71	55.78	84.95
Costs [10^4]	0.01	–	2.90	2.88	2.90	2.88
Costs on elec. energy [€]	611.36	–	598.41	413.99	640.27	414.46
Energy therm. gen. [10^4 kWh]	3.95	–	3.76	3.28	3.98	3.29
Energy elec. cons. [10^3 kWh]	8.53	–	7.81	6.90	8.36	6.91
COP	4.63	–	4.81	4.75	4.76	4.76
Volume spread [m^3]	24.57	–	14.2	33.72	16.03	46.72

**Fig. 6.** Comparison of operation mode profile for MI-MPC and different storage tank volume levels.**Fig. 7.** MI-MPC with optimized operation mode.

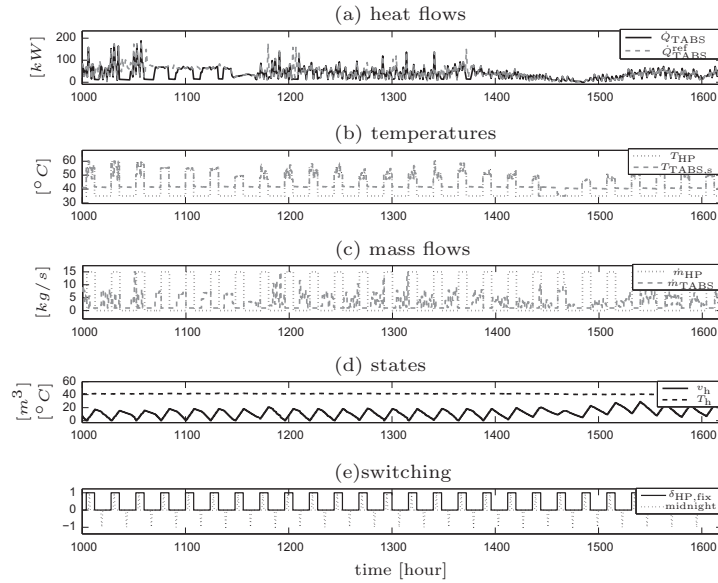


Fig. 8. MPC with fixed operation mode profile.

For a stratified storage tank full with hot water, the minimum volume for achieving a feasible solution is 20.8 m³. The MI-MPC yields better results in terms of the mean error which is an essential requirement with regard to the user comfort because the HiLe-MPC already makes use of the temperature tolerance band at minimal energy demand. Therefore, deviations to the requested energy amount result most likely in a user comfort band violation.

Variation of the stratified storage tank volume results in two major outcomes: Firstly, only the MI-MPC achieves feasible solutions for small tank volumes and secondly, the change in the strategy for the stratified storage tank management differs for small to middle size in different decisions for δ_{HP} , whereas for middle to big volume only the decision for the operation mode changes, see Fig. 6(a)–(c).

Figs. 7 and 8 show a cutout of a simulation for the heating period from December 2013 until March 2014 for the TABS system. The heat demand has characteristics from strongly variant to almost stationary, so that the difference of the controllers' strategies becomes apparent. The controller with the fixed operation mode profile runs a cyclically recurring strategy, which is successful in terms of ME if the reference trajectory is quite stationary. When the heat demand becomes higher in frequency the MI-MPC benefits from its flexibility in

operation. The difference of the controllers strategies lie as well in the management of the storage tank as well as in the usage of different temperature levels. Important to mention is, that with the given set of constraints for operation and capacities for control inputs, the MPC with the fixed operation mode profile only yields feasible optimization results for very large storage tanks, whereas the MI-MPC is implementable also for small sizes. Table 6 show the results for the whole period regarding the comparison metrics. The effects on the gap between the ME as well as the costs and the volume spread of the short run analysis are intensified over the long period, meaning that the more weight is put on the comfort the more beneficial is the implementation of the MI-MPC.

5.4. Robustness analysis

In order to prove robustness of the MI-MPC with respect to disturbances of the heat load prediction (which has been assumed deterministic in the optimization problem in Section 4.3), some unknown bias and random noise is added to the deterministic heat load prediction. The closed-loop performance is then evaluated for different levels of this stochastic disturbance.

For the robustness analysis an approximated Pareto front is computed for a fixed set of weights $Q, R(t+k), S, T$, as introduced in Section 4.1 and varying α between [0, 1]. Fig. 9(a)–(d) shows the approximated Pareto fronts and the convex hulls for different lengths of N_p . For all simulation runs a stratified storage tank volume of 39 m³ is chosen.

Since the MI-MPC optimization problem is generally non-convex, [22], the approximation of the Pareto front is not necessarily convex either. Furthermore, this approximated Pareto front is only one among a family of curves, each corresponding to a certain set of fixed weights, nevertheless not yielding the effective Pareto front. Identifying the global Pareto front is a global optimization problem; its solution would be available by e.g. executing a genetic algorithm to find the optimal set of weights. Initially a set of randomly chosen genomes would have to be evaluated according to

Table 6
Performance comparison for long term simulation for $v_h^{\max} = 260$ m³.

Metrics	MI-MPC	MPC
ME	18.37	59.95
Costs [10 ⁴]	116.56	115.79
Costs on elec. energy [10 ⁴ €]	3.05	1.97
Energy therm. gen. [10 ⁴ kWh]	190.41	162.90
Energy elec. cons. [10 ³ kWh]	406.56	328.39
COP	4.69	4.96
Volume spread [m ³]	11.89	106.68

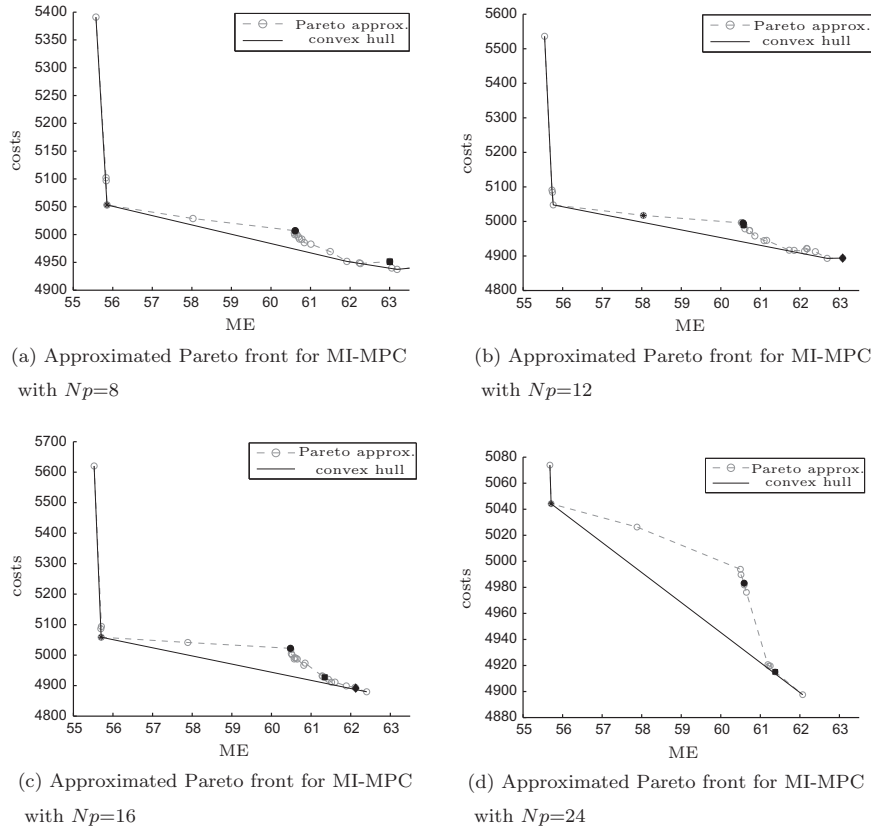


Fig. 9. Approximated Pareto fronts for $Np = 8$, $Np = 12$, $Np = 16$ and $Np = 24$.

their fitness, i.e. their contribution to the optimal Pareto front. In an iterative process, the successive ones would have to be modified and again evaluated in order to achieve the best combination of weights.

Secondly, the deterministic output reference $y_{\text{ref}}^{\text{det}}$ is overlaid with a fixed bias over the entire simulation period and a randomly generated white noise in order to get a disturbed reference trajectory $y_{\text{ref}}^{\text{dist}}$. The bias is given by the sine of the low pass filtered reference trajectory $y_{\text{ref}}^{\text{lpf}}$, while the white noise is randomly generated offline for each step over the prediction horizon Np with an amplitude of one tenth of the standard deviation σ of the deterministic standard trajectory $y_{\text{ref}}^{\text{det}}$:

$$y_{\text{ref}}^{\text{dist}}(t+k) = y_{\text{ref}}^{\text{det}}(t+k) + \lambda \cdot \sin(y_{\text{ref}}^{\text{lpf}}(t+k)) + \sigma/10 \cdot \zeta(t+k), \quad (31)$$

where ζ is a random number $\in [0, 1]$. In order to show the MI-MPCs robustness, the deterministic reference trajectory is substituted by the disturbed one $y_{\text{ref}}^{\text{dist}}$. The amplitude of the sinus is successively increased in each simulation run by increasing the parameter λ from 1 to 8 at four given levels of α . Fig. 10(a)–(d) shows the results compared to the ones without bias and noise. The symbols, stars, circles, squares and diamonds represent the results for the same level of α . For low α the distances from the disturbed results to the optimal ones on the approximated Pareto front regarding both axes are less than the distances for higher α . In Fig. 10(a)–(c) the results for higher α are widely scattered.

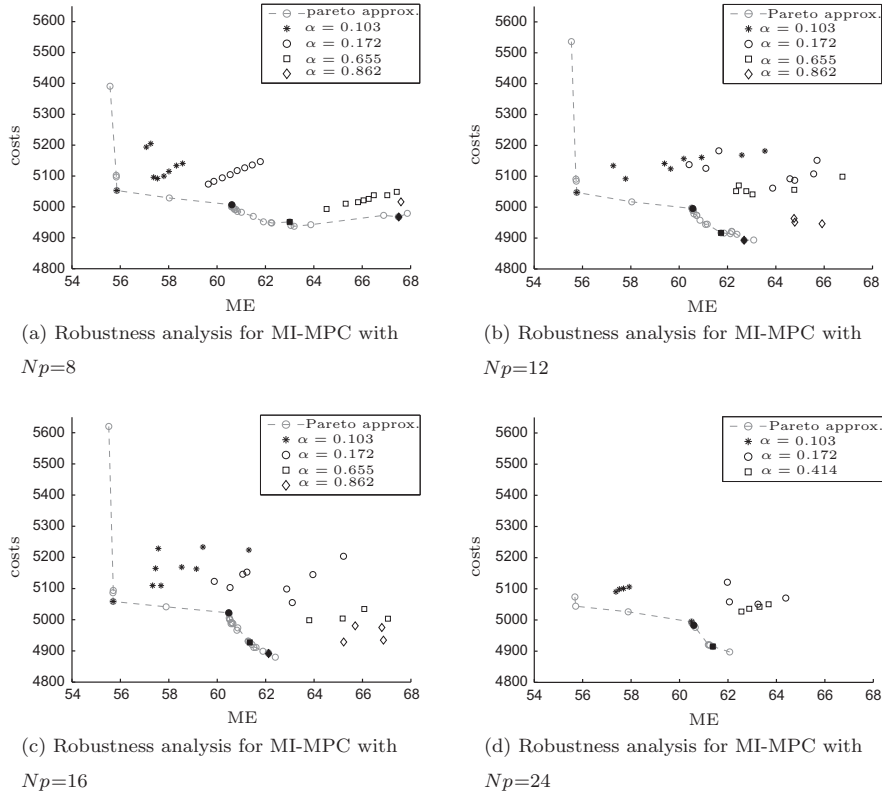
The utilized robustness measure τ is the mean sum of the weighted distances to the corresponding optimal result on the

approximated Pareto front in terms of ME and costs. It allows the direct comparison of the results for different prediction horizons Np . τ_i is given by:

$$\tau_i = \frac{1}{N} \sum_{j=1}^N \sqrt{(1 - \alpha_i) \cdot (\text{ME}_{ij}^{\text{dist}} - \text{ME}_i^{\text{det}})^2 + \alpha_i \cdot (\text{costs}_{ij}^{\text{dist}} - \text{costs}_i^{\text{det}})^2}. \quad (32)$$

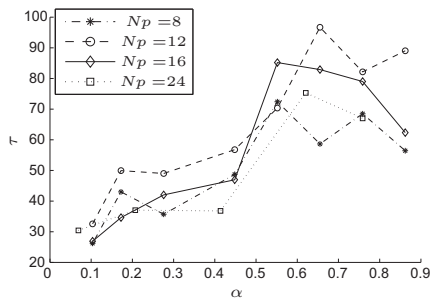
Fig. 11 shows the results for τ for the four different prediction horizons as in Figs. 9 and 10. As the robustness analysis is done for $\lambda \in \{1, 2, \dots, 8\}$ eight results with increasing white noise are compared to the optimal result. According to the definition of τ in Eq. (32), the MI-MPC becomes the more robust the smaller τ is. It is shown that for a large prediction horizon the MI-MPC shows less distance to the corresponding optimal result on the approximated Pareto front than for smaller prediction horizons. However, if the weighting parameter α is in the interval from 0.1 to 0.45 the MI-MPC is robust even for smaller horizons. If one considers also the absolute costs and the ME as demonstrated in Fig. 10, an α of around 0.1 can be recommended for the given application.

The results considering the system's COP are given in Table 7 in terms of mean value and standard deviation. The two statistical parameters are calculated over the 8 different values of λ at each level of α and different prediction horizons. The highest COP mean value is reached for $\alpha = 0.172$ for all prediction horizons. The system's COP standard deviation is small throughout all simulation runs, although with the variation of λ up to 8 very high disturbance is caused.

Fig. 10. Robustness analysis for $N_p = 8$, $N_p = 12$, $N_p = 16$ and $N_p = 24$.Table 7
COP statistics for robustness analysis.

N_p	Metrics	$\alpha_1 = 0.103$	$\alpha_2 = 0.172$	$\alpha_3 = 0.655$	$\alpha_4 = 0.862$
8	Mean value	4.8377	4.8422	4.7491	4.7492
	Standard deviation	0.0306	0.0111	0.0220	0.0245
12	Mean value	4.7783	4.8222	4.7530	4.7623
	Standard deviation	0.0271	0.0285	0.0410	0.0392
16	Mean value	4.7378	4.7635	4.7003	4.6376
	Standard deviation	0.0192	0.0238	0.0275	0.0450
24	Mean value	$\alpha_1 = 0.103$ 4.7328	$\alpha_2 = 0.172$ 4.7356	$\alpha_3 = 0.414$ 4.6931	
	Standard deviation	0.0365	0.0159	0.0075	

COP statistics for robustness analysis at different levels of the weighting parameter α .

Fig. 11. Robustness metrics for MI-MPC with $N_p = 8$, $N_p = 12$, $N_p = 16$, $N_p = 24$.

6. Conclusion

In this paper a mixed-integer MPC (MI-MPC) has been presented for building heating management with a stratified storage tank. In contrast to other studies in this field, this approach covers the unit commitment problem with switching aggregate, as well as taking their minimum up- and down times into account. The considered stratified storage tank operates in three operation modes, depending on the state of the heat pump. Therefore, the resulting hybrid PWA model, based on first order differential equations, includes discrete and continuous manipulated variables. A validation of the model is currently not possible due to a lack of measurements on the stratified storage tank in the demonstration building. However, for future work the implementation of an appropriate observer is planned in order to substitute the missing plant data. The control strategies are shown in comparison to MPC formulations with a fixed operation tank profile. The simulation results are evaluated according to the mean error, the costs and the system's COP value depending on the volume of the stratified tank. One can see that for small tanks, the MPC with an a priori operation mode profile runs into an infeasible problem, whereas the MI-MPC delivers optimal solutions. Additionally, a robustness analysis has been performed and the approximated Pareto front of the MILP given. For this analysis the originally deterministic heat load reference trajectory has been disturbed. The considered parameter of this analysis was α , putting more emphasis either on the ME or on the costs. Simulation studies with larger prediction horizons have proved beneficial. However, for small $\alpha = 0.1$ robustness is achieved even for small N_p yielding less computational burden than for larger prediction horizons.

7. Acknowledgement

This work was supported by the project “SMART MSR” (FFG, No. 832103) in cooperation with evon GmbH.

Appendix A

The coefficients for the linear system models in (2), (17)–(19) in Sections 3.1 and 3.2 are given in Table A.8.

For the time-continuous linear PWA model (22), the system matrices are derived from the linearized physical first order model, (2), (17)–(19) in SubSections 3.1 and 3.2 where the coefficients in Table A.8 give the matrix entries.

$$A_{1,c} = \begin{pmatrix} 0 & 0 \\ c_6 & c_7 \end{pmatrix}$$

$$B_{1,c} = \begin{pmatrix} 0 & \frac{1}{r^2 \pi \rho} & -\frac{1}{r^2 \pi \rho} & 0 & 0 \\ c_3 & c_4 & c_5 & 0 & 0 \end{pmatrix}$$

$$C_{1,c} =$$

$$D_{1,c} = \begin{pmatrix} c_8 \cdot cp & 0 & c_9 \cdot cp & 0 & 0 \\ 1 & 0 & 0 & 0 & 0 \\ 0 & 0 & 0 & c_1 \cdot cp & c_2 \cdot cp \end{pmatrix}$$

$$A_{2,c} = \begin{pmatrix} 0 & 0 \\ 0 & \frac{-2k}{r \rho \cdot cp} \end{pmatrix}$$

$$B_{2,c} = \begin{pmatrix} 0 & \frac{1}{r^2 \pi \rho} & -\frac{1}{r^2 \pi \rho} & 0 & 0 \\ 0 & 0 & 0 & 0 & 0 \end{pmatrix}$$

$$C_{2,c} = \begin{pmatrix} 0 & c_{17} \cdot cp \\ 0 & c_{13} \\ 0 & 0 \end{pmatrix}$$

$$D_{2,c} = \begin{pmatrix} c_{14} \cdot cp & c_{15} \cdot cp & c_{16} \cdot cp & 0 & 0 \\ c_{10} & c_{11} & c_{12} & 0 & 0 \\ 0 & 0 & 0 & c_1 \cdot cp & c_2 \cdot cp \end{pmatrix}$$

$$A_{3,c} = \begin{pmatrix} 0 & 0 \\ 0 & \frac{-2k}{r \rho \cdot cp} \end{pmatrix}$$

$$B_{3,c} = \begin{pmatrix} 0 & \frac{1}{r^2 \pi \rho} & -\frac{1}{r^2 \pi \rho} & 0 & 0 \\ 0 & 0 & 0 & 0 & 0 \end{pmatrix}$$

$$C_{3,c} = \begin{pmatrix} 0 & c_{18} \cdot cp \\ 0 & 1 \\ 0 & 0 \end{pmatrix}$$

$$D_{3,c} = \begin{pmatrix} 0 & 0 & c_{19} \cdot cp & 0 & 0 \\ 0 & 0 & 0 & 0 & 0 \\ 0 & 0 & 0 & c_1 \cdot cp & c_2 \cdot cp \end{pmatrix}$$

The matrices for the time-discrete system are derived by Laplace transformation for $t_s = 1$:

Table A.8

Coefficients of linearized system model.

c_1	$\dot{m}_{FC} _0$
c_2	$(T_{FC,s} - T_{FC,r}) _0$
c_3	$(\dot{m}_{HP} - \dot{m}_{TABS})/(z_h \cdot r^2 \pi) _0$
c_4	$(T_{HP} - T_h)/(z_h \cdot r^2 \pi) _0$
c_5	$(T_h - T_{HP})/(z_h \cdot r^2 \pi) _0$
c_6	$((\dot{m}_{TABS} - \dot{m}_{HP})(T_{HP} - T_h) \cdot r^2 \pi)/(z_h \cdot r^2 \pi)^2 _0$
c_7	$((\dot{m}_{TABS} - \dot{m}_{HP})/(z_h \cdot r^2 \pi) - (2r \pi \cdot k)/(r^2 \pi \cdot cp)) _0$
c_8	$\dot{m}_{TABS} _0$
c_9	$(T_{HP} - T_{TABS,r}) _0$
c_{10}	$\dot{m}_{HP}/\dot{m}_{TABS} _0$
c_{11}	$(T_{HP} - T_h)/\dot{m}_{TABS} _0$
c_{12}	$((T_h - T_{HP}) \cdot \dot{m}_{HP})/\dot{m}_{TABS} _0$
c_{13}	$((\dot{m}_{TABS} - \dot{m}_{HP}) \cdot T_h)/\dot{m}_{TABS} _0$
c_{14}	$\dot{m}_{HP} _0$
c_{15}	$(T_{HP} - T_h) _0$
c_{16}	$(T_h - T_{TABS,r}) _0$
c_{17}	$(\dot{m}_{TABS} - \dot{m}_{HP}) _0$
c_{18}	$\dot{m}_{TABS} _0$
c_{19}	$(T_h - T_{TABS,r}) _0$

$$A_i = e^{A_{i,c} t_s}, \quad (A.1)$$

$$B_i = \int_0^{t_s} e^{A_{i,c} \zeta} B_{i,c} d\zeta = \Psi B, \quad (A.2)$$

$$\text{with} \quad (A.3)$$

$$\Psi = A_{i,c}^{-1} (e^{A_{i,c} t_s} - I), \quad (A.4)$$

$$C_i = C_{i,c}, \quad (A.5)$$

$$D_i = D_{i,c}. \quad (A.6)$$

References

- [1] I.E. Agency, Energy efficiency policies for new buildings [cited 2015-01-21]. <http://www.iea.org/publications/freepublications/publication/Building_Codes.pdf>.
- [2] Dagdougui H, Minciardi R, Ouammi A, Robba M, Sacile R. Modeling and optimization of a hybrid system for the energy supply of a “green” building. *Energy Convers Manage* 2012;64:351–63.
- [3] Sun Y, Wang S, Xiao F, Gao D. Peak load shifting control using different cold thermal energy storage facilities in commercial buildings: a review. *Energy Convers Manage* 2013;71:101–14.
- [4] Figueiredo J, Martins J. Energy production system management-renewable energy power supply integration with building automation system. *Energy Convers Manage* 2010;51(6):1120–6.
- [5] Prívára S, Vána Z, Cigler J, Oldewurtel F, Komárek J. Role of mpc in building climate control. *Comput Aided Chem Eng* 2011;29:728–32.
- [6] Prívára S, Cigler J, Vána Z, Oldewurtel F, Sagerschnig C, Žáčková E. Building modeling as a crucial part for building predictive control. *Energy Build* 2013;56:8–22.
- [7] Oldewurtel F, Parisio A, Jones CN, Gyalistras D, Gwerder M, Stauch V, et al. Use of model predictive control and weather forecasts for energy efficient building climate control. *Energy Build* 2012;45:15–27.
- [8] Killian M, Mayer B, Kozek M. Hierarchical fuzzy mpc concept for building heating control.
- [9] Bemporad A, Morari M. Control of systems integrating logic, dynamics, and constraints. *Automatica* 1999;35(3):407–27.
- [10] Ma Y, Borrelli F, Hencsey B, Coffey B, Bengesa S, Haves P. Model predictive control for the operation of building cooling systems. *IEEE Trans Control Syst Technol* 2012;20(3):796–803.
- [11] Berkenkamp F, Gwerder M. Hybrid model predictive control of stratified thermal storages in buildings. *Energy Build* 2014;84:233–40.
- [12] Široký J, Oldewurtel F, Cigler J, Prívára S. Experimental analysis of model predictive control for an energy efficient building heating system. *Appl Energy* 2011;88(9):3079–87.
- [13] Parisio A, Rikos E, Glielmo L. A model predictive control approach to microgrid operation optimization. *IEEE Trans Control Syst Technol* 2014;22(5):1813–27.
- [14] Parisio A, Rikos E, Tzamalís G, Glielmo L. Use of model predictive control for experimental microgrid optimization. *Appl Energy* 2014;115:37–46.
- [15] Henze GP, Kalz DE, Felsmann C, Knabe G. Impact of forecasting accuracy on predictive optimal control of active and passive building thermal storage inventory. *HVAC&R Res* 2004;10(2):153–78.
- [16] Mayer B, Killian M, Kozek M. Cooperative and hierarchical fuzzy mpc for building heating control. In: *IEEE international conference on fuzzy systems (FUZZ-IEEE)*, 2014. IEEE; 2014. p. 1054–9.

- [17] Mayer B, Killian M, Kozek M. Modeling workflow for a building model for control purposes. In: 3rd International conference on systems and control (ICSC), 2013. IEEE; 2013. p. 551–6.
- [18] Camacho EF, Alba CB. Model predictive control. Springer Science & Business Media; 2013.
- [19] Vrettos E, Lai K, Oldewurtel F, Andersson G. Predictive control of buildings for demand response with dynamic day-ahead and real-time prices. In: Control conference (ECC), 2013 european. IEEE; 2013. p. 2527–34.
- [20] Lofberg J. Yalmip: a toolbox for modeling and optimization in matlab. In: IEEE international symposium on computer aided control systems design, 2004. IEEE; 2004. p. 284–9.
- [21] Gurobi optimizer reference manual [online] (2014) [cited 2014-11-02].
- [22] Borrelli F, Bemporad A, Morari M. Predictive Control for linear and hybrid systems. Cambridge University Press, In press; 2014 [cited 2014-11-20]. <<http://www.mpc.berkeley.edu/mpc-course-material>>.

2.2 Publication B

Barbara Mayer, Michaela Killian, and Martin Kozek.

A branch and bound approach for building cooling supply control with hybrid model predictive control.

Energy and Buildings, Volume 128, 2016, pages 553-566, ISSN: 0378-7788.

DOI: 10.1016/j.enbuild.2016.07.027

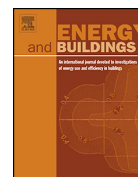
Own Contribution

Problem statement, selection of methods and algorithms for modeling, control design, implementation and simulation, as well as structuring, writing and editing the paper was done by the applicant under the supervision of the third author and mentor. Discussion of methodology and results as well as editing and proof read was done by second author.



Contents lists available at ScienceDirect

Energy and Buildings

journal homepage: www.elsevier.com/locate/enbuild

A branch and bound approach for building cooling supply control with hybrid model predictive control

Barbara Mayer^{a,*}, Michaela Killian^b, Martin Kozek^b^a FH Joanneum, Institute of Industrial Management, Werk-VI-Strasse 46, 8605 Kapfenberg, Austria^b Vienna University of Technology, Institute of Mechanics and Mechatronics, Getreidemarkt 9, 1060 Vienna, Austria

ARTICLE INFO

Article history:

Received 14 January 2016

Received in revised form 8 July 2016

Accepted 12 July 2016

Available online 14 July 2016

Keywords:

Hybrid model predictive control

Branch and bound

Building cooling supply system

Building automation

ABSTRACT

In this article a branch and bound approach for hybrid model predictive control of a building cooling supply is presented. This specific algorithm is the core part of a mixed-integer model predictive controller (MI-MPC) for energy efficient management of a cooling supply incorporating active storage connected to a switching chiller. The MI-MPC is applied to the model of the cooling system of a large office building in Salzburg, Austria. An efficient modelling strategy combines data-driven black-box identification and analytically derived white-box modelling for the purpose of predictive control. The validation of the resulting linear and hybrid energy supply models is done by an open loop simulation. Simulation results of the proposed control structure show excellent performance compared to the implemented conventional control strategy resulting in an increased usage of at least 50% of renewable energy sources, a cut in energy costs of about 50%, and an optimised operation of the active storage while accurately delivering the prescribed cooling power trajectory. The approach is thus promising for industrial application.

© 2016 Elsevier B.V. All rights reserved.

1. Introduction

The building sector is responsible for about 40% of the final energy consumption in the EU since 2004 [1]. It is therefore economically, politically and environmentally important to save energy in buildings. Focus has been put on the building physical structure such as passive heating and cooling systems. However, saving fossil energy additionally requires maximising the usage of renewable energy sources such as free cooling systems, geothermal sourcing or photovoltaic systems. Usually, the amount of energy and the respective availability highly depend on weather conditions and do not coincide with the energy demand of the building. This is why energy storage becomes necessary. Thermal energy storage is either realised as thermally activated building systems (TABS) or by active storage such as stratified water storage tanks. This paper focuses on the control of the cooling supply for two cooling systems, a TABS and a fan coil system (FC) in a large office building supplied by several energy sources. These two cooling systems are supplied by three cooling circuits comprising free cooling, geothermal sources and a chiller with a stratified storage tank.

Conventional building energy management usually relies on proportional–integral–derivative (PID) and rule-based controllers [2]. In contrast, model predictive control (MPC) has been proven as a promising technology for such building systems in recent years [3] with first application results, e.g. [4]. A model predictive control structure with three parallel MPCs, two linear MPCs (LMPC) and one mixed-integer MPC (MI-MPC), is presented for the LoLe. The constrained MPCs' goal is to maximise the usage of renewable energy sources limited by disturbances such as the ambient temperature, to minimise the energy costs while minimising the deviation to the energy demand of the building. The management of the stratified storage tank is an additional task for the corresponding MPC [5]. Fig. 1 gives an overview of the proposed control structure for the supply of the two cooling systems TABS and FC. \dot{Q}_i^{ref} and \dot{Q}_i^{act} denote the reference cooling demand and the actual cooling supply for supply $i \in \{\text{TABS}, \text{FC}\}$. The disturbances ϑ_G , T_{amb} and T_{FCr} are the difference of the supply to the return water temperature for the geothermal source, the ambient temperature and the return water temperature of the FC system.

Switching aggregates such as chillers require additional constraints such as minimum up- and down times. Furthermore, they directly influence the operation of the active storage, such that the optimisation problem contains both discrete and continuous variables. The resulting constrained mixed-integer quadratic problem (MIQP) and the dedicated hybrid model representing the corresponding supply circuit form the elementary parts of the

* Corresponding author. Tel.: +43 386233600 6347.

E-mail addresses: barbara.mayer@fh-joanneum.at (B. Mayer), michaela.killian@tuwien.ac.at (M. Killian), martin.kozek@tuwien.ac.at (M. Kozek).

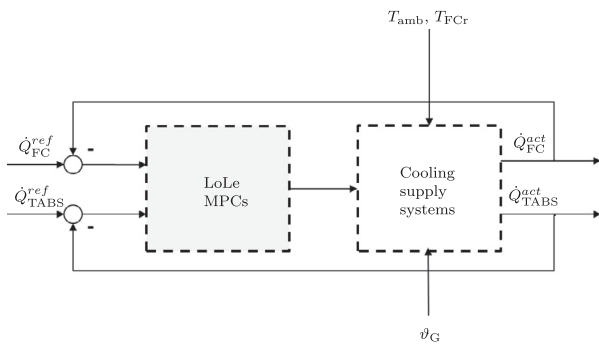


Fig. 1. Simplified control structure for the supply for TABS and FC cooling system.

introduced MI-MPC [6]. In [7] a review of optimisation techniques for active thermal storage is presented including branch and bound as well as metaheuristic methods, respectively.

Predictive control concepts for optimising the energy management in buildings and micro grids have been developed in the last years. [8] has given an overview of the performance of MPC compared to other control approaches for general heating, ventilation, and air conditioning (HVAC) systems, whereas [9] has discussed state-of-the-art control strategies for the integration of thermal storage in buildings. Another approach is to consider the underlying process as hybrid control system which are systems that involve both continuous and discrete dynamics and continuous and discrete controls. The continuous dynamics of such a system is usually modelled by a continuous or discrete-time state space system [10]. [11,5] have presented hybrid system formulations for cooling systems including two different operation modes (charging, discharging) assuming that these two modes are scheduled by an a priori fixed operation plan. In [12] a hierarchical control structure has been presented decomposing slow passive and fast active thermal storage, whereby the discrete variables for the storage's operation mode are substituted by the continuous duration of one mode with a priori fixed successions of operation modes. In [13] a two-stage optimisation algorithm is presented to obtain an optimal scheduling for a building energy management system within a smart grid by solving mixed integer linear programs (MILP). Several model predictive control concepts with mixed integer non-linear program (MINLP) have also been developed for micro grids, e.g. [14], thermal storage connected with buildings within a grid [15] or buildings including the unit commitment problem [6]. Nevertheless, solving a MIQP, which is a special category of MINLP for online control purposes, either means enumerating all possible combinations of integer variables in order to solve individual quadratic problems (QPs) or to utilise complex commercial solvers as used in e.g. [14,6]. However, branch and bound is a method that can solve MIQP more efficiently than a total enumeration without the necessity of commercial solvers.

Branch and bound algorithms have already been proposed for hybrid systems as well as for unit commitment problems. In [16] a branch and bound algorithm is introduced for the control of hybrid systems based on the proposition that firstly binary variables are associated with conditions on continuous states and secondly that switches are rare and a priori known. This behaviour is used for a specific tree exploration strategy where those QPs are solved first where the number of switches is limited. In [17] a suboptimal branch and bound approach is presented for explicit hybrid MPC. For solving unit commitment problems, early papers of [18,19] have shown how to build up the search tree and to define the fathoming and search strategy. Nevertheless, the algorithm of [18] is restricted by the assumption that the units will only switch their mode once



Fig. 2. The building studied – the University in the centre of Salzburg, Austria.

in a 24-h horizon. More recently, [20] has introduced a merged approach of logic programming and the efficient and flexible search technique of branch and bound.

However, none of these approaches has focused on the unit commitment problem with hybrid systems. This paper combines some approaches introduced in [21], within the basic idea of [20]. Firstly, the search space is reduced by applying physically motivated constraints on aggregates and storage, and secondly, the hybrid search tree is efficiently solved by a fathoming and search strategy.

Modelling of building systems is a crucial part for predictive building control [22]. Models for real time predictive controllers should be as simple and yet as accurate as possible. Basically, there exist three fundamental modelling approaches for cooling systems: (i) analytically derived modelling based on thermodynamical principles as in [11,5] or on resistance capacitance (RC) networks [23] (ii) grey-box or (iii) black-box identification. [24,22] give an overview and analysis of different identification tools, most importantly deterministic-physical modelling or probabilistic semi-physical modelling. [25,26] show a fuzzy black-box method for the identification of local linear networks.

In this work both analytically derived modelling and black-box identification based on historic data with a linear regression method are used exclusively for the formulation of the LoLe models representing the cooling supply circuits, see Fig. 1, without respecting the comfort zones in the HiLe.

Model identification and building modelling, respectively, as well as the performance of the proposed predictive control structure are shown on a representative modern large office building comprising both active and passive storage supplied by several energy sources.

The remainder of this paper is structured as follows: Section 2 gives a description of the building studied and its cooling system. In Section 3 the three models, one for each dedicated MPC, are formally described and the model validation is shown. The overall control structure and the controllers are introduced in Section 4. The simulation results for the building studied are shown in Section 5 and finally, a conclusion is drawn in Section 6.

2. Case study description

2.1. Building features

The building studied is the University of Salzburg comprising 27,000 m² in the centre of Salzburg, Austria, see Fig. 2. This representative modern building has five floors above ground containing several large and numerous smaller meeting rooms, offices and lecture rooms. For this study, the energy demand of the second and third floor of the building is considered. The two floors comprise about 500 rooms of some 13,000 m², almost all used as offices. Its

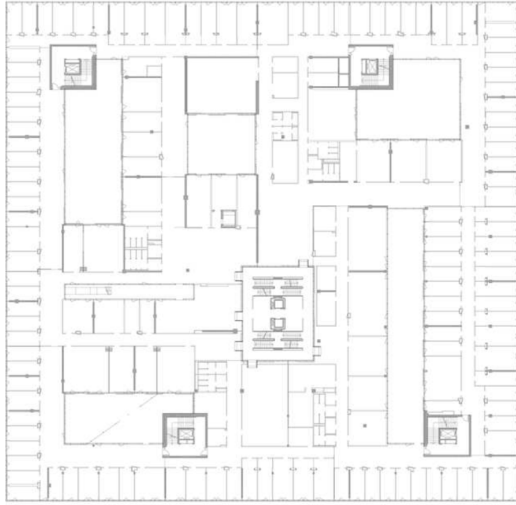


Fig. 3. The plan view of the office floors.

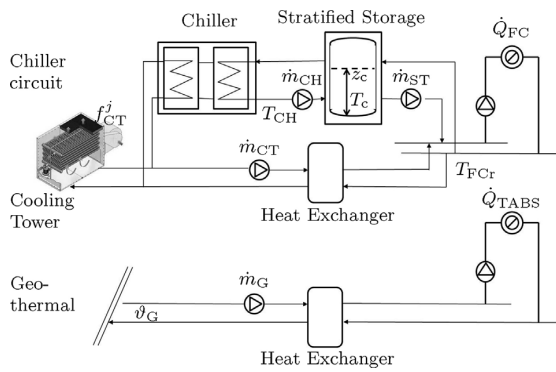


Fig. 4. Cooling supply systems for FC and TABS.

gross volume heated is about 40,000 m³ which is about a third of the overall building's heated volume. The plan view for the two almost identical floors is given in Fig. 3.

For the study of this energy consumption zone only the control of room temperature is considered. The air exchange rate for office rooms is fixed and air conditioning is not used for heating nor cooling the building. The two floors considered are supplied both by TABS and FC system, whereas the two cooling systems are connected to different energy sources: a chiller with stratified storage tank, a free cooling tower and geothermal source. The corresponding cooling supply systems are shown in Fig. 4. This building is representative for demonstrating the proposed predictive control concept as it is a modern large office building comprising active and passive storage and various energy sources. Since each supply circuit is considered separately the resulting modular MPC concept is applicable to new buildings as well as for retrofitting.

2.2. Overall cooling system

The considered cooling system is represented by two independent energy supply systems, the slow TABS and the fast FC system with time constants of 36 h and 4 h respectively. The TABS supply is directly provided by the geothermal source, whereas the cooling energy for the FC system is either generated by the chiller or by the free cooling system. Note that free cooling by definition is

Table 1
Definition of variables for all models.

Variables	Type	Model
\dot{m}_G	Input	Geothermal model
ϑ_G	Disturbance	Geothermal model
\dot{Q}_{TABS}	Output	Geothermal model
T_{CH}	Continuous input	Hybrid chiller model
\dot{m}_{CH}	Continuous input	Hybrid chiller model
\dot{m}_{ST}	Continuous input	Hybrid chiller model
ch_{on}	Discrete input	Hybrid chiller model
z_c	Continuous state	Hybrid chiller model
T_c	Continuous state	Hybrid chiller model
\dot{Q}_{FC}	Continuous output	Hybrid chiller model
\dot{m}_{CT}	Input	Free cooling model
f_{CT}^j	Input	Free cooling model
T_{amb}	Disturbance	Free cooling model
T_{FCr}	disturbance	Free cooling model
rH_{amb}	Disturbance	Free cooling model
\dot{Q}_{FC}	Output	Free cooling model

an approach to lowering the air temperature in a building by using natural cool air or water instead of mechanical refrigeration. For this building the evaporation of water in ambient air inside the cooling tower is a source of cooling energy. Fig. 4 shows the three supply circuits and the two decoupled supply systems delivering the cooling energy for the building.

The chiller delivers cold water with temperature T_{CH} and mass flow \dot{m}_{CH} to the stratified storage tank. However, the cooling energy is provided for the FC system with mass flow \dot{m}_{ST} and respective water supply temperature T_c . Depending on the difference of the two mass flow rates the stratified storage tank's operation mode changes which affects the cold water temperature T_c and the position of the thermocline z_c . In Section 3.3 the corresponding model is formally explained in detail. The cooling tower either supplies the chiller's secondary circuit (chiller active) or runs the free cooling system. Associated with the free cooling circuit are the fan speed of the cooling tower f_{CT} at stage $j \in \{1, 2\}$, the mass flow \dot{m}_{CT} from the cooling tower to the heat exchanger and the return water temperature T_{FCr} from the building. The geothermal circuit contains a pump delivering mass flow \dot{m}_G and a heat exchanger. ϑ_G denotes the difference of the supply to the return water temperature from and to the geothermal source.

The corresponding simplified models for predictive control purposes are formulated in the subsequent sections. Table 1 lists all variables associated with the three models. A model validation is given in Section 5.2.2.

3. Cooling models

3.1. Geothermal model

The geothermal source provides water only for the cooling supply of the TABS which is entirely decoupled from the FC system. The corresponding nonlinear static model in Eq. (1) is based on thermodynamic principles directly implemented in Matlab. Hence, modelling is done in a generic way, not using a specific building modelling tool. Only the coefficient of performance (COP) of the heat exchanger was identified from historic data, its definition is given in Appendix B, Eq. (B.2). The constant specific heat capacity of water is cp and $\vartheta_G = T_{TABSs} - T_{TABSr}$.

$$\dot{Q}_{TABS} = \underbrace{COP}_{const.} \cdot \vartheta_G \cdot \underbrace{\dot{m}_G \cdot cp}_{const.} \quad (1)$$

In order to utilise a linear MPC the model is linearised in Eq. (2):

$$\Delta \dot{Q}_{TABS} = \underbrace{COP \cdot cp}_{const.} (\dot{m}_{G|0} \cdot \Delta \vartheta_G + \vartheta_{G|0} \cdot \Delta \dot{m}_G) \quad (2)$$

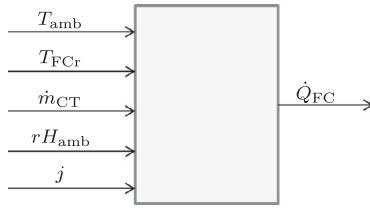


Fig. 5. Inputs and output for the specific black-box model for free cooling.

The Δ -variables denote the deviation of the variables to the operating point listed in [Appendix A](#).

3.2. Free cooling model

As depicted in [Fig. 4](#) free cooling is based on the cooling tower. Free cooling is exclusively used if the chiller is inactive. The ambient temperature, T_{amb} , constrains the cooling tower's operation for free cooling. Within the cooling tower the return water is sprinkled over a specific PVC-packing which is ventilated by the fan in order to use the evaporation heat to cool down the supply water. The fan can be run in two speed stages $j \in \{1, 2\}$ providing different levels of cooling power. Main disturbances are given by the ambient temperature T_{amb} and the return water temperature T_{FCr} . Another disturbance for the free cooling system is relative outdoor air humidity rH_{amb} . Modelling cooling towers analytically aims at detailed complex models with non-linear dynamics of high order which are not suitable for the usage within MPCs. Hence, black-box identification is expedient if historic data of the cooling tower in operation is available. Data for identification of the cooling tower covering six months of operation have been taken from the building management system. For the black-box identification linear regression models are used to explain the inputs to output behaviour shown in [Fig. 5](#). The system can be approximated by two linear static models, one for each fan speed j . The formal description is given in [Eq. \(3\)](#).

$$\dot{Q}_{FC}(j) = c_{j,1} \cdot T_{amb} + c_{j,2} \cdot T_{FCr} + c_{j,3} \cdot \dot{m}_{CT} + c_{j,4} \cdot rH_{amb} + c_{j,5} \quad (3)$$

Within the identification routine the parameters $c_{j,i}$ have to be estimated using historic data of the free cooling system in operation. Note that the model in [Eq. \(3\)](#) is linear in the parameters $c_{j,i}$, thus least squares methods can be employed for optimal parameter estimation [\[27\]](#). If measurements of individual input variables are not available due to a lack of sensors, the corresponding coefficients are set to zero and the output has to be explained by the remaining inputs. Note that in terms of control all model inputs are either disturbances (T_{amb} , T_{FCr} , and rH_{amb}) or manipulated variables (\dot{m}_{CT}). There are no feedback loops implemented for air conditioning of the building studied. Therefore, it is not equipped with sensors for the relative humidity and the coefficients $c_{j,4}$ have to be set to zero. All model coefficients for the models identified for the building studied are given in [Appendix A](#).

3.3. Hybrid chiller model

The chiller is a switching aggregate with latency times, such that minimum up and down times have to be respected. Once the chiller is on, the mass flow \dot{m}_{CH} from the chiller to the stratified storage tank is variable between 30% and 70% of the pump's maximum capacity, while it is zero otherwise. Furthermore, the storage tank can operate in two basic modes: charging and discharging. These operation modes depend on the status of the chiller (on/off), ch_{on} , and on the difference of the mass flows to, \dot{m}_{CH} , and from, \dot{m}_{ST} , the storage tank [\[6\]](#). These two mass flows together with the supply temperature from the chiller, T_{CH} form

the continuous manipulated variables to the system while the status of the chiller, ch_{on} , is a discrete input variable. This system can be expressed by a hybrid system state-space formulation with discrete as well as continuous inputs. General results on hybrid system representations are given in [\[21\]](#). See also [\[6\]](#) for the development of the analytically derived nonlinear dynamic system, the linearisation, and the formulation as a piecewise affine (PWA) system. [Eq. \(4a\)–\(4b\)](#) is an equivalent compact representation of the PWA system with time-variant matrices [\[21\]](#).

$$x(t+1) = A_t x(t) + B_{1t} u(t) + B_{2t} \delta(t) + B_{3t} z(t), \quad (4a)$$

$$y(t) = C_t x(t) + D_{1t} u(t) + D_{2t} \delta(t) + D_{3t} z(t), \quad (4b)$$

subject to

$$E_{2t} \delta(t) + E_{3t} z(t) \leq E_{1t} u(t) + E_{4t} x(t) + E_{5t}. \quad (4c)$$

The model contains continuous states, $x(t) = \{z_c(t), T_c(t), \dot{Q}_{FC}(t)\}$, three continuous manipulated variables, $u_c(t) = \{T_{CH}(t), \dot{m}_{CH}(t), \dot{m}_{ST}(t)\}$, one discrete input, $u_d(t) = \{ch_{on}(t)\}$, and one continuous output $y(t) = \{\dot{Q}_{FC}(t)\}$. All inputs together are summarised in $u(t)$ with $u(t) = \{u_c(t), u_d(t)\}$.

The δ -variables are auxiliary discrete variables representing the hybrid modes, charging or discharging – with active or inactive chiller:

$$\begin{aligned} \delta_1 &= 1 \leftrightarrow ch_{on} = 1 \wedge \dot{m}_{CH} > \dot{m}_{ST} \\ \delta_2 &= 1 \leftrightarrow ch_{on} = 1 \wedge \dot{m}_{CH} \leq \dot{m}_{ST} \\ \delta_3 &= 1 \leftrightarrow ch_{on} = 0 \wedge \dot{m}_{CH} \leq \dot{m}_{ST} \end{aligned} \quad (5)$$

The z -variables are auxiliary continuous representatives of the states at each mode, denoted by $z_i(t) = \delta_i(t)x(t)$ for $i = 1, 2, 3$, which encapsulate the non-linearity.

The logical conditions arising with the discrete modes and the resulting hybrid system can be collected in a compact form as mixed-integer linear inequalities [\[21\]](#). $E_{1t}, E_{2t}, E_{3t}, E_{4t}, E_{5t}$ in [Eq. \(4c\)](#) are matrices which represent these inequalities in compact form. Most important matrices are listed in [Appendix A](#).

4. Control structure

4.1. Complete control structure

The complete control structure is split into two independent parts. One closed loop consisting of only one LMPC is responsible for the TABS, while the control of the FC system is alternatively provided by an LMPC or an MI-MPC. [Fig. 6](#) gives an overview over the complete control structure embedded into an hierarchical building control concept. ϑ_B^{ref} and ϑ_B^{ref} denote the required respectively actual building zone indoor temperature. Here, this proposed structure is embedded into an overall hierarchical predictive building control concept designed for industrial application, introduced in [\[25,28\]](#), where the energy supply level, the low level (LoLe), is decoupled from the building's energy consuming level in the comfort zones, high level (HiLe). For this study we assume only proper operation of any HiLe controller providing a prediction of the required cooling power (see e.g. [\[29\]](#)). This proposed structure is limited by the suboptimality resulting due to the hierarchy but it allows to easily include additional circuits and energy sources, since each supply circuit is considered separately resulting in a modular MPC concept, which is ideal for industrial application.

The reference trajectories for the cooling demand of the TABS, \dot{Q}_{TABS}^{ref} , and the FC system, \dot{Q}_{FC}^{ref} , are predetermined over the complete prediction horizon by the predictive controller of the buildings' comfort area (HiLe) [\[25,6\]](#). The LMPC for the TABS controls the geothermal system. The only manipulated variable is the mass flow

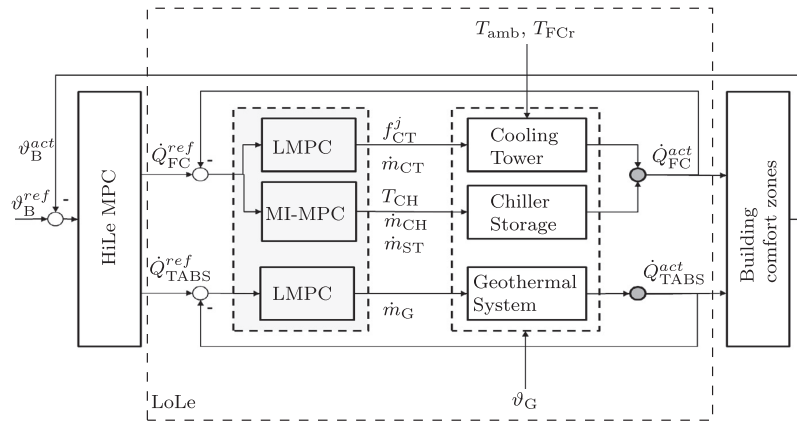


Fig. 6. Overall control structure for cooling circuits supplying FC and TABS.

from the geothermal pipes, \dot{m}_G , to the heat exchanger. The only disturbance is the difference of the supply and return water temperature ϑ_G . The closed loop for the FC system consists of two alternatively working MPCs, the LMPC controlling the free cooling circuit and the MI-MPC is responsible for the chiller circuit. Both have the same controlled variable, \dot{Q}_{FC} , but only one may be active at a given time. Fan speed f_{CT}^j and the mass flow from the cooling tower, \dot{m}_{CT} , act on the free cooling circuit as well as the disturbances ambient temperature, T_{amb} , and return water temperature, T_{FCr} . Due to the fact that the two controllers act with different manipulated variables bump-less switching between the controllers is ensured as long as the change of MI-MPC's states is consistently performed.

4.2. Linear MPC

MPC control methods are designed for complex multivariable control problems. At each sampling time, starting at the current state, an open-loop optimal control problem is solved over a finite horizon. An explicit model is used to predict the future outputs. At the next time step, the minimisation of the objective function is repeated starting from the new state and over a shifted horizon, leading to a receding horizon strategy. Various MPC methods differ in the model used to represent the plant, the cost function to be minimised and the disturbances to take into account [30]. Linear MPCs rely on a linear (dynamic) model, and can explicitly consider constraints in all variables. The two LMPCs for this work have a quadratic optimisation target, similar to the objective of the MI-MPC, see Eq. (6). They only differ in the model they rely on. The FC model for free cooling, Eq. (3), uses a linear model with absolute inputs, whereas the TABS geothermal model, Eq. (2), is a linearised model with Δ -variables which denote the deviation from the corresponding operating point. Within the MPC optimisation routine these models are constraints to the optimisation task. The inputs to the models are disturbances or manipulated variables, whereas the models' outputs denote the controlled variables of the controller. Note that manipulated variables are those variables the controller is free to choose at each time instance in order to optimise the controlled variable.

4.3. MI-MPC with branch and bound

The four subsequent Sections introduce the MI-MPC formulation, give basic notions on the branch and bound method and present the branch and bound algorithm for the hybrid system and the unit commitment problem motivated in Section 3.3.

4.3.1. MI-MPC formulation

In Section 3.3 a linear hybrid system with discrete and continuous inputs was obtained which is used within the MI-MPC. The goal of the MI-MPC, Eq. (6), is the minimisation of the error to the given reference trajectory \dot{Q}_{FC}^{ref} , while minimising the energy costs arising due to the manipulated variables. According to the a moving horizon control strategy [30], at time $t+0$ an optimal solution for the manipulated variables $U^* = \{u_{t|t}^*, \dots, u_{t+Np-1|t}^*\}$ is calculated for the complete horizon Np . Only the first element $u_{t|t}^*$ is actually applied to the plant, then the optimisation problem is repeated at time $t+1$ with the updated states x_{t+1} . This implies an efficient management of the stratified storage tank and a solution of the unit commitment problem, arising due to the switching chiller with its minimal up and down times, resulting in the following optimisation problem:

$$J^* = \min_{\Delta u \in U} \sum_{k=0}^{Np-1} \|\Delta \dot{Q}_{FC}^{ref}(t+k) - \Delta \dot{Q}_{FC}^{act}(t+k)\|_{Q_y}^2 + \min_{\Delta u \in U} \sum_{k=0}^{Np-1} \|\Delta u(t+k)\|_{Q_u}^2 \quad (6)$$

subject to:
model and inequalities in Eq. (4),

$$\delta_i(t+k) \in \{0, 1\}, \quad (7a)$$

$$\sum_i \delta_i(t+k) = 1, \quad (7b)$$

$$u_{min} \leq u(t+k) \leq u_{max}, \quad (7c)$$

$$x_{min} \leq x(t+k) \leq x_{max}, \quad (7d)$$

$$ch_{on}(t+k) - ch_{on}(t+k-1) \leq ch_{on}(\omega_{up}), \quad (7e)$$

$$ch_{on}(t+k-1) - ch_{on}(t+k) \leq 1 - ch_{on}(\omega_{down}), \quad (7f)$$

where u_{min} and u_{max} , respectively x_{min} and x_{max} , denote the the capacity limits of the manipulated variables and the physical bounds of the stratified storage. The constraints on latency times with minimum up and down times are given in Eq. (7e) and Eq. (7f) with $\omega_{up} = t+k, t+k+1, \dots, \min(t+Np, t+k+T_{HP}^{up}-1)$ and $\omega_{down} = t+k, t+k+1, \dots, \min(t+Np, t+k+T_{HP}^{down}-1)$. Eq. (7b) denotes that at each time only one hybrid mode can be active. Due to the quadratic cost function this optimisation problem aims at solving a mixed-inter quadratic problem (MIQP) each time step $t+k$. The weighting matrices Q_y and Q_u are penalising the deviation

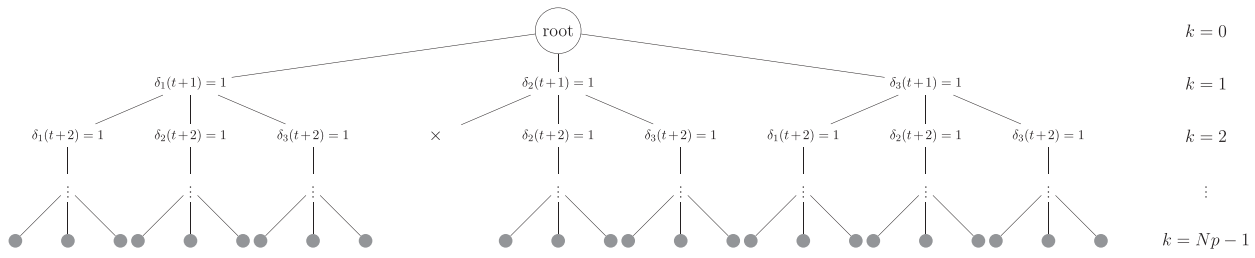


Fig. 7. The binary tree for the hybrid chiller system optimisation with branch and bound.

to the reference and the energy costs caused by the inputs. All Δ -variables denote the deviation from the corresponding operating point.

4.3.2. Branch and bound basic notions

The branch and bound method is based on the relaxation of the integrality constraint Eq. (7a), i.e. integer and particularly binary variables are allowed to span over the whole continuous interval. The relaxed MIQP can be represented as a problem specific tree structure such as Fig. 7 for the introduced predictive optimisation target. A tree consists of nodes and branches. The first node is called the root node, which is the only node of the tree without parent. All other nodes have one unique parent, but a parent can have $n \geq 0$ subsequent nodes, called its children. Taking one node with all its children and deleting the branch to its father is called subtree. Fig. 7 shows the tree related to the specific problem formulation in Section 4.3.1. The first node represents the root node and nodes without children are marked as leaves, represented as grey circles at the end of the tree. The depth k of a node is its number of predecessors up to the root. The maximum depth over all nodes represents the length of the tree, which is $Np - 1$ for the corresponding predictive optimisation problem. In this example the fourth branch is terminated at depth 2, such that no further children are searched.

4.3.3. Search space reduction

According to the hybrid model structure the decision tree consists of three branches at each time step which corresponds to one layer in depth of the tree, leading to a maximum number of 3^{Np} leaves for a prediction horizon Np . In order to reduce this large number of branches to be searched, a modified forward checking method of [20] has been developed. For the reduction of the search space for the branch and bound algorithm three additional equations correlating with the minimum up and down times of the chiller, the physical constraints balances of the stratified storage tank, and the total amount of theoretically supplied energy from the storage are checked while building up the search tree level by level.

minimum up- and down-times, Eqs. (7e) and (7f), (8)

$$\dot{m}_{CH}^{\max} \cdot c_{on}(t+k) - \dot{m}_{ST}^{\min} \cdot c_{off}(t+k) + v_c(t+0) < v_c^{\max}, \quad (9)$$

$$\dot{m}_{CH}^{\min} \cdot c_{on}(t+k) - \dot{m}_{ST}^{\max} \cdot c_{off}(t+k) + v_c(t+0) > v_c^{\min}, \quad (10)$$

$$\dot{Q}_{FC}^{ref}(t+k) - \dot{Q}_{ST}^{\max} \leq e_{FC}^{\max}, \quad (11)$$

where $c_{on}(t+k)$, respectively $c_{off}(t+k)$, is the number of hours the chiller has been active, respectively inactive, up to time $t+k$. \dot{Q}_{ST}^{\max} denotes the maximum energy that can be provided by the storage tank with T_c at the operating point and e_{FC}^{\max} the maximum error tolerated for the FC energy supply. If inequality (11) is not fulfilled, the storage tank has not enough cooling energy without the activation of the chiller at time $t+k$. Therefore, the branch with inactive chiller is not added as a child branch to the parent node at level $t+k-1$.

4.3.4. Branch and bound approach

MIQP can be solved by commercial solvers, e.g. [14,6]. However, for industrial applications a method without the need of expensive solvers is desirable. The above problem differs from a QP through the integrality constraints Eq. (7a). One approach to get rid of the integer variables is to enumerate all possible combinations of integer variables. A more effective method is the branch and bound algorithm which relaxes the original problem by replacing integrality constraints with simple bounds, as $\delta_i \in [0, 1]$ in the binary case. If the solution to a relaxed subproblem is not integral, but has a cost worse than the best MILP solution found so far, that branch can be terminated, or “fathomed”, as further branching will only increase the cost. Then the corresponding node is marked, such as exemplarily shown in Fig. 7. The search terminates when all branches have been searched. Note that the longer the prediction horizon Np is and the shorter the minimum up and down times are, the greater the length of the tree and the more branches have to be searched. For more information on the principles of the branch and bound method, see e.g. [31,32].

Fig. 8 shows the developed branch and bound algorithm for the corresponding MIQP including the unit commitment problem and explained as follows:

- Init:** The MIQP (model, objective and constraints) is defined. Initialise list of problems to be solved by $QP_{list} = \emptyset$. Relax all integrality constraints ($u^d \in [0, 1]$ instead of $u^d \in \{0, 1\}$). Set $J^* = \infty$, $u^* = [\infty, \dots, \infty]$. Add the root node to the list of problems: $QP_{list} = [\text{root}]$.
- Reduce search space:** Take the root node and apply the search space reduction routine, see Section 4.3.3 by using forward checking implying the constraint check. The feasible tree is set up with depth Np and sampling time $T_s = 1$ h. A second tree is set up similarly with a larger sample time $T_s > 1$ h and depth Np/T_s to calculate the minimum upper bound J_{min}^{ub} for the optimisation problem by enumerating all subtrees. Only the first tree is used within the further algorithm.
- Check QP list:** If the list of problems QP_{list} is empty then stop. The output is given by J^* and u^* . Else go to 4.
- Solve QP:** Remove first QP from the list of problems and solve the QP by setting the already determined binary variables and leaving the relaxation of the integrality constraints to the unknown binary variables.
- Check if solution is feasible:** If the solution is feasible and the solution is better than the best upper bound J_{min}^{ub} , store solution $\tilde{J} = J$, $\tilde{u} = u$, else the node is fathomed and the subtree is not expanded; go to 3.
- Check integrality constraint:** If the binary variables satisfy $u^d \in [0, 1]$ go to 7, else go to 8.
- Set best solution:** Set $J^* = \tilde{J}$ and $u^* = \tilde{u}$ and go to 3.
- Expand tree:** Expand the tree by adding the children of the current node. Add the QPs to the list of QPs and go to 3.

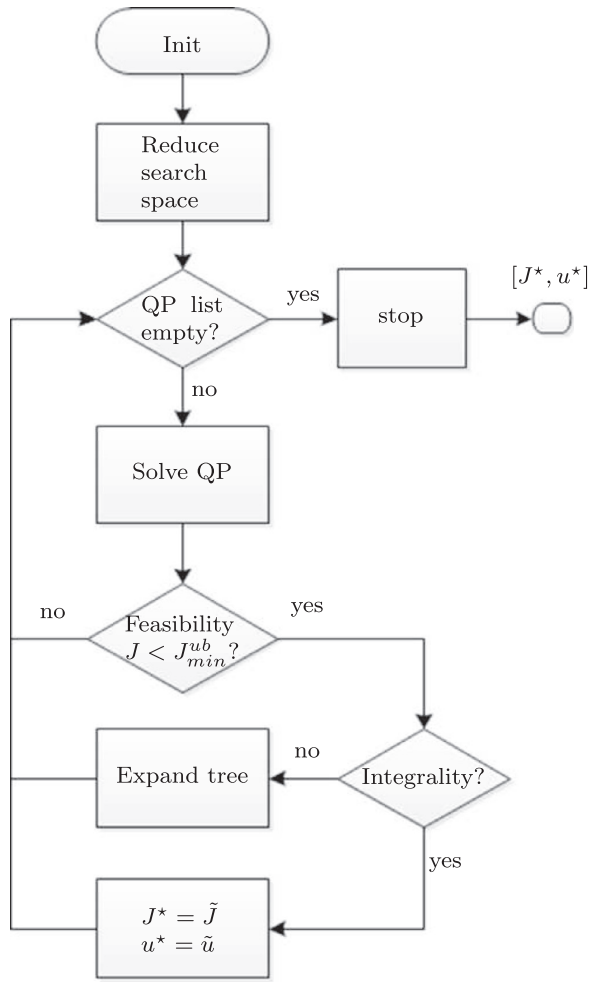


Fig. 8. Branch and bound algorithm for hybrid MI-MPC and unit commitment problem.

5. Simulation results

5.1. Model validation

In this section a validation of the models, Eqs. (2)–(4), is given. For this open loop analysis, the measured input data and disturbances obtained from the historic data base of the studied building's control system are used to generate the corresponding simulated cooling supply, which is compared to the measured output \dot{Q}_i^{meas} . Fig. 9 depicts the corresponding workflow: Firstly, the measured data from the realised implementation is taken. Secondly, the open loop simulation is conducted where the measured supply variables denote the input to the model. Thirdly, the simulated cooling supply is compared to the historically measured cooling supply. In Fig. 10 the measured and predicted outputs are shown for the geothermal, the free cooling and the chiller model introduced in Section 3. The validation period is chosen differently for all the models such that the corresponding model is active over the whole period. The quality of the models is measured with the mean percentage fit (MPF) from the predicted to the measured output:

$$MPF_m = 1 - \frac{1}{N} \sum_{n=1}^N \frac{|\dot{Q}_i^{meas} - \dot{Q}_{i,m}^{pred}|}{|\dot{Q}_i^{meas}|}, \quad (12)$$

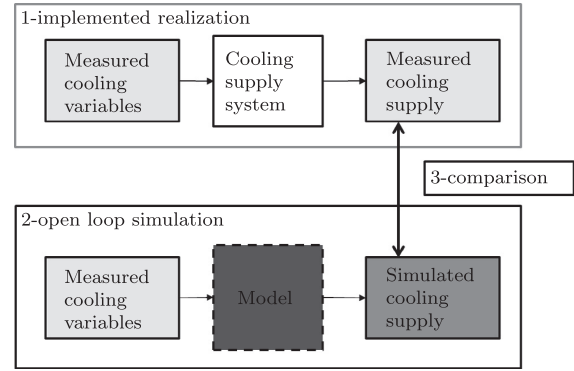


Fig. 9. Setup and workflow for the open loop model validation.

Table 2

The mean percentage error for validation of the three models and the corresponding period.

MPF _{geothermal}	MPF _{free cooling}	MPF _{chiller}
92.12%	92.59%	80.41%

for $i \in \{\text{FC}, \text{TABS}\}$ and $m \in \{\text{geothermal}, \text{free cooling}, \text{chiller}\}$ and N the length of the validation period in hours. The mean percentage fit for validation of the three models and the corresponding period is given in Table 2.

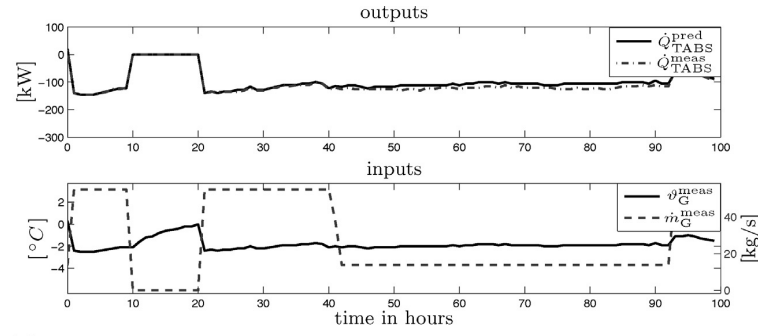
Note that the MPF defined in (12) can only reach 100% for both a perfect model and noise-free measurements. In the presence of inevitable measurement noise the results for MPF will be smaller than 100% even for perfect models. Thus, the results presented in Table 2 are excellent for geothermal and free cooling models, respectively. It also provides a justification to omit the relative Humidity rH_{amb} in the freecooling model. The result for the chiller model is slightly worse. However, this is also caused by the poor data quality available. For the usage within the closed loop predictive control structure the accuracy of the models is only important for the length of the prediction horizon $N_p = 12$ h, since in each optimisation step, the prediction starts with the actual plant data. The results for the proposed control structure with a prediction horizon of 12 h presented in Section 5.2.2 are promising, such that the balance between accuracy and simplicity is obtained.

5.2. Closed loop simulations

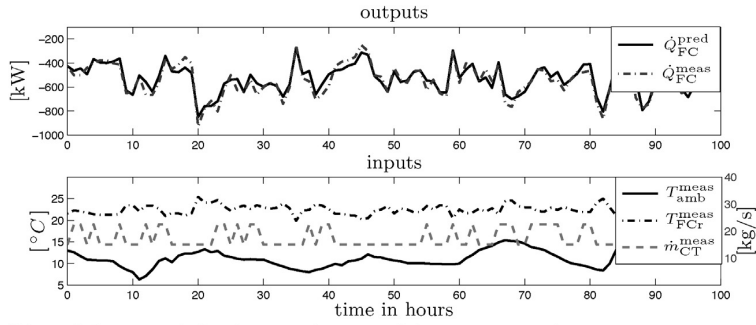
This section contains simulation results for the closed loop system, i.e. the models described in Section 3 are used within the MI-MPC given in Section 4. The closed loop simulations are presented for two intervals: May 2014 and June–August 2014.

5.2.1. Simulation setup

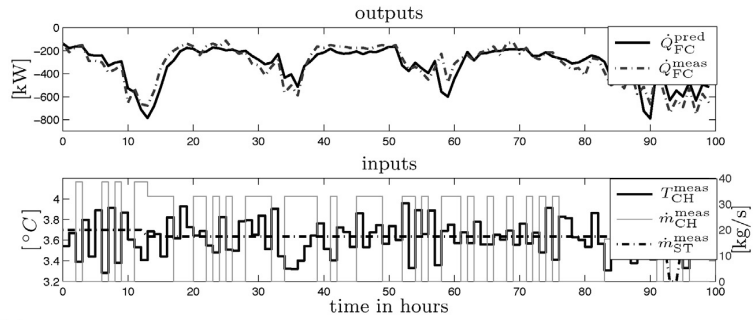
The simulation setup for the closed loop simulation is similar to the setup of the open loop analysis, Section 5.1. The setup and workflow is shown in Fig. 11. Firstly, the measured data from the implemented realisation is taken. Secondly, the closed loop simulation is conducted. The measured cooling supply denotes the reference to the predictive controllers (LMPCs and MI-MPC). Thirdly, the simulated data is compared to the historic measured data. The closed loop system is simulated based on the models and equations presented in Section 3. The reference to the predictive controller structure is the measured cooling supply, \dot{Q}_i^{ref} , taken from the historic data base. The closed loop simulation results, simulated cooling supply \dot{Q}_i^{sim} , and the simulated cooling variables for the MPCs are compared to the corresponding measured data.



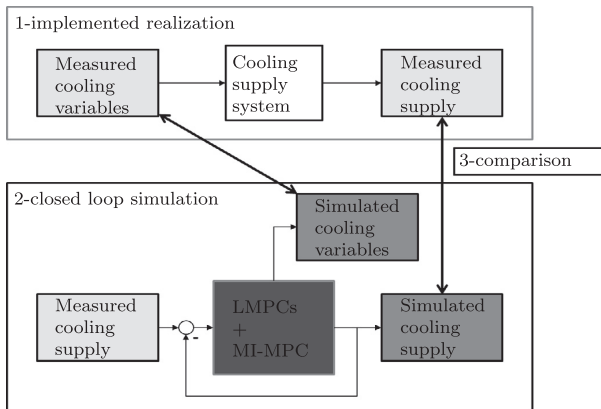
(a) Validation of the geothermal model starting with 06.06.2014 14:00.



(b) Validation of the free cooling model starting with 08.04.2014 20:00.



(c) Validation of the hybrid chiller model starting with 16.06.2014 19:00.

Fig. 10. Validation of the geothermal, the free cooling and the chiller model.**Fig. 11.** Setup and workflow for the closed loop simulation.

The corresponding admissible operating margins of the cooling supply circuit, see Eq. (7c), for pumps and the chiller are given by:

$$T_{CH} \in [2, 10][^{\circ}\text{C}]$$

$$\dot{m}_{CH} \in \{0\} \cup [30, 39][\text{kg/s}]$$

$$\dot{m}_{ST} \in [24, 60][\text{kg/s}]$$

$$T_c \in [0, 20][^{\circ}\text{C}]$$

$$z_c \in [0.1, 2][\text{m}].$$

The coefficient of thermal conductivity k is $0.01 \text{ W/m}^2 \cdot ^{\circ}\text{C}$ and the ambient temperature in the basement is assumed to be constant at 20°C . The minimum on/off-times for the heat pump for this work are given by $T_{CH}^{\text{up}} = T_{CH}^{\text{down}} = 1 \text{ h}$. The prediction horizon is 12 h and the sampling time is 1 h. The cooling energy demand of the building for the FC system, \dot{Q}_{FC} , and the TABS, \dot{Q}_{TABS} , as well as the disturbances and inputs for the conventional controller results are taken from

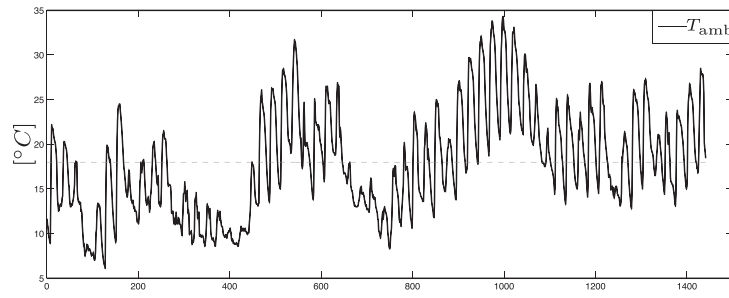


Fig. 12. Ambient temperature from 1st of May 2014 midnight with the upper bound of 18 °C for free cooling denoted by the dashed grey line.

historic data archived by the distributed automation system of the building studied.

The performance of the proposed control structure is compared to the conventional, currently implemented control strategy. This concept is based on several PID-controllers and logic within the programmable logic controller (PLC) ensuring that no technical constraint is violated. The supply water temperatures T_{FCs} and T_{TABs} as well the cooling tower's pump \dot{m}_{CT} are controlled by a PID-controller. The management of the stratified storage tank and the operation of the chiller are simply done by an additional constraint on the temperature of the cool water in the tank, T_c . If T_c is higher than 16 °C, the chiller is activated and if it is lower than 6 °C the chiller is switched off.

5.2.2. Transition period: spring

The month of May represents the transition period with widely varying ambient temperature (see Fig. 12) and cooling energy demand.

Fig. 13 shows the performance of the proposed predictive control structure for the corresponding simulation run. The first subplot in Fig. 13 shows the cooling power trajectories \dot{Q}_{FC} and

\dot{Q}_{TABs} . The proposed control structure is able to deliver the required power for little as well as for high energy demand. However, the TABs supply meets the reference even better than the FC supply does. The second subplot shows the continuous supply input variables of the chiller introduced in Section 3.3, whereas the third subplot shows the mass flow of free cooling which is the only manipulated variable of the free cooling system, Eq. (3), for the corresponding LMPC. The fourth subplot shows the geothermal supply with the disturbance ϑ_G and manipulated variable \dot{m}_G introduced in Eq. (2). The vertical lines represent midnight. Note that an aggregate is not active if the corresponding mass flow is zero and active if greater than zero. The chiller and free cooling are alternately operating. While minimising the deviation to the required cooling energy the predictive controllers' second aim is to minimise the energy costs. Hence, free cooling is used whenever possible. The limiting factor for its usage is the ambient temperature, Fig. 12, since free cooling is disabled for $T_{amb} > 18$ °C.

5.2.3. Cooling period: summer

The biggest advantage of the proposed control structure arises for operation during summer. Figs. 14 and 15 show the first 600 h

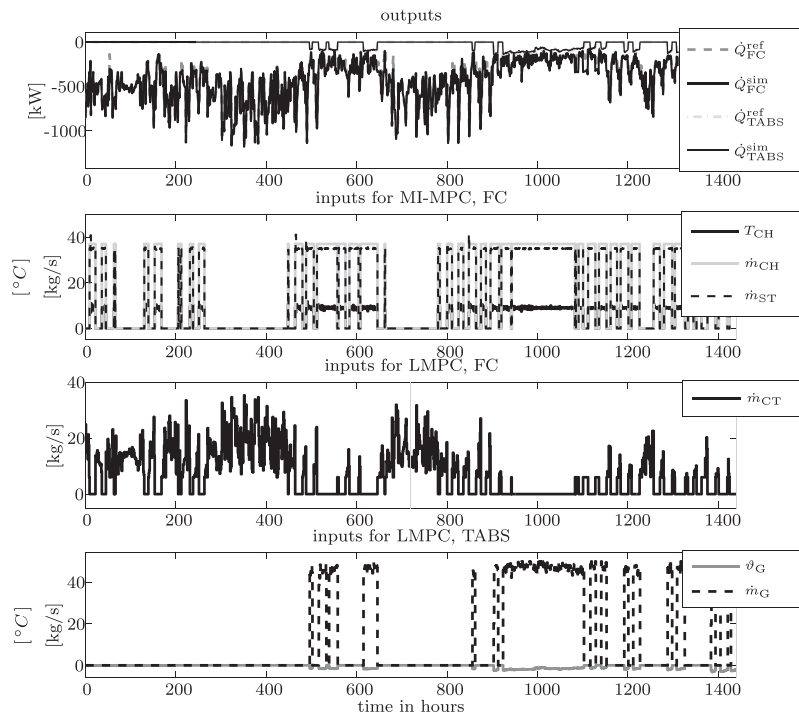


Fig. 13. Closed loop result of proposed control structure starting from 1st of May 2014.

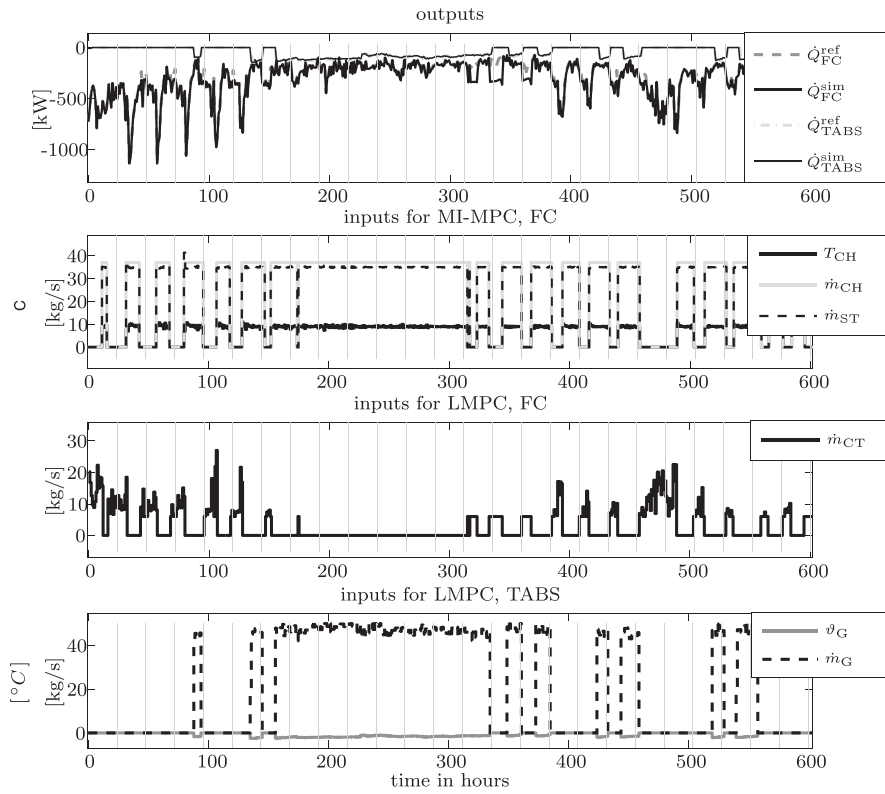


Fig. 14. First 600 h snapshot of the closed loop result of proposed control structure for simulation of June–August 2014.

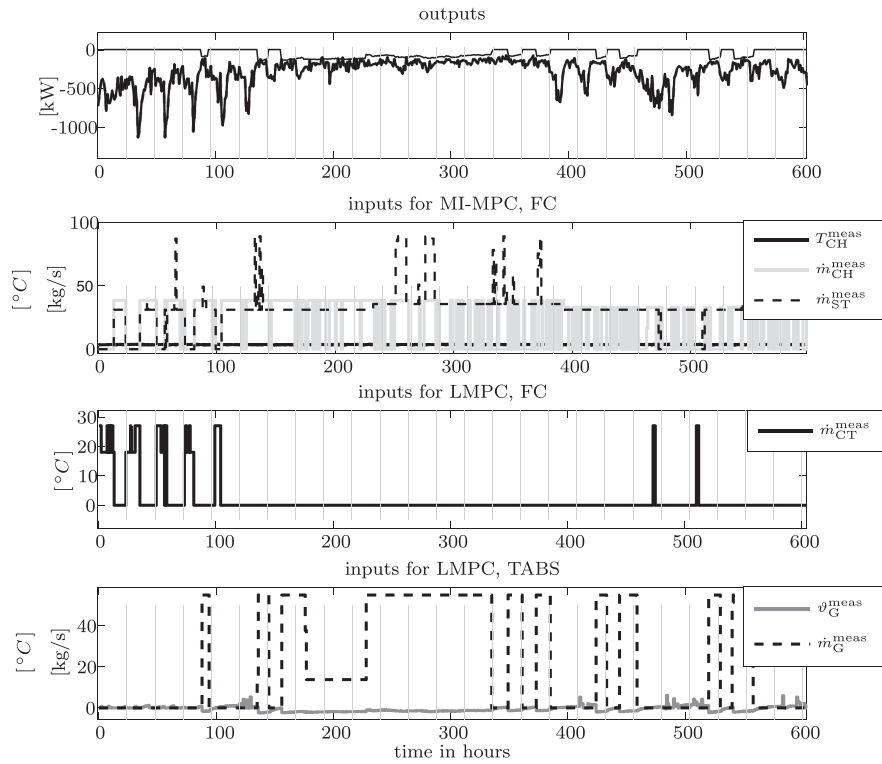


Fig. 15. First 600 h snapshot of the closed loop of conventional control strategy for simulation of June–August 2014.

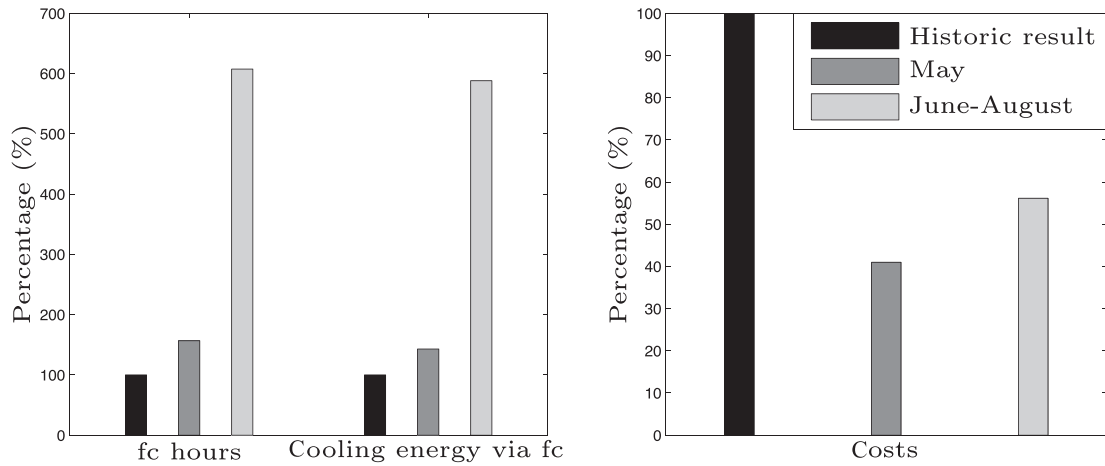


Fig. 16. Comparison of the simulation results (conventional controller = 100%) for May and June–August for free cooling (fc) hours, the cooling energy via free cooling, and costs in percent.

of the simulation run. The structure of the plots is the same as in Fig. 13.

The first subplot in Figs. 14 and 15 shows again the cooling power trajectories \dot{Q}_{FC} and \dot{Q}_{TABS} . The MPC structure is clearly able to deliver the required cooling power. Comparing the second subplots showing the activity of the chiller, the proposed control requires far less switching operations than the conventional control. Moreover, \dot{m}_{CH} and \dot{m}_{ST} are operated synchronously, while for conventional control they showed decoupled behaviour with a temporarily much higher mass flow \dot{m}_{ST} . This means that the proposed controller keeps the thermocline constant by balancing the mass flow to and from the storage.

The third subplot shows the mass flow of free cooling. The proposed concept uses a fine amplitude discretisation optimised for the respective system state, while the conventional control only uses three amplitude values (0, 18, 26 kg/s).

The fourth subplot shows geothermal supply. The main picture is the same for both control concepts. However, the proposed control structure varies the mass flow during on-time while the conventional structure supplies a fixed value. Since ϑ_G is an external disturbance to the geothermal system the two curves are identical.

5.3. Estimation of savings

A quantitative estimation of possible savings by the proposed control concept focuses on two main indicators: (1) increase in free cooling hours, and (2) number of chiller transitions. The first indicator can be related to additional cooling energy supplied by the ambience and the consequent monetary savings. The second indicator is related to maintenance costs, as chiller wear is mainly caused by on/off cycles.

The following results are taken from the closed loop simulations presented in Section 5.2. The proposed control strategy leads to an increased number of free cooling hours in comparison to the conventional controller shown in the first column and row of Table 3.

The proposed controller increases the resulting number of active free cooling hours by more than 50% and as an effective consequence, less power is required from the pumps of the chiller circuit and the chiller itself. The amount of cooling energy via free cooling in May varies considerably, and the costs for electric energy

Table 3

Comparison of the predictive and the conventional control strategy in terms of number of free cooling (fc) hours, the cooling energy via free cooling, and costs.

	May		June–August	
	MPC	CC	MPC	CC
fc hours	760	485	729	120
Cooling energy via fc in [kWh]	406.97	284.95	365.85	62.21
Costs in 10 ³ [€]	11.48	28.03	23.67	42.17

for cooling can be reduced by about 50% for this period. The costs are calculated with a price of €0.12 for a kWh of electric energy. The amount of electric energy E_{el} consumed by the pumps and the chiller are given by:

$$E_{el} = \sum_{n=1}^N k_1 \cdot \dot{m}_G(n) + k_2 \cdot \dot{m}_{CT}(n) + k_3 \cdot \dot{m}_{ST}(n) + \sum_{n=1}^N \frac{\dot{m}_{CH}(n) \cdot (T_{CT} - T_{CH}(n)) \cdot cp}{COP_{CH}},$$

where COP_{CH} is the coefficient of performance of the chiller, which is calculated from historic data with 3.9 based on the definition of Eq. (B.1). The water supply temperature from the cooling tower to the chiller T_{CT} is assumed to be constant at 12 °C and the coefficients k_1 , k_2 and k_3 are derived from the characteristic curves of the pumps. The coefficients are given in Appendix A.

Fig. 16 shows the results for the MPC structure given in Table 3 relatively to the conventional controller, meaning that 100% represent the respective historic result for the two simulation periods. In the left plot free cooling hours, retrieved energy from free cooling, and in the right plot related costs are shown.

In Table 4 and Fig. 17 the decrease of chiller transitions is presented for the two simulation periods. Note that the MI-MPC reduces the number of transitions from the chiller state *off* to the state *on* between 73% and 79% depending on the simulation period compared to the implemented rule based controller.

It should be noted that the related cost reduction is difficult to assess, as wear and maintenance costs vary strongly between individual implementations.

Table 4
Comparison of the predictive and the conventional control strategy in terms of number of chiller transitions.

	May		June–August	
	MPC	CC	MPC	CC
Nr. transitions	41	152	70	327

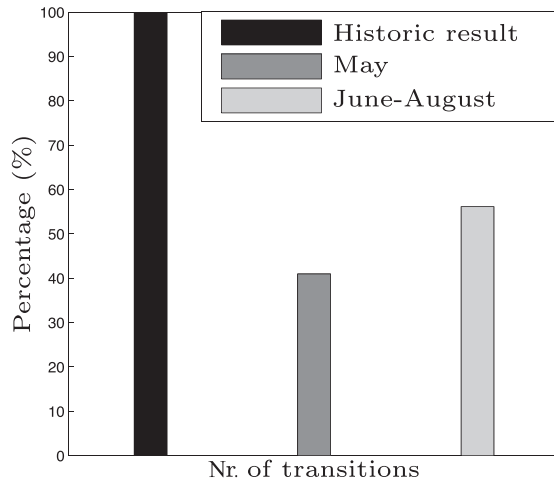


Fig. 17. Comparison of the simulation results (conventional controller = 100%) for May and June–August for number of transitions from chiller state in percent.

Summarised, the two control strategies deviate from each other in three points: (i) free cooling is used more frequently by the MPC concept and its supply energy is increased (ii) the energy costs of the proposed controller structure are lower than the current expenses and (iii) the management of the chiller circuit and the stratified storage tank are more efficient as the number of transitions of the chiller states can be reduced by the MI-MPC. Table 3 shows the comparison results based on these three criteria. Furthermore, the predictive controllers are characterised by a high flexibility with respect to additional optimisation targets and constraints, as was shown by the technical constraint on the heat exchanger. For instance, maintenance costs represented by start-up and shut-down costs of aggregates can easily be added to the optimisation function as well as time-varying prices for electric energy are applicable in time-varying penalty matrices $Q_{ii}(t+k)$.

6. Conclusion

This paper has presented an efficient energy management control concept for cooling supply systems in large office buildings comprising active and passive storage such as stratified storage tanks. The corresponding switching aggregates with different charging modes are the key elements for hybrid cooling systems consisting of continuous and integer variables.

The contribution of the study is a dedicated flexible predictive control structure with a core MI-MPC, which is capable of gaining optimal solutions for conflicting goals: accurate delivery of a prescribed cooling power trajectory at maximum usage of renewable energy resources and minimum costs. The considered costs for the resulting effective storage tank management can reflect life cycle or maintenance costs etc. caused by pumps and switching aggregates. The controller's predictive character is furthermore

advantageous for potentially variable electricity prices and therefore beneficial for a building's smart grid integration. Additionally, the proposed specific branch and bound algorithm is introduced to solve the corresponding constrained mixed-integer quadratic optimisation problem on-line without the need of commercial solvers.

The main outcomes of the simulations show excellent performance compared to the implemented conventional control for a large office building in Salzburg, Austria. The proposed MPC structure increases the usage of renewable energy sources by at least 50% and cuts energy costs by about 50%. Furthermore, a reduction of the number of switching cycles of the chiller of about 70% can be achieved by an optimised operation of the stratified storage tank.

Simulation results of the proposed predictive control structure are very promising for the future implementation in the building studied. Even more, it is quite likely that future building management systems will be based on hybrid system models within MI-MPC realisations, as the potential for cost saving and integration of renewables is high. The proposed control concept including the algorithm is universally applicable for new buildings as well as for retrofitting. The correct parametrization is the only part which has to be adapted for a specific building. However, as the hybrid character is inherent for any energy system with various energy sources and switching aggregates with storage, this study forms a promising basis for the application of a MI-MPC structure for a wider field of energy systems. Future work is likely to be invested on further development of appropriate branching rules and search space reduction for the branch and bound algorithm, since in the worst case, the computational effort increases exponentially with the problem size.

Acknowledgements

This work was supported by the project "SMART MSR" (FFG, No. 832103) in cooperation with evon GmbH.

Appendix A. Coefficients and matrices of cooling system models

The coefficients for the linear system models in Eq. (3) are given in Table A.5. The operating points for the linearisation of the geothermal model, Eq. (2), and the hybrid chiller model, Eq. (4), are given in Table A.6. For the time-discrete linear hybrid chiller model

Table A.5
Coefficients of the free cooling model.

$c_{1,1}$	$c_{1,2}$	$c_{1,3}$	$c_{1,4}$	$c_{1,5}$
2.36	3.49	−97.38	0	−5000
$c_{2,1}$	$c_{2,2}$	$c_{2,3}$	$c_{2,4}$	$c_{2,5}$
5	−50	−110	0	−5500

Table A.6
Operating points for the geothermal and the hybrid chiller model.

Geothermal model				
$\dot{m}_{G o}$		$\vartheta_{G o}$		
46 [kg/s]		−0.1 [°C]		
Hybrid chiller model				
$T_{CHS o}$	$\dot{m}_{CH o}$	$\dot{m}_{ST o}$	$z_{c o}$	$T_{c o}$
8 [°C]	36 [kg/s]	35 [kg/s]	1 [m]	9 [°C]

in the compact form of Eq. (4), the system matrices are derived from the linearised physical first order model [6], and discretised with sampling time $T_s = 1$:

$$\begin{aligned} A &= 0_{3,3} \in \mathbb{R}^{3 \times 3} \\ B_1 &= 0_{3,4} \in \mathbb{R}^{3 \times 4} \\ B_2 &= 0_{3,4} \in \mathbb{R}^{3 \times 4} \\ B_3 &= \begin{bmatrix} I_{3,3} & I_{3,3} & I_{3,3} \end{bmatrix} \in \mathbb{R}^{3 \times 9} \\ C &= \begin{bmatrix} 0 & 0 & 1 \end{bmatrix} \in \mathbb{R}^{1 \times 3} \\ D_1 &= 0_{1,4} \in \mathbb{R}^{1 \times 4} \\ D_2 &= 0_{1,4} \in \mathbb{R}^{1 \times 4} \\ D_3 &= 0_{1,9} \in \mathbb{R}^{1 \times 9} \\ E_1 &\in \mathbb{R}^{50 \times 4} \\ E_2 &\in \mathbb{R}^{50 \times 4} \\ E_3 &\in \mathbb{R}^{50 \times 9} \\ E_4 &\in \mathbb{R}^{50 \times 3} \\ E_5 &\in \mathbb{R}^{50 \times 1} \end{aligned}$$

The coefficients of the pumps k_1 , k_2 , and k_3 are given by:

$$\begin{aligned} k_1 &= 0.022 \\ k_2 &= 0.135 \\ k_3 &= 0.029 \end{aligned}$$

Appendix B. Definition of COPs and technical specification

The definition of the coefficient of performance (COP) for the chiller is given by the ratio between the usable cooling power \dot{Q}_c^u and the electric power P_{el} added:

$$COP_{CH} = \frac{\dot{Q}_c^u}{P_{el}} \quad (B.1)$$

The definition of the coefficient of performance (COP) for a heat exchanger is given by the ratio between the usable cooling power \dot{Q}_c^u and the cooling power from the energy supply \dot{Q}_c^s :

$$COP_{HE} = \frac{\dot{Q}_c^u}{\dot{Q}_c^s} \quad (B.2)$$

In Table B.7 the technical specification of aggregates and pumps of the building studies are given.

Table B.7
Technical specifications of aggregates and pumps.

Aggregate	Type	Operating point	Connected load
Chiller	Water-cooled, screw compressor	6°C supply temp.	1.145 kW cooling capacity
Free cooling tower	CT with two speed fan	1500/750 r.p.m.	540 kW cooling capacity
Geothermal source	56 probes 200 m deep	Water–glycol–mix 34%	
Pump CT (\dot{m}_{CT})	Block pump	102 m ³ /h	7.5 kW
Pump CH (\dot{m}_{CH})	Inline pump	171 m ³ /h	3.0 kW
Pump ST (\dot{m}_{ST})	Inline pump	172 m ³ /h	7.5 kW
Pump G (\dot{m}_G)	Inline pump	166 m ³ /h	3.0 kW

References

- [1] L. Pérez-Lombard, J. Ortiz, C. Pout, A review on buildings energy consumption information, *Energy Build.* 40 (3) (2008) 394–398, <http://dx.doi.org/10.1016/j.enbuild.2007.03.007>.
- [2] B. Paris, J. Eynard, S. Grieu, T. Talbert, M. Polit, Heating control schemes for energy management in buildings, *Energy Build.* 42 (10) (2010) 1908–1917, <http://dx.doi.org/10.1016/j.enbuild.2010.05.027>.
- [3] S. Privara, Z. Vána, J. Cigler, F. Oldewurtel, J. Komárek, Role of MPC in building climate control, *Comput. Aided Chem. Eng.* 29 (2011) 728–732.
- [4] J. Široky, F. Oldewurtel, J. Cigler, S. Privara, Experimental analysis of model predictive control for an energy efficient building heating system, *Appl. Energy* 88 (9) (2011) 3079–3087, <http://dx.doi.org/10.1016/j.apenergy.2011.03.009>.
- [5] F. Berkenkamp, M. Gwerder, Hybrid model predictive control of stratified thermal storages in buildings, *Energy Build.* 84 (2014) 233–240, <http://dx.doi.org/10.1016/j.enbuild.2014.07.052>.
- [6] B. Mayer, M. Killian, M. Kozek, Management of hybrid energy supply systems in buildings using mixed-integer model predictive control, *Energy Convers. Manag.* 98 (2015) 470–483, <http://dx.doi.org/10.1016/j.enconman.2015.02.076>.
- [7] R. Ooka, S. Ikeda, A review on optimization techniques for active thermal energy storage control, *Energy Build.* 106 (2015) 225–233, <http://dx.doi.org/10.1016/j.enbuild.2015.07.031>.
- [8] A. Afram, F. Janabi-Sharifi, Theory and applications of HVAC control systems – a review of model predictive control (MPC), *Build. Environ.* 72 (2014) 343–355, <http://dx.doi.org/10.1016/j.buildenv.2013.11.016>.
- [9] Z.J. Yu, G. Huang, F. Haghighat, H. Li, G. Zhang, Control strategies for integration of thermal energy storage into buildings: state-of-the-art review, *Energy Build.* 106 (2015) 203–215, <http://dx.doi.org/10.1016/j.enbuild.2015.05.038>.
- [10] M.S. Branicky, V.S. Borkar, S.K. Mitter, A unified framework for hybrid control: model and optimal control theory, *IEEE Trans. Autom. Control* 43 (1) (1998) 31–45.
- [11] Y. Ma, F. Borrelli, B. Hancey, B. Coffey, S. Bengae, P. Haves, Model predictive control for the operation of building cooling systems, *IEEE Trans. Control Syst. Technol.* 20 (3) (2012) 796–803, <http://dx.doi.org/10.1109/TCSST.2011.2124461>.
- [12] C.R. Touretzky, M. Baldea, A hierarchical scheduling and control strategy for thermal energy storage systems, *Energy Build.* 110 (2016) 94–107, <http://dx.doi.org/10.1016/j.enbuild.2015.09.049>.
- [13] J. Gruber, F. Huerta, P. Matatagui, M. Prodanović, Advanced building energy management based on a two-stage receding horizon optimization, *Appl. Energy* 160 (2015) 194–205, <http://dx.doi.org/10.1016/j.apenergy.2015.09.049>.
- [14] A. Parisio, E. Rikos, G. Tzamalís, L. Glielmo, Use of model predictive control for experimental microgrid optimization, *Appl. Energy* 115 (2014) 37–46, <http://dx.doi.org/10.1016/j.apenergy.2013.10.027>.
- [15] Y. Zhao, Y. Lu, C. Yan, S. Wang, MPC-based optimal scheduling of grid-connected low energy buildings with thermal energy storages, *Energy Build.* 86 (2015) 415–426, <http://dx.doi.org/10.1016/j.enbuild.2014.10.019>.
- [16] A. Bemporad, D. Mignone, M. Morari, An efficient branch and bound algorithm for state estimation and control of hybrid systems, in: *Proceedings of the European Control Conference*, Citeseer, 1999.
- [17] D. Axehill, T. Besselmann, D.M. Raimondo, M. Morari, A parametric branch and bound approach to suboptimal explicit hybrid MPC, *Automatica* 50 (1) (2014) 240–246, <http://dx.doi.org/10.1016/j.automatica.2013.10.004>.
- [18] A.I. Cohen, M. Yoshimura, A branch-and-bound algorithm for unit commitment, *IEEE Trans. Power Appar. Syst.* 102 (2) (1983).
- [19] G. Lauer, N. Sandell, D. Bertsekas, T. Posbergh, Solution of large-scale optimal unit commitment problems, *IEEE Trans. Power Appar. Syst.* 101 (1) (1982) 79–86, <http://dx.doi.org/10.1109/TPAS.1982.317243>.
- [20] K.-Y. Huang, H.-T. Yang, C.-L. Huang, A new thermal unit commitment approach using constraint logic programming, in: *20th International Conference on Power Industry Computer Applications*, IEEE, 1997, pp. 176–185, <http://dx.doi.org/10.1109/PICA.1997.599394>.
- [21] A. Bemporad, M. Morari, Control of systems integrating logic, dynamics, and constraints, *Automatica* 35 (3) (1999) 407–427, [http://dx.doi.org/10.1016/S0005-1098\(98\)00178-2](http://dx.doi.org/10.1016/S0005-1098(98)00178-2).
- [22] S. Privara, J. Cigler, Z. Vána, F. Oldewurtel, C. Sagerschnig, E. Žáčková, Building modeling as a crucial part for building predictive control, *Energy Build.* 56 (2013) 8–22, <http://dx.doi.org/10.1016/j.enbuild.2012.10.024>.
- [23] F. Oldewurtel, A. Parisio, C.N. Jones, D. Gyalistras, M. Gwerder, V. Stauch, B. Lehmann, M. Morari, Use of model predictive control and weather forecasts for energy efficient building climate control, *Energy Build.* 45 (2012) 15–27, <http://dx.doi.org/10.1016/j.enbuild.2011.09.022>.
- [24] S. Privara, Z. Vána, E. Žáčková, J. Cigler, Building modeling: selection of the most appropriate model for predictive control, *Energy Build.* 55 (2012) 341–350, <http://dx.doi.org/10.1016/j.enbuild.2012.08.040>.
- [25] M. Killian, B. Mayer, M. Kozek, Hierarchical fuzzy MPC concept for building heating control, in: *Proc. IFAC 19th World Congress of the International Federation of Automatic Control (IFAC'14)*, Capetown, South Africa, 2014, pp. 12048–12055, <http://dx.doi.org/10.3182/20140824-6-ZA-1003.00772>.
- [26] M. Killian, B. Mayer, M. Kozek, Effective fuzzy black-box modeling for building heating dynamics, *Energy Build.* 96 (2015) 175–186, <http://dx.doi.org/10.1016/j.enbuild.2015.02.057>.
- [27] L. Ljung, *System Identification – Theory for the User*, 2nd edition, PTR Prentice Hall, Upper Saddle River, NJ, 1999.

- [28] B. Mayer, M. Killian, M. Kozek, Cooperative and hierarchical fuzzy MPC for building heating control, in: 2014 IEEE International Conference on Fuzzy Systems (FUZZ-IEEE), IEEE, 2014, pp. 1054–1059, <http://dx.doi.org/10.1109/FUZZ-IEEE.2014.6891573>.
- [29] M. Killian, B. Mayer, A. Schirrer, M. Kozek, Cooperative fuzzy model predictive control, IEEE Trans. Fuzzy Syst. (2016), <http://dx.doi.org/10.1109/TFUZZ.2015.2463674>.
- [30] E.F. Camacho, C.B. Alba, *Model Predictive Control*, Springer Science & Business Media, 2013.
- [31] C.A. Floudas, *Nonlinear and Mixed-Integer Optimization: Fundamentals and Applications*, Oxford University Press, 1995.
- [32] L.A. Wolsey, G.L. Nemhauser, *Integer and Combinatorial Optimization*, John Wiley & Sons, 2014.

2.3 Publication C

Barbara Mayer, Michaela Killian, and Martin Kozek.

Hierarchical model predictive control for sustainable building automation.

Sustainability, Volume 9, 2017, ISSN: 2071-1050.

DOI: 10.3390/su9020264

Own Contribution

Problem statement, selection of methods and algorithms for modeling, control design, implementation and simulation, as well as structuring, writing and editing the paper was done by the applicant under the supervision of the third author and mentor. Discussion of methodology and results as well as editing and proof read was done by second author.



Article

Hierarchical Model Predictive Control for Sustainable Building Automation

Barbara Mayer ^{1,*}, Michaela Killian ² and Martin Kozek ²

¹ Institute of Industrial Management, FH JOANNEUM, Alte Poststraße 149, 8020 Graz, Austria

² Institute of Mechanics and Mechatronics, TU WIEN, Getreidemarkt 9, 1060 Wien, Austria; michaela.killian@tuwien.ac.at (M.K.); martin.kozek@tuwien.ac.at (M.K.)

* Correspondence: barbara.mayer@fh-joanneum.at; Tel.: +43-316-5453-6347

Academic Editor: Behzad Sodagar

Received: 29 June 2016; Accepted: 2 February 2017; Published: 13 February 2017

Abstract: A hierarchical model predictive controller (HMPC) is proposed for flexible and sustainable building automation. The implications of a building automation system for sustainability are defined, and model predictive control is introduced as an ideal tool to cover all requirements. The HMPC is presented as a development suitable for the optimization of modern buildings, as well as retrofitting. The performance and flexibility of the HMPC is demonstrated by simulation studies of a modern office building, and the perfect interaction with future smart grids is shown.

Keywords: building automation; model predictive control; optimization of building operation; flexibility; retrofit tool; smart building

1. Introduction

Buildings are responsible for 40% of energy consumption in the EU. Thus, the European legislation passed energy performance and efficiency directives to extend the green footprint of buildings [1], affecting designers, investors and operators. The operational energy consumption of buildings is responsible for most of the environmental burdens [2]; thus, pressure is put on operators to run buildings efficiently in order to reduce the consumption of fossil energy. Investors are legally responsible for integrating renewable energy sources in the building. However, such systems are only efficient if an intelligent operating strategy maximizes their usage.

Building operation is closely linked with building automation and its implemented control systems. Since buildings have life spans surpassing 50 years, building automation has to be flexible to meet the requirements of today and the needs of the next decades. Changing conditions will occur due to climate change. This is extraordinarily relevant because climate plays a unique and primary role as it directly affects the thermal load and thus energy performance of the building [3]. In Central Europe, more chillers will be installed in order to satisfy the user thermal comfort. Thus, the challenge is to operate these aggregates in an energy-efficient way and to save maintenance costs over the entire life cycle by minimizing wear and usage. Additional demands on building automation are also made by power grids requiring direct influence on the energy demand of the building (demand response). The opportunities and potential for both energy efficiency and demand response depend on the existing building and equipment infrastructure and on the flexibility of building automation systems providing technical support to the smart grid [4]. Load curtailment can lead to a reduction of energy consumption or at least to a preferable load shift for the grid. The other way around, the buildings' operators gain economic viability by paying lower prices for being curtailed.

Sustainability in buildings affects the whole buildings' life cycle from design over construction, operation and maintenance to deconstruction for better integration of environmental, societal, functional and cost concerns [5]. Building automation is the key instrument of the operation

and maintenance phase. Thus, sustainable building automation is gained by flexibly meeting the current and prospective requirements of the directly interacting groups: the users (thermal comfort), the operators (cost efficiency) and the power grid (demand response).

However, building automation is traditionally based on rule-based controllers (RBC) and conventional proportional-integral-derivative (PID) controllers, which are disadvantageous for this purpose due to their rigid characteristics. Firstly, they are designed for planned building physics often differing from its realization. Hence, the PID/RBC structures cannot in most cases reflect the nonlinear (switching) nature of the underlying system. Even if a perfect model would be available, PID and RBC have only limited flexibility to obtain an optimal control. Secondly, PID-controllers cannot incorporate predictions of disturbances and only react on control errors, and thirdly, though they are easy to implement, their parameters are not intuitively changeable.

In recent years, advanced process control approaches have been evaluated for building control [6]. One of their most powerful representatives is model predictive control (MPC). MPC is an optimization tool based on the dynamic process model capable of incorporating disturbances and constraints. The optimal process inputs are computed by respecting possibly contradicting goals formulated as objective function and set-points [7]. MPC has had a substantial impact in many fields in practice [8] and is probably one of the most successful modern control algorithms. MPC has also been proven as a promising technology for building systems in recent years [9], with the first application results, e.g., [10]. Due to its flexibility, MPC enables building automation to meet the requirements for sustainable operation and maintenance affecting environmental, societal, functional and economic concerns. MPC is thus the best suited control concept for: (i) maximizing user comfort and the usage of renewable energy sources; (ii) minimizing life cycle costs of aggregates, such as chillers; (iii) flexibility towards changes in operational targets and the requirements of smart grids; and can be (iv) part of a retrofit tool for sustainable building automation.

The main contributions of this paper are thus the definition of how building automation affects sustainability and the introduction of a hierarchical MPC (HMPC) for sustainable building automation with beneficial qualities for the directly interacting groups. Simulation results of a hierarchical MPC concept show the performance of MPC for sustainable building automation, especially regarding its flexibility towards possibly changing optimization requirements. Additionally, quantitative differences between the state-of-the art PID and RBC concept and the HMPC are given for a demonstration building.

The paper is structured as follows: Section 2 gives an overview of MPC in buildings and the definition of sustainability in building automation. The proposed hierarchical MPC concept as one promising example of MPC in building automation is presented in Section 3. In Section 4, simulation results are given showing the performance of the HMPC concept regarding sustainability. These results are further discussed from the perspectives of a prospective user, investor or operator in Section 5. Finally, a conclusion is drawn in Section 6.

2. MPC in Building Automation

Within this section, the definition of how building automation affects sustainability, a comparison of MPC and conventional PID control and an overview of MPC approaches in building automation are given.

2.1. Building Automation and Sustainability

In [5], sustainability indicators for buildings are presented with the following key issues: resources consumption, environmental pressure, energy and water efficiency, indoor air quality, comfort and life cycle costs. Building automation affects sustainability in various manners influencing all of these indicators directly or indirectly in the building operation phase. Therefore, the performance of the overall building automation system becomes important for users, operators and the power grids. The demands of each group affect sustainable building automation.

Sustainability for users means a high level of thermal comfort with the opportunity to adjust certain comfort parameters by themselves [11]. Operators are interested in a reduction of costs, including life cycle costs due to maintenance. Furthermore, the expected life cycle of a building is exceptionally long, and the objective of building operation might change from cradle to grave. Thus, flexibility and an intuitive interaction with the system is required from the building automation. Flexibility is also a key factor for the interaction with smart grids. Smart grids demand smart buildings with the capability of dealing with varying prices, demand response and load curtailment [12]. In return, they offer the advantage of temporarily low prices, which are again beneficial for operational cost efficiency. Within the building operation phase, cost efficiency goes along with energy efficiency if the potential for the usage of renewable energy sources can be realized. Thus, the usage of fossil fuels can be minimized, positively affecting the environmental pressure. Finally, investors are indirectly interested in sustainable building automation since they can expect an added value of the building as long as they provide a sustainable construction with infrastructure, such as free cooling or a geothermal source. Figure 1 shows the interaction of building automation with the most affected groups and the environment.

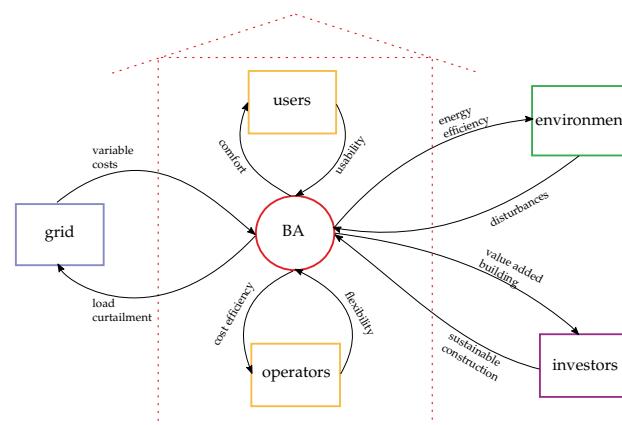


Figure 1. Interaction of building automation (BA) with users, operators, grids, investors and the environment.

Model predictive control (MPC) as introduced in Section 2.2 is a powerful tool for sustainable building automation since the following requirements can be met:

- sustainable user satisfaction, including thermal comfort and usability.
- energy efficiency, including a maximal usage of renewable energy sources.
- minimization of costs, including life cycle costs arising due to the minimization of aggregates' wear.
- flexibility towards smart grids by taking advantage of varying prices and fulfilling load curtailment.

This paper focuses on non-residential buildings, which significantly differ from residential ones concerning the extent of building automation. However, the methodology of MPC is applicable also for residential buildings.

2.2. MPC versus PID

Model predictive control (MPC) is a standard method from advanced process control; it is based on a dynamic process model, predictions of disturbances, set-points and constraints and an optimality criterion. The manipulated variables (process inputs) are optimized such that contradicting goals, such as minimal control error and minimal control effort, are met in a suitable compromise.

This optimization is performed by repeated on-line simulation of the process, its disturbances and the candidate input values to be optimized. As a result, the optimal process inputs fully respect time-varying constraints and the dynamic behavior of the process.

These features are illustrated for building automation in Figure 2.

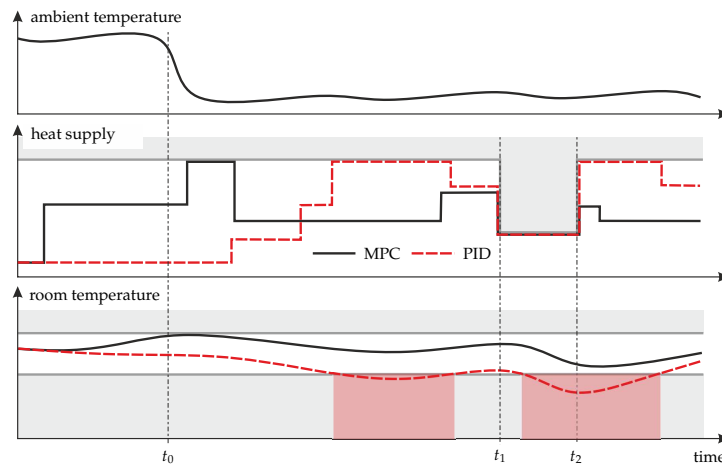


Figure 2. Comparison of MPC and PID for building automation.

In the upper plot, the ambient temperature (main disturbance) is shown. At $t = t_0$, a sudden drop in the ambient temperature occurs. The middle plot shows the heating input to the building. Two inputs from alternative control concepts are shown: PID (red, dashed) and MPC (black, continuous). Note that between $t = t_1$ and $t = t_2$, a strong constraint on the available heat input is active (e.g., caused by a grid overload). The bottom plot shows the mean temperature in the building together with an acceptable comfort band (between shaded areas).

Since MPC considers both the building's time constants, the future disturbances and future constraints, it can pre-heat the building before the problem actually occurs. Since constraints are incorporated in the optimization, both input and comfort constraints are met. PID control reacts only to the increasing control error, thus violations of the lower temperature constraints occur (see the red regions in the bottom plot).

2.3. MPC Approaches in Building Automation

In recent years, several different approaches for the application of MPC in building automation have been presented [13]. Their key differentiators are the overall control structure, the type of MPC, the underlying building model and the application. Most of the concepts consider either the user level or the energy supply level. For the control of a multi-zone user level, centralized [9], decentralized, distributed [14] or cooperative configurations [15] have been proposed in the literature. The centralized controller delivers one solution for all zones, but the optimization results in a high computational load, since it incorporates the inputs, outputs and disturbances for all zones. Solving the control task for each zone separately in several decentralized MPCs reduces the computational burden. However, decentralized MPCs are not capable of taking coupling instances into account, a drawback that can be overcome by distributed and cooperative MPC schemes by sharing information between the MPCs in a cooperative loop. In [10], a hierarchical structure was chosen where the MPC determines the set-points for the low-level PID controller, but does not affect the energy supply system.

The type of MPC used depends on the type of system model. Buildings' heating, ventilation and air conditioning (HVAC), as well as energy supply behavior are strongly non-linear systems.

Modeling is a crucial part for MPC in buildings [16], since models are expected to be as accurate and yet as simple as possible. Hence, approximation is welcome as long as model validation assures acceptable error. For the user level, models have been identified using either statistical methods [16], physical modeling [10] or black-box identification routines [17].

MPCs for cooling or heating supply systems have been presented in, e.g., [18] based on non-linear and in [19] or [20] on hybrid system models. The energy supply level is mostly modeled based on non-linear differential equations, such as energy balance equations. Most of the MPCs are deterministic, meaning that the forecast for uncertain disturbances is used as known input. However, stochastic MPCs have been proposed for problem formulations involving uncertainties [21]. Furthermore, MPC approaches have been presented for the interaction with smart grids [12,22], as well as MPC usage for the optimization of power grids [23].

3. Hierarchical Model Predictive Control

In this section, the proposed HMPC is introduced based on the example of a demonstration building representing a large modern office building. However, due to its modularity, the control concept presented in Section 3.1 is also applicable to other buildings. In Sections 3.2 and 3.3, the user level MPC and the energy supply level MPC are presented.

3.1. Hierarchical MPC Concept

A HMPC structure facilitates the flexibility to meet the requirements defined in Section 2.1. Two separately operating MPCs are independently designed, implemented and tuned and thus ideal for retrofit application, as well as for new buildings. The hierarchy splits the buildings into two layers, the user level and the energy supply level. Concerning control, the characteristics of these two layers differ significantly in their objective, the influencing disturbances and the system dynamics. The MPC on the user level, optimizing user comfort and minimizing heating/cooling energy, incorporates ambient temperature, radiance and the occupancy profile as disturbances. The system dynamics are basically slow since the thermal inertia of the building leads to time constants of several hours up to two days. The MPC on the energy supply level, supplying the necessary heating/cooling energy for the user level while fulfilling other conflicting goals, such as minimal costs, maximum usage of renewables and minimum wear, is affected as well by the ambient temperature and the water return temperatures of the building. The system dynamics are much faster than those of the user level. Furthermore, the HMPC is also an enabler for the interaction with a smart grid, since the two MPCs are flexible regarding varying prices and constraints possibly active due to load curtailment. The overall control structure is given in Figure 3.

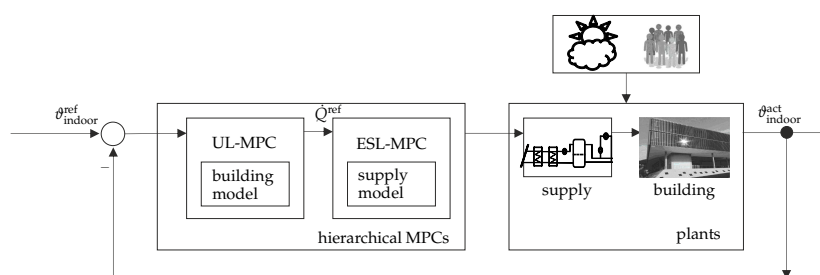


Figure 3. Hierarchical control structure with the user level (UL) MPC and the energy supply level (ESL) MPC.

The two MPCs are hierarchically operating, meaning that the optimized energy demand trajectory generated by the user level MPC \dot{Q}^{ref} is reference for the energy supply level MPC. Hence, \dot{Q} is the only coupling point.

3.2. User Level MPC

The user level MPC is employed for optimizing the user comfort and minimizing the heating and cooling energy. Since this goal can be achieved by using the orientation specific radiance and the building as passive storage, the building is divided into independently controllable zones with different orientation; see Figure 4.

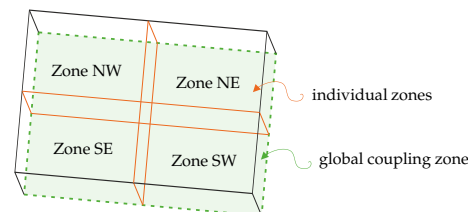


Figure 4. Example for zone splitting of the user level. The orange lines mark the individual zones, whereas the global coupling zone is surrounded in green dashed lines.

The MPC is then responsible for keeping the mean zone temperature within a predefined comfort band, taking the forecasts of the main disturbances of ambient temperature, radiance and the occupancy profile into account. While some heating or cooling systems provide energy for each zone individually, some HVAC systems supply the entire floor affecting the comfort parameter of all zones. Thus, these systems, such as ventilation systems or thermally-activated building systems (TABS), are coupling variables for all zones. In this paper, two supply systems are respected: the fan coil (FC) system supplying each zone individually and a common TABS providing all zones with heating or cooling energy. Different MPC approaches for the user level have been presented in the literature; cf. Section 2.3. However, for this study, a cooperative fuzzy MPC scheme (CFMPC) [15] is chosen, since it is most appropriate for the specific system identification approach. Depending on the seasons (winter, summer, transition), three local linear models (LLMs) are approximately characterizing the non-linearity of each zone. Note that depending on the local climate, the optimal number of LLMs can vary for a specific building. The fuzzy MPCs (FMPC) are implemented consisting of one linear MPC for each LLM, calculating the resulting control variable and the corresponding manipulated variables by applying fuzzy rules. The overall CFMPC thus includes one fuzzy MPC for each zone cooperatively acting with one global MPC for the coupling TABS control. Cooperation in this case means that two controllers, one respective FMPC of zone i and the global MPC, have to agree on one solution that is acceptable for both. This is done between all four FMPCs and the global MPC by an iterative loop with the aim that the corresponding manipulated variables converge to an optimum. Note that this approach enables flexible integration of new zones, as well as additional controlled variables: All existing MPCs can be retained without adjustments, and just the MPCs for the new parts have to be integrated in the cooperation loop.

3.2.1. Building Model

Modeling is the most time-consuming part designing a model predictive controller. Since buildings are complex processes with non-linear system dynamics, modeling is especially demanding in this field.

TS-Fuzzy Building Model

Four zones of the data-driven building model have the structure of a Takagi–Sugeno (TS)-fuzzy model. TS-fuzzy models are suitable to approximate nonlinear systems by interpolating between local linear, time-invariant autoregressive models with exogenous inputs (ARX) [24]. The basic element of a TS-fuzzy system is a set of fuzzy inference rules R^j [25]. In the following,

$\zeta = [\zeta_1, \dots, \zeta_p] \in \mathbb{R}^p$ is the vector of partition variables, and $\Xi_{j,1}, \dots, \Xi_{j,p}$ are the fuzzy sets or regions for the j -th rule \mathbf{R}^j with corresponding membership functions $\mu_{j,\Xi_1}, \dots, \mu_{j,\Xi_p}$, with $\mu_{j,\Xi_i}(\zeta_i) \mapsto [0, 1]$, for $i = 1, \dots, p$ [17]. The number of rules r_i in this work is the same as the number of local linear models (LLMs) $L_i, \forall i \in \mathbb{F}$ [17].

The elements of the fuzzy vector are usually a subset of the past input and outputs [24]. TS-fuzzy models consist of both fuzzy inference rules and local analytic linear dynamic models as follows,

$$\begin{aligned} \mathbf{R}^j: \quad & \text{IF } \zeta_1 \text{ is } F_1^j \text{ and } \dots \zeta_p \text{ is } F_p^j \\ & \text{THEN } x^{k+1} = A_j^k x^k + B_j^k u^k \\ & y^k = C_j^k x^k, \end{aligned} \quad (1)$$

where $j \in L = \{1, \dots, p\}$ denotes the number of LLMs (rules).

The degree of fulfillment of the specific j -th rule can be computed using the product operator $\mu_j(\zeta) = \prod_{i=1}^p \mu_{j,\Xi_i}(\zeta_i)$; furthermore, the normalized degree of fulfillment can be computed as:

$$\Phi_j(\zeta) = \frac{\mu_j(\zeta)}{\sum_{l=1}^L \mu_l(\zeta)}. \quad (2)$$

The overall zone model is given as a superposition of the above defined local linear models. This superposition is achieved by weighted parameter blending of the individual system matrices over all LLMs:

$$A^k = \sum_{j=1}^L \Phi_j(\zeta) A_j^k, \quad B^k = \sum_{j=1}^L \Phi_j(\zeta) B_j^k, \quad C^k = \sum_{j=1}^L \Phi_j(\zeta) C_j^k \quad (3)$$

Each zone model of the building can thus be formally written as a time-varying linear state-space system:

$$\begin{aligned} x^{k+1} &= A^k x^k + B^k u^k \\ y^k &= C^k x^k. \end{aligned} \quad (4)$$

The global coupling zone (see Figure 4) can be modeled by a linear time-invariant state-space system represented by the matrices A_g, B_g and C_g .

Note that four building zones plus the linear coupling zone have been considered, and each TS-fuzzy zone model consists of three LLMs. Each TS-fuzzy model has five inputs and the mean room temperature of the respective zone as the output (see Figure 5).

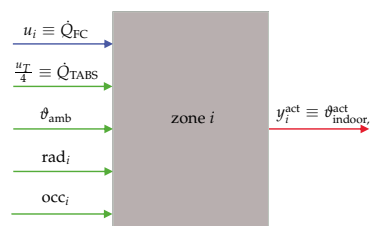


Figure 5. Input to output behavior for model identification of zone i .

Specific Building Model

For each zone of the specific building, the significant nonlinearities are given by a two-dimensional partition space spanned by the difference between heat supply and return temperatures of the manipulated variable TABS (denoted by $\Delta\theta_{\text{TABS}} = (\theta_{\text{TABS}_{\text{supply}}} - \theta_{\text{TABS}_{\text{return}}})$) and the ambient temperature (denoted by θ_{amb}). Both the choice of the partition variables and the model split have been done by expert knowledge; however, they could also be identified by a local

linear model tree algorithm (LoLiMoT) [17]. In any case, after partitioning of the measured data, classical linear identification methods like least squares can be utilized to estimate the matrices of the individual LLMs (1).

The LLMs and the specific partition space for the building are presented in Figure 6a. Note that in this building, the partition space with the model splits is identical for all zones. For more detailed information and extensive model validation, see [15,26]. It is shown there that all TS-fuzzy zone models achieve R^2 -values above 0.9 for three or more LLMs.

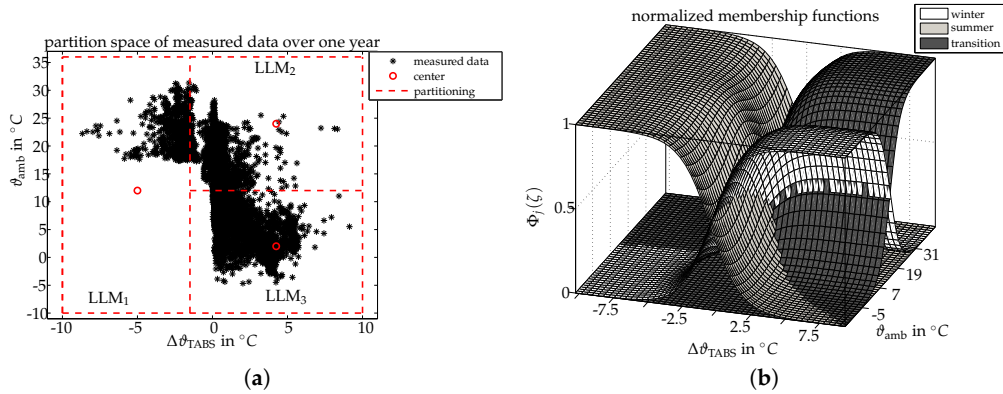


Figure 6. Two-dimensional partition space and the normalized membership function. (a) Two-dimensional partition space of the building: $(\Delta\theta_{\text{TABS}} \times \theta_{\text{amb}})$. Three local linear models (LLMs) give good performance, each corresponding to one of the seasons: 1, summer; 2, transition; and 3, winter. The measured data are represented by stars, where measured data over one year are included. (b) Normalized membership functions for one building zone (SW). Three local linear models are weighted with the shown function values depending on the ambient temperature θ_{amb} and the difference between supply and return temperatures of thermally-activated building systems (TABS) $\Delta\theta_{\text{TABS}}$.

3.2.2. Objective

The objective of the user level MPC, for each FMPC of zone $i \in \{1, \dots, 4\}$, is to maximize the user comfort and to minimize the energy demand. The resulting trade off is mathematically expressed by the quadratic objective function given in (6).

$$J_i^* = \min_{u_i} J_i(u_i) \quad (5)$$

$$J_i = \alpha \sum_{k=0}^{Np} (y_i^{\text{ref}}(k) - y_i^{\text{act}}(k))' Q_i (y_i^{\text{ref}}(k) - y_i^{\text{act}}(k)) + (1 - \alpha) \sum_{k=0}^{Np} u_i'(k) R_i u_i(k) \quad (6)$$

The control variable y_i^{act} denotes the actual mean zone temperature for the i -th FMPC and y_i^{ref} its reference value. The vector u_i represents the energy demand to be optimized for the FC system, the TABS and the given disturbances radiance and ambient temperature for zone i . The i -th FMPC calculates an optimized strategy looking Np steps ahead by minimizing the sum of the costs arising due to the deviation and the energy demand penalized with the time-invariant penalty matrices Q_i and R_i , respectively, each time step k . The optimization problem is subject to the constraints in (7) and the usage of the model introduced in the previous section. The parameter $\alpha \in [0, 1]$ is free to be

chosen by the operator in order to put either more weight on the minimization of the deviation of the user comfort parameter or on the minimization of the energy demand.

$$\begin{aligned} u_{i,\min} &\leq u_i \leq u_{i,\max} \\ y_{i,\min} &\leq y_i^{\text{act}} \leq y_{i,\max} \end{aligned} \quad (7)$$

The constraints guarantee that the optimized energy demand is kept within technically feasible limits and that the mean zone temperature does not violate a predefined comfort band. The MPC solves the corresponding optimization problem each time step k . Though the optimal strategies $U_{i,\text{FC}}^*$ for FC and U_{TABS}^* for TABS are computed for the entire prediction horizon Np , only the first elements $u_{i,\text{FC}}^*(k)$ and $u_{\text{TABS}}^*(k)$ are applied to the system, and at the next time instance, the optimization is repeated with the updated disturbances yielding a receding horizon strategy. Since the objective in (6) is a quadratic function and constraints of the form (7) have to be respected, a solver has to be chosen that is capable of solving a constrained quadratic program. For this study MATLABsolvers have been used <https://de.mathworks.com/help/optim/ug/quadratic-programming-algorithms.html>.

3.3. Energy Supply Level MPC

The energy supply level MPC is responsible for minimizing the energy costs, to maximize the usage of renewable energy sources while delivering the energy demand of the user level accurately. The energy supply level consists of several supply circuits routed from various energy sources to the supply systems incorporating heat exchangers, aggregates and water storage tanks. Figure 7 illustrates such circuits exemplarily for the fan coil (FC) supply, including free cooling, the chiller and subsequent stratified water storage tank for cooling and district heat supply for heating.

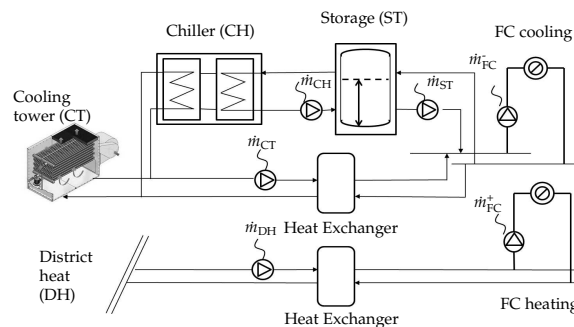


Figure 7. Fan coil (FC) circuits, including free cooling, the chiller and district heat. \dot{m} denotes the respective mass flows and ‘+’ heating, whereas ‘−’ cooling.

The proposed MPC for this level is a modular predictive control concept (MPCC) including a mixed-integer MPC (MI-MPC) [27]. This special MPC has not only all of the advantages presented in Section 2.1, but is also capable of optimizing discrete and continuous variables at the same time. This becomes necessary if the underlying system contains switching instances, such as chillers, which influence the operation mode of the subsequent storage in a discontinuous fashion. With this type of MPC, the number of transitions of the aggregates from the state off to on can be reduced significantly [28], leading to less life cycle costs due to minimal wear. The MPCC includes one MPC for each circuit, depending on the respective building’s physical structure. If supply systems are connected with circuits provided by fossil fuels, as well as by renewable energy sources, the MPCC always prefers the circuits with renewables. Given the example in Figure 7, cooling energy for FC is supplied by free cooling as long as all technical conditions such as the ambient temperature limit are fulfilled.

3.3.1. Energy Supply Model

Modeling the energy supply system for the proposed MPCC is done based on thermodynamic principles [18,20]. Circuits with heat exchangers only are treated as linear systems, approximated by linearized first order differential energy balance equations. Circuits with additional aggregates and storage are seen as hybrid systems, since the state of the aggregate δ_A affects the operation mode of the storage, such that one model is required for each mode. The resulting model is a nonlinear piecewise affine system of the following form:

$$x(t+1) = \begin{cases} A_1x(t) + B_1u(t), & \text{if } \delta_1(t) = 1 \\ A_2x(t) + B_2u(t), & \text{if } \delta_2(t) = 1 \\ A_3x(t) + B_3u(t), & \text{if } \delta_3(t) = 1, \end{cases} \quad y(t+1) = \begin{cases} C_1x(t) + D_1u(t), & \text{if } \delta_1(t) = 1 \\ C_2x(t) + D_2u(t), & \text{if } \delta_2(t) = 1 \\ C_3x(t) + D_3u(t), & \text{if } \delta_3(t) = 1, \end{cases} \quad (8)$$

with $\delta_1 \Leftrightarrow \text{charging} \wedge \delta_A = 1$, $\delta_2 \Leftrightarrow \text{discharging} \wedge \delta_A = 1$ and $\delta_3 \Leftrightarrow \text{discharging} \wedge \delta_A = 0$. Figure 8 illustrates the three basic modes: charging, discharging if the aggregate is active and discharging if the aggregate is inactive.

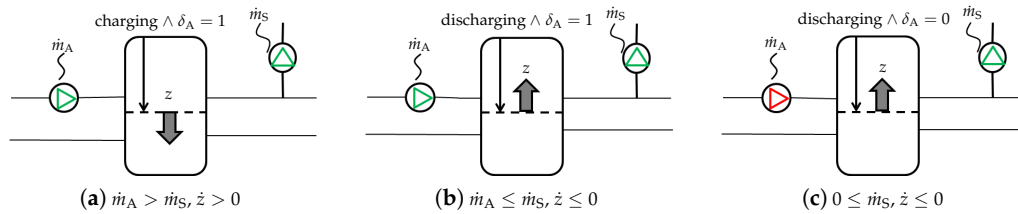


Figure 8. The three operation modes of the stratified storage tank. (a) Charging; (b) discharging while the aggregate is on; (c) discharging while the aggregate is off. \dot{m}_A denotes the mass flow from the aggregate, whereas \dot{m}_S the mass flow to the supply system. z is the thermocline of the storage.

For detailed information about the modeling, see [20], and for model validation, the reader is referred to [28].

3.3.2. Objective

For the MPC implementation, a quadratic optimization target is used, where the deviation to the reference trajectory of the cooling respective heating power is penalized with factor S . Furthermore, the energy costs represented by T_k , caused by the manipulated variables (mass flows of the pumps) are taken into account. Note that the penalty matrix T depends on the time instance k , meaning that varying prices can be respected. Both additive terms are considered for each time step k over the whole prediction horizon Np . The parameter α is again a weighting factor, which can be modified easily by the operator in order to shift the importance between the accuracy of the delivered power and the energy costs. The formal description of the objective is given by:

$$J^* = \min_{u \in U} \left[\alpha \sum_{k=0}^{Np} (\dot{Q}_j^{\text{ref}}(k) - \dot{Q}_j^{\text{act}}(k))' S (\dot{Q}_j^{\text{ref}}(k) - \dot{Q}_j^{\text{act}}(k)) + (1 - \alpha) \sum_{k=0}^{Np} u'(k) T_k u(k) \right], \quad (9)$$

where $j \in \{\text{FC}, \text{TABS}\}$ determines the supply system, and the vector u_j represents the manipulated variables, such as mass flows and supply temperatures to be optimized for the supply of the FC system and the TABS.

$$\begin{aligned} u_{j,\min} &\leq u_j \leq u_{j,\max} \\ x_{j,\min} &\leq x_j \leq x_{j,\max} \end{aligned} \quad (10)$$

The optimization problem with the target given in (9), the hybrid model introduced in (8), with constraints on the manipulated variables, and the states given in (10) result in a mixed-integer quadratic problem, which can either be solved by commercial solvers, such as [29], or approximated by, e.g., branch and bound algorithms, such as introduced in [28].

Note that the prediction horizon N_p for the energy supply level MPC is shorter than the one for the user level MPC (6 h versus 25 h) since the time constants are much smaller in the energy supply level.

4. Simulation Results

The performance of the HMPC for sustainable building automation is demonstrated based on the example of a large office building in Salzburg, Austria. The description of the demonstration building is given including the currently active PID control structure and the HMPC integration in the building automation system (BAS) before the simulation results are shown regarding the requirements set up in Section 2.1. All building and energy supply models have been identified, respectively implemented in MATLAB. The HMPC implementation, as well as the simulation have also been conducted in MATLAB.

4.1. Demonstration Building

The demonstration building for this study is a 27,000 m² University building in the center of Salzburg, Austria. It has five floors above ground containing several large and numerous smaller meeting rooms, offices and lecture rooms. For this work, focus is put on the second and third floor, which is comprised of about 500 rooms of some 13,000 m², almost all used as offices. Both floors are supplied by fan coils (FC) and a thermally-activated building system (TABS) coupling the four zones; see Figure 4. The energy supply system of this building consists of heating and cooling supply circuits for FC (see Figure 7) and TABS. The FC system is provided energy from district heat and cooling energy from free cooling or the chiller, whereas the geothermal source supplies the TABS including a heat pump in the case of heating. The results presented in the following sections are based on simulation results, but the HMPC concept is already in the test phase implemented in the demonstration building's automation system. The simulation is shown for representative snapshots of the three seasons: transition periods (13 April–12 May 2014 and 16 October–15 November 2014), summer (4 July–11 August 2014) and winter (19 January–28 February 2015). The corresponding historic data for disturbances and comparison analysis are taken from the implemented building automation system.

4.1.1. State-Of-The-Art PID Control Structure

The state-of-the-art PID-control structure designed for and currently active in the demonstration building consists of PIDs together with RBC loops. In the user level PID control, the room temperatures are based on the comfort requirements of the users. In the energy supply level, all supply temperatures are controlled by individual PIDs. The set-points are calculated in the PLC by comparing the recent past of the ambient temperature to a predefined skid. The mass flows of the corresponding supply pumps are kept constant. Switching on and off the heat pump, respectively the chiller, is decided in an RBC loop where fixed temperature limits of the stratified storage tanks are respected. Figure 9 shows the PID controllers and RBC loops within the overall building automation system.

4.1.2. HMPC Integration in the Building Automation System

The implementation of the proposed structure in existing building automation systems (BAS) is straightforward. Basically, it can be seen as part of an extended supervisory control and data acquisition (SCADA) system. As shown in Figure 9, the conventional function of (mainly feedforward) set-point generation for the underlying PID and RBC loops is replaced by the proposed

hierarchical structure. The MPCC replaces some of the local control loops; nevertheless, in most cases, the existing local control loops with their respective safety functions can be utilized. Note that disturbances (weather and occupancy) are explicitly considered by predictions.

Both CFMPC and MPCC can be directly integrated in the SCADA system, as the functions of a flexible programming structure are given in the BAS. Another solution is possible by setting up a dedicated hardware and software for the predictive controllers, which communicate by standard interfaces with the SCADA system and local controllers.

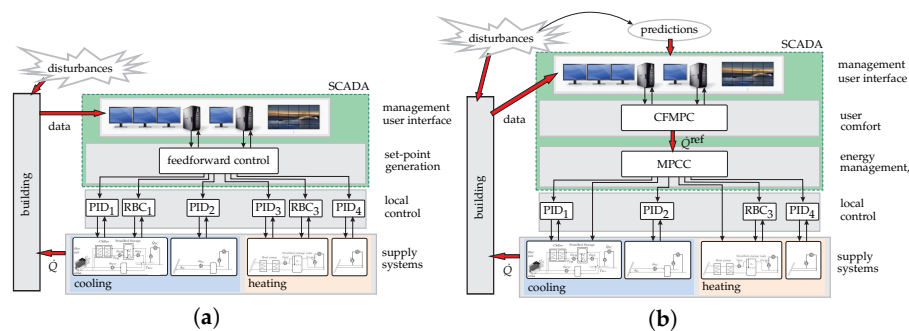


Figure 9. (a) Conventional building automation system (BAS) and (b) proposed hierarchical structure. In (a) set-points for the underlying control loops are generated by feedforward control as part of the SCADA system. In (b) a CFMPC computes the necessary heating/cooling \dot{Q}^{ref} for user comfort, and the actual heating/cooling \dot{Q} transferred to the building is optimally provided by the MPCC. Both CFMPC and MPCC are part of the updated SCADA-system.

4.2. User Satisfaction

User satisfaction in terms of sustainable building automation primarily means fulfillment of user comfort requirements. The user level MPC, here represented by the CFMPC, is capable of predicting the energy needed for the individual zones in order to keep the respective mean zone temperature not only within the comfort band, but around a predefined reference value. The comfort band for this simulation has been chosen with a tolerance of ± 2 °C of the reference value individually for each zone. Figure 10a–c shows the simulation results for the three seasons.

The plots show the reference, as well as the mean zone temperature for the four zones respectively. For all periods, the thermal comfort is guaranteed with little deviation to the constant reference value and, thus, all times within the comfort band. One can see a higher frequency in summer arising due to the higher amplitude of the radiation in summer compared to the other periods. Figure 10d shows the ambient temperature for the respective season. All disturbances are taken from snapshots of the Central Institute for Meteorology and Geodynamics in Salzburg, ZAMG. The occupancy profile is generated generically as in [15] according to the occupancy pattern for offices adapted from [30].

User satisfaction is also affected by the degree of individual control of users' respective operators. Therefore, the automation system has to enable an easy and intuitive adjustment of optimization settings. One of these parameters is $\alpha \in [0, 1]$ representing how much emphasis is either put on the thermal comfort satisfaction or on the cost minimization in the energy supply level MPC's objective. In order to demonstrate the consequence of the variation, simulation runs are conducted with α varying from 0.1–0.9. The results are given in Table 1 in terms of resulting quadratic costs and the mean absolute error (MAE) of the MPC output to the reference value for the three seasons. The building requires on average about 550 kW of cooling power in summer and 750 kW of heating power in winter. The higher α , the higher the (energy) costs and the less the error of the energy supply to the energy demand of the user level. Note that in winter, the error is generally much smaller since the energy demand from the user level is less volatile. For an industrial application, a cost reduction

is preferable, leading to a small α , which can be recommended in this case since the MAE does not vary a lot. Note that the energy costs are calculated by considering the electric effort of all pumps according to their characteristic curves, as well as the chiller with a coefficient of performance of 3.9. For more details, see [28].

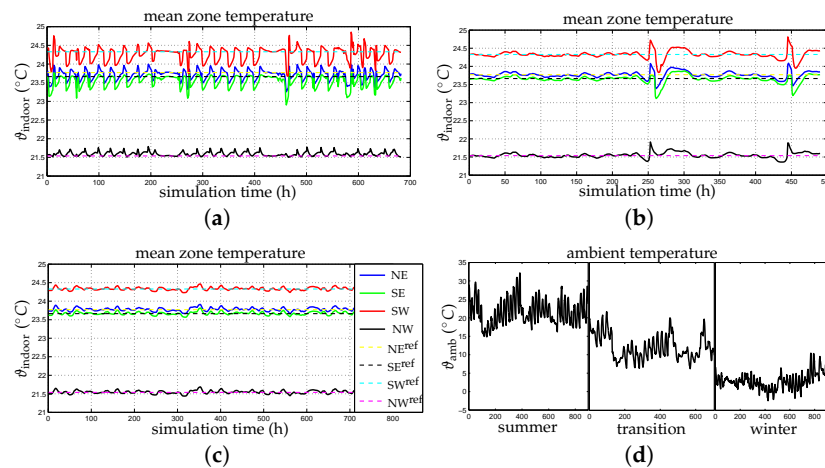


Figure 10. User level MPC results for all zones and seasons. (a) Simulation results for summer; (b) simulation results for transition; (c) Simulation results for winter; (d) ϑ_{amb} of summer, transition and winter.

Table 1. Simulation results in terms of costs and MAE (kW) for varying weighting parameter α .

α	Summer		Transition		Winter	
	Costs (10^6)	MAE	Costs (10^6)	MAE	Costs (10^6)	MAE
0.1	4.4253	2.28	1.63540	0.26	2.0305	0.014
0.5	4.4266	2.27	1.63542	0.25	2.0302	0.002
0.9	4.4267	2.26	1.63929	0.22	2.0340	0.000

4.3. Energy Efficiency

The HMPC enables an energy-efficient building operation due to the minimization of energy demand in the user level and due to maximal usage of renewable energy sources in the energy supply level. Free cooling is the representative renewable source for this study addressable in the demonstration building. Figure 11 shows the active free cooling hours according to the strategy of the HMPC and the currently-implemented PID controller in the building for spring (transition 1), summer, autumn (transition 2) and winter.

The results show a big potential for the transition period, as well as summer, since the MPCC is capable of predicting time slots of ambient temperature below the technical limit, whereas the PID controller only reacts on weather data from the past. For the entire simulation period, an additional 221 active free cooling hours have been achieved, which means an overall increase of 11%. However, for the transition periods, up to 25% more free cooling hours become feasible with the HMPC. Note that the high amount of cooling hours in winter is a result of continuous cooling of the server rooms. The total number of cooling hours in summer is 694 with the MPCC or 684 with the PID control. Further simulation results have been presented in [28], where additionally explicit costs and the cooling energy provided by free cooling are compared, resulting in about 50% less electric energy costs for cooling and the double amount of cooling energy supplied via free cooling for the transition month of May.

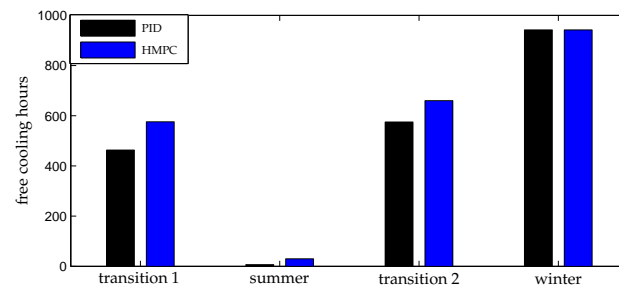


Figure 11. Free cooling hours of simulated hierarchical (HMPC) compared to the implemented PID controller.

Figure 12 shows the difference between the control strategy of the PID/RBC structure and the proposed HMPC concept. All data concerning the PID/RBC results are taken from the demonstration building's BAS database. The first subplot shows the ambient temperature. Note that the days are often quite hot, and the nights remain chilly, which can be considered as a sudden drop concerning the time constants of the building, such as demonstrated in Figure 2. The second subplot shows the differences of the cooling supply strategy. The HMPC pre-cools the building during night where the electric energy is less expensive, whereas the PID structure reacts if the ambient temperature gets hotter for some hours. The third subplot shows the resulting indoor zone temperature. Note that the HMPC can keep the temperature in the comfort band (marked with the gray lines) over the entire simulation period, but the PID sometimes violates it; see the blue marked spots. Furthermore, the HMPC reduces the variance significantly. The last subplot shows when the PID, respectively the HMPC, activates the supply via free cooling. At hours 130 and 173, the PID violates the rule that free cooling must not be activated if the ambient temperature is higher than 18 °C, whereas the HMPC uses all possible periods for free cooling by meeting this requirement.

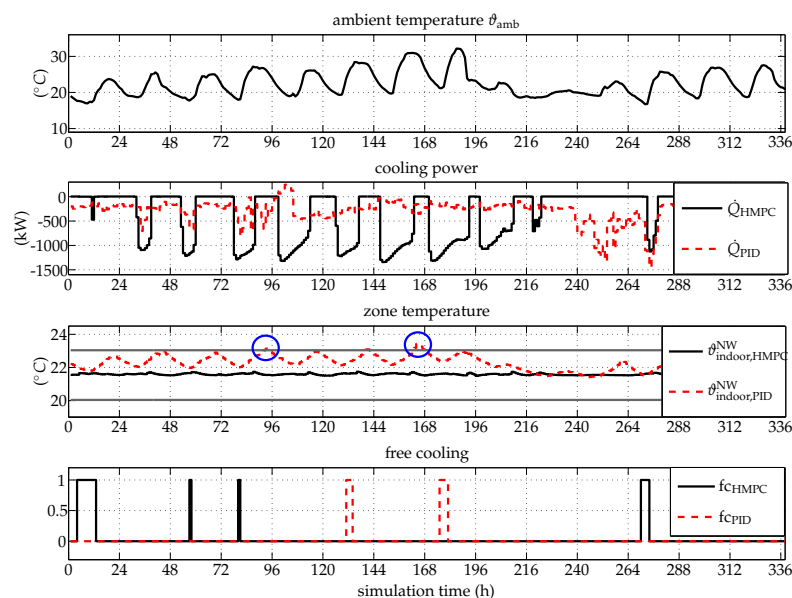


Figure 12. Comparison of PID and HMPC for a cutout in summer 2014, starting with 13 July. The blue marked spots show where the PID violates the comfort band.

4.4. Life Cycle Costs

Life cycle assessment for buildings is generally a demanding task [2]. Nevertheless, reducing costs for energy supply systems in operation and maintenance is an effective means. Applying an MPC with the optimization target presented in Section 3.3.2 minimizes the wear of aggregates, such as chillers or heat pumps. For this simulation study, the number of transitions from state off to state on from the chiller is the reference measure. Figure 13 shows the simulation results compared to the measured transitions resulting from the PID control decision in the respective seasons.

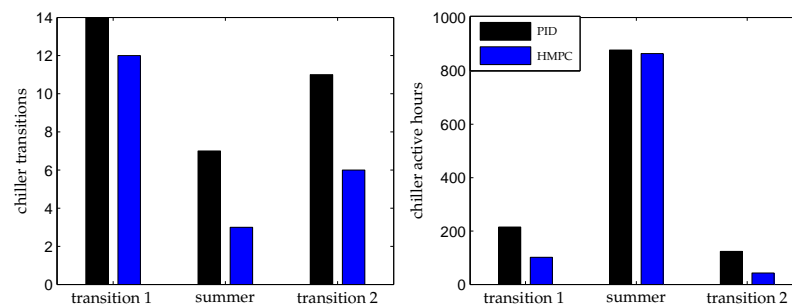


Figure 13. Chiller active hours and transitions of simulated HMPC compared to the implemented PID controller.

The number of active chiller hours can be reduced by 206 h or 17%, and simultaneously, the number of transitions from state off to state on can be reduced by 11% or 35% with the MPCC for the entire simulation period. However, the results for individual seasons are much more promising, such as a reduction of chiller transitions of up to 50% in autumn and spring. Note that in winter, the chiller has not been active, since free cooling could be activated all of the time.

4.5. Flexibility towards the Smart Grid

Demand response programs vary in their price or incentive options, but in general, accepting load shift or curtailment is monetarily beneficial for building operators. For this simulation study, the winter period is considered. The exemplary price profile is based on fixed rates depending on the time of day; see Figure 14a. For the high-peak hours in the morning, at noon and in the evening, higher prices are accepted, but in turn, the price is lower (€1.0/kWh) than the constant price of €1.2/kWh for all other hours. The energy supply level MPC predictively incorporates the varying prices and optimizes the strategy such that more energy is demanded if the price is low and less if it is high. The resulting costs are therefore a little higher during the more expensive hours, but lower for the less expensive periods compared to the MPC results with a time-invariant price profile. Figure 14b shows a snapshot of the difference of the costs from the MPC simulations with a constant and a varying price profile, resulting in an overall cost reduction of 14% or €3.230 only for the heating TABS supply in winter. For the same high-peak hours, load curtailment is demanded at lower electricity costs. Figure 14c shows this requirement for the TABS supply represented by upper constraints in gray dashed lines. The user level MPC is capable of adjusting the strategy taking the load curtailment as a time variant input constraint into account (see the pink line), while still guaranteeing the desired user comfort over the entire simulation period; see Figure 14d.

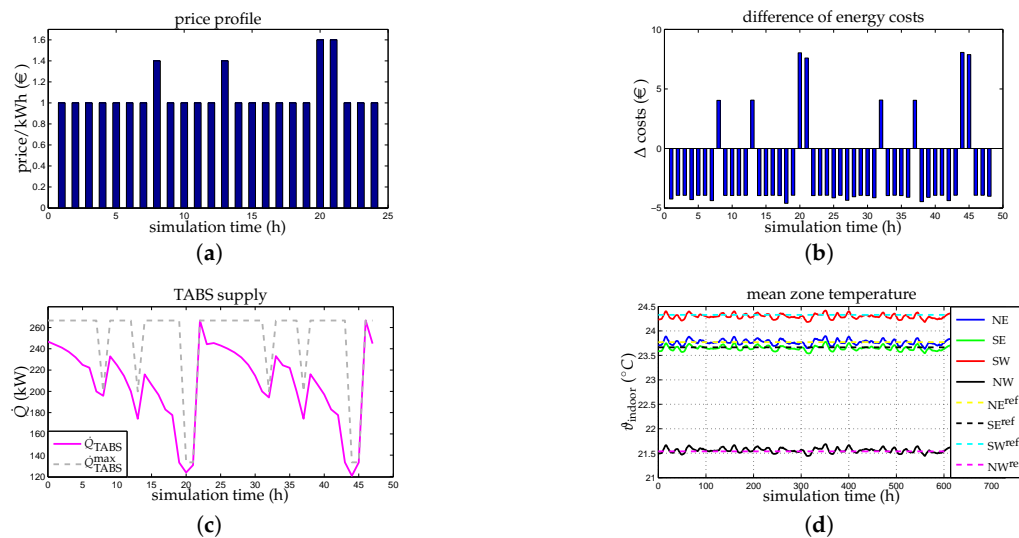


Figure 14. Simulation study for flexible pricing and load curtailment for smart grid integration. (a) Price profile with fixed rates for 24 h; (b) Δ costs for constant and varying prices; (c) load curtailment on TABS supply; (d) user comfort with load curtailment.

5. Discussion

In this section, the results are discussed, and possible obstacles and necessary measures are given for the industrial usage of the proposed MPC concept.

5.1. Perspectives

In Section 2.1, Figure 1, the interaction of building automation with the most important groups is illustrated. In the following sections, the simulation results are discussed from the perspective of the buildings' users, operators, investors and the smart grid.

5.1.1. User Perspective

Users judge the performance of building automation systems particularly in terms of thermal comfort. The simulation results in Section 4.2 show that a predictive control concept is capable of guaranteeing high user comfort with less energy demand. Even if load curtailment is accepted at some hours a day, the user comfort is kept within the predefined comfort band as illustrated in Section 4.5. Sustainability for users also means the opportunity to adjust certain comfort parameters by themselves. The objective function as a key element of MPCs is changeable within the building automation system. Thus, some tuning parameters can easily be disclosed for the users or operators. In Section 4.2, Table 1, the effect of changing the parameter α shows that the trade off between costs and thermal comfort can be regulated to some degree by the user. Note that different set-points for different zones are possible without compromising the overall optimum.

5.1.2. Operator Perspective

Operators are mainly interested in a reduction of costs, including life cycle costs. In Section 4.3, it is shown that the energy supply level MPC maximizes the usage of free cooling, which is in relation to other (fossil) sources a significantly less expensive solution. Thus, in building operation, energy efficiency is equivalent to cost efficiency. Regarding the life cycle costs the proposed energy supply level MPC reduces the aggregates' wear and therefore maintenance effort by decreasing the aggregates' transitions by 15%–50% compared to conventional PID control depending on the season. Additionally, the aggregates are less used if other (less expensive) sources are available. Thus, the

chiller has 17% less active hours over the year. In Section 4.5, it is shown that the energy supply level MPC can additionally take advantage of varying prices by saving up to 10% for the chosen price profile.

5.1.3. Smart Grid Perspective

Smart grids demand smart buildings with the capability to deal with varying prices, demand response and load curtailment. The results in Section 4.5 clearly show that the HMPC concept meets these requirements and becomes therefore beneficial for a smart grid integration and simultaneously for a reduction of energy costs.

5.1.4. Investor Perspective

Providing sustainable construction with infrastructure, such as free cooling or geothermal source, is expensive. However, investors can expect a value added building if sustainable building automation is implemented, and a return on invest is possible since the infrastructure can be used efficiently. Moreover, the added flexibility of the proposed HMPC concept results in a robust building automation system, easily adaptable to future demands. It is thus also a contribution to risk mitigation.

5.2. Possible Obstacles and Necessary Measures

Several simulation studies [10,31], as well as the first prototypes of MPC implementations for large non-residential buildings [32] show the performance and the readiness level for industrial solutions of this intelligent control scheme. Nevertheless, some obstacles might complicate successful implementations and future market penetration. In the following sections, possible obstacles are addressed, and necessary measures are given.

5.2.1. Trained Personnel

An industrial usage of MPC as a key component in building automation requires the automation suppliers to employ experts in the field of building modeling and experienced control engineers for MPC design and implementation. The availability of competent and trained experts in this field may be the real bottleneck for market penetration. On the other side, also operating personnel are necessary who are willing to apply advanced control approaches not commonly used. For retrofitting projects, it has been proven advisable to involve operators early in the control design and implementation phase in order to integrate their knowledge of the process and the building's specifics on the one side and to let them participate on the engineering progress to dismantle the fear from the new technique on the other side.

5.2.2. Data Acquisition

Building modeling is a crucial part for the MPC's performance. Hence, for model identification, historic data from the building in operation are essential. The more powerful the automation system is regarding the data base structure, data acquisition and archiving, the better the basis for the resulting models. If input data or data from disturbances are missing or not appropriately assignable to its timestamps, the model quality may be poor. Therefore, the accessibility of sensors, as well as of, for instance, weather data from external systems is important.

5.2.3. Hardware Requirements

The proposed MPC approach works with existing building infrastructures for heating and cooling supply. However, the performance depends on the availability of information of the energy supply and building process. For the closed loop control of thermal comfort parameters, it is necessary to obtain actual measures of indoor room temperatures, energy supply to the respective zones, water supply and return temperatures, mass flows of pumps, etc. This requires the

implementation, availability and integration of the corresponding sensors to the building automation system. In turn, all actuators, such as pumps or valves must be addressable in order to execute new set-points computed by the MPC.

6. Conclusions

The paper has presented a hierarchical model predictive controller (HMPC) for sustainable building automation. The proposed MPC structure sustainably affects the directly influenced groups, such as users, operators, investors, the environment or the power grid. The HMPC is capable of maximizing user comfort and the usage of renewable energy sources while minimizing energy demand and costs for buildings in operation. Additionally, it allows the integration of the resulting smart building in the smart grid. Furthermore, due to the HMPCs flexibility, changing legislative requirements can easily be applied with little investment, since only the optimization target of the HMPC has to be adapted. For example, a time-variant constant proportion of renewable energy sources can be guaranteed. The performance of the exemplarily proposed HMPC is demonstrated regarding the demands of the respective group by simulation results of a modern office building. For users, thermal comfort is guaranteed throughout all seasons, and the variation of a user-adjustable parameter shows the resulting trade off between user comfort and energy costs. Operators benefit monetarily from energy-efficient strategies and lower life cycle costs, since free cooling is used up to 25% more often than by the conventional PID controller instead of more expensive fossil sources. Furthermore, the aggregates' wear is minimized due to a reduction of transitions from state off to on of up to 50%. Furthermore, an easy smart grid integration is possible, since the predictive character of the MPC is ideal to take advantage of flexible prices and to meet temporarily active load curtailment without violating the thermal comfort band. Finally, possible obstacles for a successful implementation of MPC in building automation are addressed, and necessary measures for a prosperous industrial development of MPC for sustainable building automation are given.

Acknowledgments: This work was supported by the project “SMART MSR” (FFG, No. 832103) in cooperation with evon GmbH.

Author Contributions: This study was carried out by Barbara Mayer under the supervision of Martin Kozek. The HMPC was developed by Michaela Killian (user level MPC) and Barbara Mayer (energy supply level MPC) under the supervision of Martin Kozek. This paper has been written by Barbara Mayer and proof read by Michaela Killian. The data were analyzed by Michaela Killian and Barbara Mayer under the supervision of Martin Kozek.

Conflicts of Interest: The authors declare no conflict of interest.

References

1. European Commission. “Buildings”. Available online: <https://ec.europa.eu/energy/en/topics/energy-efficiency/buildings> (accessed on 14 May 2016).
2. Khasreen, M.M.; Banfill, P.F.G.; Menzies, G.F. Life-Cycle Assessment and the Environmental Impact of Buildings: A Review. *Sustainability* **2009**, *1*, 674–701.
3. Waddicor, D.A.; Fuentes, E.; Sisó, L.; Salom, J.; Favre, B.; Jiménez, C.; Azar, M. Climate change and building ageing impact on building energy performance and mitigation measures application: A case study in Turin, northern Italy. *Build. Environ.* **2016**, *102*, 13–25.
4. Siano, P. Demand response and smart grids—A survey. *Renew. Sustain. Energy Rev.* **2014**, *30*, 461–478.
5. Bragança, L.; Mateus, R.; Koukkari, H. Building Sustainability Assessment. *Sustainability* **2010**, *2*, 2010–2023.
6. Dounis, A.I.; Caraiscos, C. Advanced control systems engineering for energy and comfort management in a building environment—A review. *Renew. Sustain. Energy Rev.* **2009**, *13*, 1246–1261.
7. Maciejowski, J.M. *Predictive Control: With Constraints*; Pearson Education: Upper Saddle River, NJ, USA, 2002.
8. Camacho, E.F.; Alba, C.B. *Model Predictive Control*; Springer Science & Business Media: Berlin, Germany, 2013.

9. Oldewurtel, F.; Parisio, A.; Jones, C.N.; Gyalistras, D.; Gwerder, M.; Stauch, V.; Lehmann, B.; Morari, M. Use of model predictive control and weather forecasts for energy efficient building climate control. *Energy Build.* **2012**, *45*, 15–27.
10. Široký, J.; Oldewurtel, F.; Cigler, J.; Přívara, S. Experimental analysis of model predictive control for an energy efficient building heating system. *Appl. Energy* **2011**, *88*, 3079–3087.
11. Shahzad, S.S.; Brennan, J.; Theodossopoulos, D.; Hughes, B.; Calautit, J.K. Building-Related Symptoms, Energy, and Thermal Control in the Workplace: Personal and Open Plan Offices. *Sustainability* **2016**, *8*, 331.
12. Miletić, M.; Schirrer, A.; Kozek, M. Load management in smart grids with utilization of load-shifting potential in building climate control. In Proceedings of the 2015 International Symposium on Smart Electric Distribution Systems and Technologies (EDST), Vienna, Austria, 8–11 September 2015; pp. 468–474.
13. Afram, A.; Janabi-Sharifi, F. Theory and applications of HVAC control systems—A review of model predictive control (MPC). *Build. Environ.* **2014**, *72*, 343–355.
14. Moroşan, P.D.; Bourdais, R.; Dumur, D.; Buisson, J. Building temperature regulation using a distributed model predictive control. *Energy Build.* **2010**, *42*, 1445–1452.
15. Killian, M.; Mayer, B.; Kozek, M. Cooperative fuzzy model predictive control for heating and cooling of buildings. *Energy Build.* **2016**, *112*, 130–140.
16. Přívara, S.; Cigler, J.; Váňa, Z.; Oldewurtel, F.; Sagerschnig, C.; Žáčková, E. Building modeling as a crucial part for building predictive control. *Energy Build.* **2013**, *56*, 8–22.
17. Nelles, O. *Nonlinear System Identification: From Classical Approaches to Neural Networks and fuzzy Models*; Springer Science & Business Media: Berlin, Germany, 2001.
18. Ma, Y.; Kelman, A.; Daly, A.; Borrelli, F. Predictive control for energy efficient buildings with thermal storage. *IEEE Control Syst. Mag.* **2012**, *32*, 44–64.
19. Berkenkamp, F.; Gwerder, M. Hybrid model predictive control of stratified thermal storages in buildings. *Energy Build.* **2014**, *84*, 233–240.
20. Mayer, B.; Killian, M.; Kozek, M. Management of hybrid energy supply systems in buildings using mixed-integer model predictive control. *Energy Convers. Manag.* **2015**, *98*, 470–483.
21. Oldewurtel, F.; Jones, C.N.; Parisio, A.; Morari, M. Stochastic model predictive control for building climate control. *IEEE Trans. Control Syst. Technol.* **2014**, *22*, 1198–1205.
22. Schirrer, A.; Konig, O.; Ghaemi, S.; Kupzog, F.; Kozek, M. Hierarchical application of model-predictive control for efficient integration of active buildings into low voltage grids. In Proceedings of the 2013 Workshop on Modeling and Simulation of Cyber-Physical Energy Systems (MSPES), Berkeley, CA, USA, 20 May 2013.
23. Parisio, A.; Rikos, E.; Tzamalís, G.; Glielmo, L. Use of model predictive control for experimental microgrid optimization. *Appl. Energy* **2014**, *115*, 37–46.
24. Abonyi, J. *Fuzzy Model Identification for Control*; Birkhauser Boston: Cambridge, MA, USA, 2002.
25. Takagi, T.; Sugeno, M. Fuzzy identification of systems and its applications to modeling and control. *IEEE Trans. Syst. Man Cybern.* **1985**, *SMC-15*, 116–132.
26. Killian, M.; Mayer, B.; Kozek, M. Effective fuzzy black-box modeling for building heating dynamics. *Energy Build.* **2015**, *96*, 175–186.
27. Mayer, B.; Killian, M.; Kozek, M. Modular Model Predictive Control Concept for Building Energy Supply Systems: Simulation Results for a Large Office Building. In Proceedings of the EUROSIM, Oulu, Finland, 12–16 September 2016.
28. Mayer, B.; Killian, M.; Kozek, M. A branch and bound approach for building cooling supply control with hybrid model predictive control. *Energy Build.* **2016**, *128*, 553–566.
29. Gurobi Optimization. *Gurobi Optimizer Reference Manual*; Gurobi Optimization, Inc.: Houston, TX, USA, 2016.
30. Chang, W.K.; Hong, T. Statistical analysis and modeling of occupancy patterns in open-plan offices using measured lighting-switch data. *Build. Simul.* **2013**, *6*, 23–32.

31. Oldewurtel, F.; Sturzenegger, D.; Morari, M. Importance of occupancy information for building climate control. *Appl. Energy* **2013**, *101*, 521–532.
32. Sturzenegger, D.; Gyalistras, D.; Morari, M.; Smith, R. Model predictive climate control of a swiss office building: Implementation, results, and cost-benefit analysis. *Control Systems Technology. IEEE Trans. Control Syst. Technol.* **2015**, *24*, 1–12.



© 2017 by the authors; licensee MDPI, Basel, Switzerland. This article is an open access article distributed under the terms and conditions of the Creative Commons Attribution (CC BY) license (<http://creativecommons.org/licenses/by/4.0/>).

2.4 Publication D

Michaela Killian, Barbara Mayer, and Martin Kozek.

Cooperative fuzzy model predictive control for heating and cooling of buildings.

Energy and Buildings, Volume 112, 2016, pages 130–140, ISSN: 0378-7788.

DOI: 10.1016/j.enbuild.2015.12.017

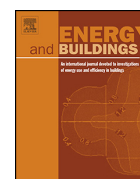
Own Contribution

Problem statement, selection of methods and algorithms for modeling, control design, implementation and simulation, as well as structuring, writing and editing the paper was done by the first author under the supervision of the third author and mentor. Discussion of methodology and results as well as editing and proof read was done by the applicant and second author.



Contents lists available at ScienceDirect

Energy and Buildings

journal homepage: www.elsevier.com/locate/enbuild

Cooperative fuzzy model predictive control for heating and cooling of buildings

M. Killian^{a,*}, B. Mayer^b, M. Kozek^a^a Vienna University of Technology, Institute of Mechanics and Mechatronics, Getreidemarkt 9, 1060 Vienna, Austria^b FH Joanneum, Werk-VI-Strasse 46, 8605 Kapfenberg, Austria

ARTICLE INFO

Article history:

Received 10 July 2015

Received in revised form

10 December 2015

Accepted 11 December 2015

Available online 14 December 2015

Keywords:

Grey-box modelling

Fuzzy MPC

Cooperative FMPC

Building control

ABSTRACT

This paper presents a cooperative fuzzy model predictive control (CFMPC) for heating and cooling of buildings. Because of different supply zones, the large time constants and the non-linear building dynamics with respect to the different seasons, a CFMPC concept is proposed. The overall non-linear building is split into different zones, which are consisting of input-coupled Takagi-Sugeno (TS)-fuzzy models. Each such TS-fuzzy model is constituted by a local linear model network (LLMN). The LLMN consists of local linear models (LLM), which are representing the different seasons: winter, transition season (fall and spring), and summer. The control of each LLM is realized by model predictive control (MPC). For each building zone the associated MPCs are output-blended by the fuzzy membership functions, which leads to fuzzy model predictive control (FMPC). In addition to the FMPCs a global MPC is controlling the thermally activated building systems, which affect all other zones. To coordinate the different controllers a cooperative iteration-loop is assumed, which leads to cooperative fuzzy model predictive control (CFMPC). The concept is developed for a specific demonstration building and can be easily adapted for other complex buildings. A simulation example demonstrates that the proposed CFMPC achieves a performance increase with less energy consumption, as compared to FMPC controllers and historical measured data of the demonstration building.

© 2015 Elsevier B.V. All rights reserved.

1. Introduction

1.1. Motivation and contribution

Energy efficient climate control is an important current task, hence there has been a growing rethinking in energy savings. The building sector accounts for about 40% of the total energy consumption [1]. In order to guarantee user comfort in complex office-buildings an intelligent automation system has to be implemented. Such controversial optimization problems, as minimizing energy cost while maximizing user comfort, are suitable for model predictive control (MPC). Furthermore, external disturbances for buildings as weather (ambient temperature and radiance) can be explicitly handled by MPCs. Also internal disturbances caused by occupancy, large time-delays caused by the building's heat capacity, strong couplings between different supply zones, and

constraints in all variables can be incorporated in the MPC optimization. This complete coverage of the control problem together with the possibility to directly balance the trade-off between comfort and energy saving makes a strong point for MPC in building automation. Since one of the most time-consuming parts for the design of model-based controllers is the model design [2], it is essential to choose the best fitting model structure. Therefore, this work presents a grey-box modelling method for buildings, which approximates the non-linear building behaviour with local linear models (LLM). This non-linear behaviour is mainly caused by the seasonal changes in building dynamics, which is especially important when designing indoor-room temperature control for both heating and cooling. Conventional non-predictive control concepts can robustly compensate these non-linearities only by accepting performance losses. The standard in building control is currently rule-based control utilizing expert knowledge combined with PID-control for manipulated variables [3]. In order to avoid this disadvantage non-linear concepts such as fuzzy predictive control have to be employed. Because of the aforementioned large time constants the combination with MPC is favourable. The use of LLMs lead to a special type of non-linear MPC (NMPC),

* Corresponding author.

E-mail addresses: michaela.killian@tuwien.ac.at (M. Killian), barbara.mayer@fh-joanneum.at (B. Mayer), martin.kozek@tuwien.ac.at (M. Kozek).

Nomenclature

ARX	auto-regressive model with exogenous input
CFMPC	cooperative FMPC
FC	fan coil
FMPC	fuzzy MPC
$h_{F_i}^q$	cooperative iteration-update of zone i
h_r^q	cooperative iteration-update of coupling zone
k_σ	steepness of the membership function
LLM	local linear model
LLMN	local linear model network
LoLiMoT	local linear model tree
\dot{m}	mass flow in $\text{kg} \cdot \text{s}^{-1}$
MISO	multi-input single-output
MPC	model predictive control
NARX	non-linear ARX
NE	north-east
NMPC	non-linear MPC
NW	north-west
occ_i	occupancy of zone i in %
\dot{Q}_{F_i}	heat flow of zone i in kW
\dot{Q}_T	heat flow of coupling zone in kW
\dot{Q}_Σ	sum of all heat flows in kW
rad_i	radiance of zone i in W/m^2
SE	south-east
SW	south-west
TABS	thermally activated building system
TS	Takagi-Sugeno
ϑ_{amb}	ambient temperature in K
y_i^{act}	actual indoor room temperature of zone i in K
y_i^{ref}	reference indoor room temperature of zone i in K
\bar{y}^{act}	actual mean indoor room temperature in K
\bar{y}^{ref}	reference mean indoor room temperature of coupling zone in K
$\Delta \vartheta_j$	difference between heat flow and heat return for supply source j

the so-called fuzzy MPC (FMPC) [4]. If several zones of a building are controlled by dedicated FMPCs a coordinated controller scheme provides additional advantages. In order to coordinate different buildings zones, including coupling zones, a cooperative FMPC (CFMPC) is introduced. In addition, the proposed models for the CFMPC cover all seasons, hence, heating as well as cooling are shown for a specific demonstration building. Building climate control in general includes several systems as heating, ventilation and air conditioning (HVAC) systems, lighting systems, and many more.

In this work the focus is put on the control of indoor-room temperature, which is controlled by both fan coils (FC) and thermally activated building system (TABS). The proposed concept is applicable to other control configurations; especially if ventilation and air conditioning (VAC) significantly contributes to indoor-room temperature it must be included in the control concept as an additional manipulated variable.

The main contributions of this work are for one thing non-linear grey-box models, which are valid for all seasons (heating and cooling). In addition, the second main part of the work is the cooperative FMPC structure. This CFMPC provides a novel, more flexible and intelligent opportunity for temperature control of the office rooms of a complex multi-zone building. The scope of the control design is to provide separate FMPC controllers independently designed for each building zone, and to incorporate the strong coupling of the activated concrete core by a cooperative scheme. A comparison between a rule-based PID-controller [3] and two

predictive controllers (linear MPC and fuzzy MPC) is performed in this work.

1.2. State-of-the-art system identification

Classical system identification algorithms are useful in the case of MPC [5]. Black-box models are known as purely data-driven models. Such a data-driven algorithm is the local linear model tree (LoLiMoT) algorithm, which has been introduced in [6,7]. LoLiMoT approximates non-linear systems with LLMs, which leads to an overall fuzzy model. Another black-box method for building models are subspace identification methods, like n4SID, which provides a model in state-space form [2], this is purely linear. Furthermore, other methods as the prediction error method or a deterministic semi-physical modelling method are introduced in [2].

The next category is grey-box models. These model types are hybrid models that use simplified physical descriptions to simulate the behaviour. Model coefficients are identified based on the operating data of the building. Therefore, the combination of black-box and white-box model is called grey-box [8].

In [9], a comparison is given between black-box and grey-box models for HVAC systems. It was found that artificial neural networks perform best followed by the auto-regressive model with exogenous input (ARX) and the grey-box model. In this work, the grey-box model is based on an ARX-algorithm, but one of the most important tasks is done by expert knowledge, the choice of the so-called partition space [6]. This fact leads to a grey-box model in this work.

The last general group of models is white-box models, which are purely physical. A lot of mature white-box software tools such as EnergyPlus and TRNSYS have been widely used [8]. The choice of the model type is depending on three main factors: effort, complexity and accuracy. The cost for parameterizing of white-box models is very high, but the resulting accuracy is high as well. In the case of MPC design the order and complexity of white-box models implies an enormous effort, because of the necessary model reduction and possible problems such as underlying switching control loops. Therefore, black-box and grey-box models are more suitable for the design of MPC. In this work the grey-box approach is chosen, based on a black-box model as the incorporation of expert knowledge additionally reduces the dimension of the partition space in the LoLiMoT method [7].

The use of Takagi-Sugeno (TS)-fuzzy models is widespread for fuzzy identification [10]. These models can be extracted from LLMs and can be directly fed into the FMPC design [11]. Fuzzy identification for control in general is illustrated in [12]. FMPC using TS-fuzzy models is a smart way to use general linear MPC optimization formulations, while afterward blending the different controller outputs with a non-linear validity function [13]. In case of buildings a fuzzy modelling approach is given in [14]. Skrzanc et al. [14] have introduced two different types of modelling: theoretical and experimental. The theoretical approach is based on energy balances, which is described by differential equations.

The grey-box model, in this application, is based on TS-fuzzy models, and the controller is based on non-linear output-blending.

1.3. State-of-the-art MPC

Classical MPC approaches are presented in [15]. However, thermal behaviour of buildings is typically non-linear especially when considering both heating and cooling. As already mentioned, this work illustrates a cooperative concept including more than one FMPC (CFMPC) [16]. The authors of [17] present an energy efficient MPC for temperature control, based on a model from a simulation package. The authors of [18] use fuzzy logic-based advanced on-off control for thermal control in residential buildings. They achieved a

reduction of energy consumption while improving the control performance. The focus in [17] is on controlling the vapor compression cycle in an air-condition system, which is used for cooling. An MPC only for a building heating system is introduced in [19], in contrast to [20], where only building cooling systems are taken into account. In opposition to [17,19,20], in this work the building is controlled for heating and cooling.

In this work, not only a straight-forward FMPC for buildings is shown. A more intelligent algorithm for more than one FMPC is given, a coordinated FMPC (CFMPC) [16]. This problem formulation is similar to distributed MPCs [21], both leading to a suboptimal solution. The authors of [21] present a distributed MPC structure for thermal regulation in buildings with an inner cooperation-loop. In [21], a simulated building with 3 rooms (one room is one zone) is presented. Moreover, only heating is proposed. In contrast to [21], in this work a real demonstration building with 4 zones, each zone includes approximately 61 rooms per floor, is shown. Therefore, the complexity in the recent work is much higher and the optimization problem for all seasons is more challenging. Furthermore, in [21], only output-coupling is taken into account, which is irrelevant in sense of building temperature control where the room/zone differences are very small. It is much more complex to consider input-coupled systems, as it is presented in the recent work.

Furthermore [22], illustrates the concept of suboptimal MPCs. Scokeart et al. [22] establish conditions under which suboptimal MPCs are stabilizing. The theoretical background of cooperative MPCs is given in [23], where the theoretical assumptions are discussed and proved. In addition [24,25], introduce a hierarchical concept for MPCs, respectively FMPCs. Also in this work, such a hierarchical scheme is assumed to exist, but it is assumed that a suitable energy management system (EMS) as introduced in [26] is existing.

Added flexibility of CFMPC is given by the possibility to either add or omit specific zones of the building with minimum effort, depending on the building's current usage. Furthermore, CFMPC achieves higher control performance with slightly less energy consumption. Both stability and convergence are secured by theoretic results [16]. While many state-of-the-art MPCs in buildings just control heating or cooling systems, the presented CFMPC is able to provide control for all seasons, both in terms of heating and cooling.

The remainder of this work is structured as follows: in Section 2, a general formulation of the grey-box modelling is given and the most important tasks are introduced. A general description of the demonstration building and the final building model are given in Section 3. The methodology of cooperative fuzzy model predictive control (CFMPC) for the specific building is outlined in Section 4. Simulation and validation results are presented in Section 5, and Section 6 summarizes the results.

2. Grey-box model

It is common for modelling a process to use one of the introduced methods: white-box models, black-box models or grey-box models [9]. White-box models require the understanding of the system physics and use physical parameters for modelling the system dynamics. But these models are usually not suitable for model predictive control of buildings because of their high order and complexity. Black-box models are purely data-driven models [7].

In the recent work, grey-box models were used for modelling the building. A balance between good generalization and high accuracy is given by grey-box models. In addition, this approach validly presents a grey-box model for building control, both for heating as well as for cooling.

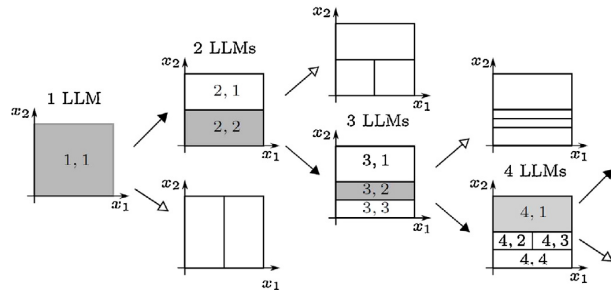


Fig. 1. First four iterations of LoLiMoT algorithm for a two-dimensional input space ($m=2$).

2.1. Grey-box model as local linear model network

In this work, a local linear model network (LLMN) approach is chosen for modelling the different building zones. The so-called local linear model tree (LoLiMoT) algorithm combines a heuristic strategy for partition space decomposition with weighted least squares optimization or output error optimization [6]. It therefore provides a local linear model (LLM) approximation of globally non-linear dynamic systems.

The main part of the algorithm are Gaussian Kernel functions, which are fitted to a rectangular partitioning of the m -dimensional input or *partition space* performed by a decision tree with axis-orthogonal splits at the internal nodes (Fig. 1). Each local model belongs to one hyper-rectangle in the center of which the fitting point is placed. New hyper-rectangles are found by testing the possible splits in all dimensions and taking the one with the highest performance improvement. The choice of the partition space is the key point of this LoLiMoT algorithm; it should describe the strongest non-linearities in the process to reach the best results. The algorithm is described in detail in [6,7].

For the global non-linearities in the building, the LLMs are blended with mentioned Gaussian Kernel functions, which leads to fuzzy modelling, see Section 2.2 and subsequently to fuzzy model predictive control (FMPC).

It is known that buildings are complex non-linear dynamic processes. Therefore, the behaviour of the specific building is approximated by LLMs, where the partitioning variable ϑ_{amb} is chosen by expert knowledge. This fact turns the modelling into a grey-box model.

Both analysis of historical data and expert knowledge (building operators) indicate the choice of the different LLMs, which are given by the seasons: winter, transition season (fall and spring), summer. Thus, the partition space for the specific building is 1-dimensional. Therefore, ϑ_{amb} is the only variable for the validity of the different local models. Furthermore, each split of the partition space is equivalent to fuzzy inference rules and can be mathematically formulated as Takagi-Sugeno (TS)-fuzzy models, see Section 2.2 [11].

The parameters of each input to output transfer function are estimated from historical data. The model validation of each zone is given in Section 5.2.

2.2. Takagi-Sugeno (TS)-fuzzy model

TS-fuzzy models are suitable for approximating systems by interpolating between local linear, time-invariant auto-regressive models with exogenous inputs (ARX) [12]. The resulting output of the LoLiMoT algorithm, see Section 2.1, are parameters for an ARX-model. Therefore, the equivalence to a TS-fuzzy model is obtained.

The basic element of a TS-fuzzy system is a set of fuzzy inference rules. In general, each inference rule consists of two elements: the IF-part (antecedent) and the THEN-part (consequent) [10], the set of rules is given by \mathcal{R} in this work.

Here $\zeta = [\zeta_1, \zeta_2, \dots, \zeta_p] \in \mathbb{R}^p$ is the vector of input fuzzy variables. The elements of the fuzzy vector are usually a subset of the past input and outputs [12]. This vector is defined as:

$$\zeta \in \{y^k, \dots, y^{k-n_a+1}, u_s^{k-\tau}, \dots, u_s^{k-n_b-\tau+1}\} \in \mathbb{R}^p, \quad (1)$$

where y is the output, u_s is the input s where s denotes the specific input parameter or number of input, n_a is the maximum lag considered for the output and n_b is the maximum lag considered for the input terms. Furthermore, τ is the discrete dead time.

The overall system is approximated by a collection of coupled multiple-input single-output (MISO) discrete-time TS-fuzzy models of the input-output non-linear ARX (NARX) type

$$y^{k+1} = \sum_{j=1}^r \Phi_j(\zeta) y_j^{k+1}, \quad (2)$$

where r denotes the global number of rules. The degree of fulfillment of the specific j th rule can be computed using the product operator $\mu_j(\zeta) = \prod_{i=1}^p \mu_{j,i}(\zeta_i)$, where Ξ_i are the antecedent fuzzy set or regions for the j th rule \mathcal{R}^j . Furthermore, the normalized degree of fulfillment can be computed as

$$\Phi_j(\zeta) = \frac{\mu_j(\zeta)}{\sum_{i=1}^r \mu_i(\zeta)}. \quad (3)$$

The membership function is parameterized properly by the centers, the spreads and the steepness value k_σ [6,12,10].

Note, $\Phi_{i,l}$ denotes the fuzzy membership function for LLM_i of LLMN_l , which is expressed by $\text{LLM}_{i,l}$, $i \in \mathbb{I}$, $l = \{1, \dots, L_i\} = \mathbb{L}$. In the remainder of this work \mathbb{F} denotes the number of FMPCs, which is equivalent to the number of LLMNs, and is set to the number of buildings zones, which are considered to be 4 zones, thus, $\mathbb{F} = \{1, 2, 3, 4\}$. Note, the number of LLMs L_i is the same as the number of rules r , therefore $L_i \equiv r$ holds, here $L_i \equiv r$ is assumed to be equal to 3 for all $i \in \mathbb{I}$. In this work, *blended* describes the mixture between LLMs, where $\sum_{l=1}^{L_i} \Phi_{i,l} = 1$ holds $\forall i \in \mathbb{I}$. Blended zones are the areas in the partition space where the LLMs are overlapping each other.

Note, the manipulated variables of the FMPCs, $\forall i \in \mathbb{F}$ are given by output blending, not by parameter blending, see Section 4.3.

3. Building model

The building presented in this work is a 27,000 m² university building in the center of Salzburg, Austria. It has five floors above ground containing several large and numerous smaller meeting rooms, offices and lecture rooms. The facade of this special building has a glass ratio of about 70% and outside blinds over 2 floors, see



Fig. 2. Photo of the University building in Salzburg, Austria. © Luigi Caputo.

Fig. 2. On each floor. The building contains 250 office rooms, the footprint of these floors is identical and each has an effective area of about 6500 m². The building contains four shafts, which connect the piping for the cooling and heating supply and return with the supply level in the basement. The modelling of this specific building is based on these four main shafts, because each of these shafts supplies one building zone. These zones are distributed according to the building's orientation, which is equal to the cardinal direction. This fact makes the modelling more difficult, since the radiance input is given as a mixture from North-East (NE – zone₁), South-East (SE – zone₂), South-West (SW – zone₃) and North-West (NW – zone₄). For control purposes, the building model is split into these four independent zones and one coupling zone, see Fig. 3. Energy supply in this specific building is provided by a concrete activated floor distributing supply water in a second circuit, which means that this building has a thermally activated buildings system (TABS – coupling zone). Another supply into the building is based on Fan Coils (FC), which are required for the fast dynamics. The time constant of TABS is given by approximately 48h, in contrast to which the time constant for FC is assumed to be 4 h.

The energy demand of each zone i , respectively the coupling zone TABS, is denoted by $\dot{Q}_{F,i}$, $i \in \mathbb{F}$, and \dot{Q}_T . Note, it is assumed that a suitable energy management system (EMS) exists, which is able to provide the requested energy demand of the cooperative fuzzy model predictive control (CFMPC) scheme. An appropriate energy management system is presented in [26,24].

The coupling zone is controlled by TABS, which spans over all 4 zones and feeds the energy into the building through the concrete floor. TABS has a slow dynamic, but a very high thermal coefficient. Hence, it is beneficial to provide the building with a base level of energy. Each individual zone is managed by FC, which are able to control fast and react to short-term disturbances.

In the recent approach for the specific building, 13 models were made for control purposes depending on historical data and expert knowledge, see Section 2.1. For each FMPC _{i} , $i \in \mathbb{F}$, 3 models ($L_i \equiv 3$)

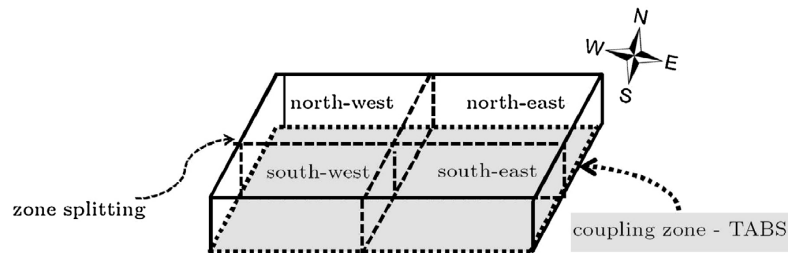


Fig. 3. Zone splitting for modelling the university building in Salzburg, Austria.

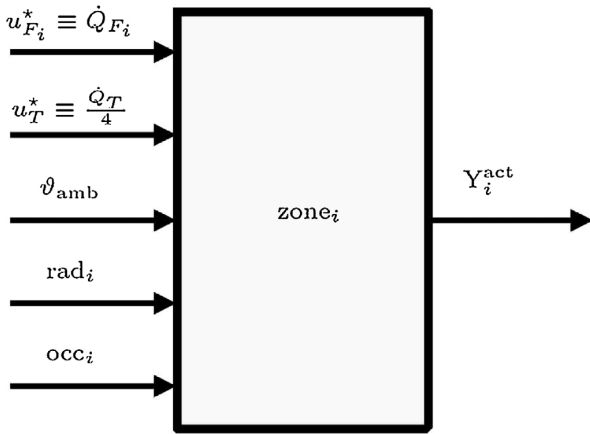


Fig. 4. Scheme of input-output relation for each MISO $zone_i$ model, $\forall i \in \mathbb{F}$. The manipulated variables after the cooperation loop are denoted by $u_{F_i}^*$ for FC of zone $_i$ and u_T^* for TABS. The heat supply \dot{Q}_T is divided by 4, because each zone comprises one quarter of the floor. Furthermore, ϑ_{amb} denotes the ambient temperature in K, rad_i the radiance input in the i th zone in W/m^2 , occ_i the occupancy in zone $_i$ in %, and Y_i^{act} represents the actual average indoor room temperature in zone $_i$ in K, $\forall i \in \mathbb{F}$.

are in use, constituting the LLMs. In addition, one global model for the whole floor (TABS) is designed for the global MPC (MPC $_T$).

The 3 LLMs of each FMPC are dedicated to the relevant seasons: winter, transition season (spring and fall), and summer. Therefore, for the zone-FMPCs, 12 LLMs are needed and 1 additional model for MPC $_T$, which is also valid for all seasons. The CFMPC is able to control the building over the whole year, because the fuzzy rules are switching between the three different seasons.

Note, for heat flow $\dot{Q}_j, j = \{T, F_i\}, i \in \mathbb{F}$ of TABS and FC the following relation holds:

$$\dot{Q}_j = \underbrace{\dot{m}_j}_{const.} \cdot \Delta \vartheta_j \cdot \underbrace{c_p}_{const.}, \quad (4)$$

where c_p , the specific heat capacity of water, is assumed to be constant and has no sub fix j , $\Delta \vartheta_j$ denotes the temperature difference between the supply and the return auf the j th control input, $j = \{T, F_i\}, i \in \mathbb{F}$. Also, the mass flows \dot{m}_j are assumed to be constant, further $j = \{T, F_i\}, \forall i \in \mathbb{F}$. The heat supplies are given in kW (heating – positive; cooling – negative) in the remainder of this work. The summation of the manipulated variables

$$\dot{Q}_{\Sigma} = \sum_{i \in \mathbb{F}} |\dot{Q}_{F_i}| + |\dot{Q}_T|, \quad (5)$$

is sent to the suitable EMS [26], where the energy supply is optimized and delivered to the building. All zones $_i$ of the plant are MISO-models, the input-output relation is demonstrated in Fig. 4.

Note that the effect of existing HVAC systems on indoor-room temperature must be included in the model. The best approach would be to include the dynamic response of the HVAC together with other heating and cooling systems in the grey-box model. It would then constitute just another manipulated variable. An alternative is given by considering the HVAC as an disturbance to the indoor-room temperature control; this known disturbance could consequently be included in the CFMPC concept.

4. Cooperative fuzzy model predictive control

Linear MPC refers to a class of control algorithms that compute manipulated variables by utilizing a linear process model [15]. However, many systems are inherently non-linear. This motivates

the use of non-linear MPCs (NMPC). Here a non-linear and generally non-convex optimization problem has to be solved. To avoid non-convex optimization, a set of LLMs can be extracted from a TS-fuzzy model [11], which is then used by the MPC algorithm [27,13,12]. The overall control structure in this specific problem leads to FMPCs and subsequently to CFMPC – because of the different building zones and one coupling zone, see Section 3. The concept of the CFMPC in general is presented in [16].

In the following, the index i of FMPCs is taken from the set $\mathbb{F} = \{1, 2, 3, 4\}$, and the associated $L_i \in \mathbb{L}$ LLMs for FMPC $_i, \forall i \in \mathbb{F}$, are denoted by the index $l \in \mathbb{L} = \{1, 2, 3\}$.

4.1. CFMPC for specific building

In this section, the CFMPC structure for the specific building is introduced. The CFMPC controls the average indoor-room temperature in the office rooms by manipulating supply temperatures of both FCs and TABS, while considering main disturbances given by ambient temperature, radiance, and occupancy. In Fig. 5 the control concept for 4 FMPCs (FMPC $_i, \forall i \in \mathbb{F}$) cooperating with 1 global coupling MPC (MPC $_T$) is illustrated.

The controlled variable is the average indoor room temperature of each zone denoted by $Y_i^{act}, \forall i \in \mathbb{F}$. In Fig. 5, Y_i^{ref} describes the reference trajectory for the i th FMPC of the closed-loop system, and Y_i^{act} represents the actual value. For the coupling zone, the mean \bar{Y}^{ref} of the other 4 reference values is taken, and the actual mean indoor room temperature is given as \bar{Y}^{act} .

The manipulated variables before the cooperative iteration-loop are denoted by $u_j, j = \{T, F_i\}, \forall i \in \mathbb{F}$. The “T” denotes “TABS” and “F $_i$ ” denotes the control by FC for zone $_i$. After the cooperation, the manipulated variables are star-variables u_j^* . Furthermore, three main disturbances to the building are considered:

- ambient temperature denoted by “ ϑ_{amb} ” in K,
- radiance denoted by “rad” in W/m^2 ,
- occupancy denoted by “occ” in %, adapted from [28].

The cooperative iteration-loop is introduced in Section 4.2. Note that the manipulated variables u_j (and consequently u_j^*) are equal to the energy demand \dot{Q}_j , see Section 3 Eqs. (4) and (5). Furthermore, the disturbances “rad” and “occ” are split into rad_i and occ_i depending on the zones, $\forall i \in \mathbb{F}$.

The global plant (see Fig. 5 “building”) consists of 4 parallel input-coupled zones, and each FMPC controls one zone. The manipulated coupling variable u_T^* influences all 4 zones. These zones are each defined by one LLMN, split into the cardinal directions, see Section 3. As introduced in Section 2.2, ARX transfer functions can be transformed state-space matrices. Therefore, the overall non-linear building plant, consisting of 4 input-coupled zones (by TABS), is possible to be presented in time-variant state-space matrices. These matrices are given as: $A_i^k, \bar{B}_i^k, C_i^k, \forall i \in \mathbb{F}$. Note in contrast to the output-blended controller, for the global plant parameter-blended matrices are assumed. This means that the system matrix at time k is calculated as: $A_i^k = \sum_{l \in \mathbb{L}} A_{i,l}^k \Phi_{i,l}, \forall i \in \mathbb{F}$.

Note $\bar{B}_i^k = [B_i^k; E_i^k]$ is a stacked matrix for the input-matrix and the disturbance-matrix, for details see Section 4.3. In contrast to parameter-blending, the manipulated variable for each FMPC is computed by output-blending:

$$u_i^k = \sum_{l \in \mathbb{L}} u_{i,l}^k \Phi_{i,l}. \quad (6)$$

The fuzzy membership functions $\Phi_{i,l}$ are given for the fuzzy input vector depending on all LLMs $_{i,l}, \forall i \in \mathbb{F}$ and $l \in \mathbb{L}$.

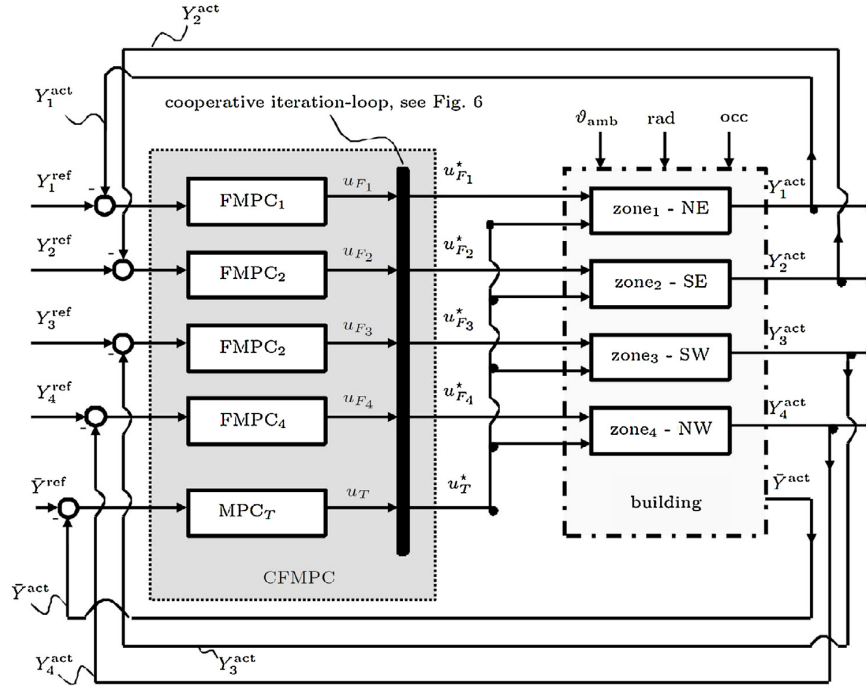


Fig. 5. CFMPC scheme for the specific building. The scheme shows the structure of a CFMPC, which is used for the demonstration building, with 4 different zones.

In this cooperative control structure (based on Fig. 5), four FMPCs are in cooperation with one global MPC. Each manipulated variable of the i th FMPC is a disturbance to the global MPC, and the manipulated variable of MPC_T is an additional disturbance to each $FMPC_i$, $\forall i \in \mathbb{F}$.

4.2. Cooperative iteration-loop

The cooperative iteration-loop is computed between consecutive time steps. Furthermore, only u_i for $FMPC_i$ and u_T for MPC_T , $\forall i \in \mathbb{F}$, are iteratively updated, all other variables are assumed to be constant during the iteration-loop (e.g. external disturbances). The functions

$$u_{F_i}^q = h_{F_i}^q(\cdot | u_T^q), \quad (7)$$

$$u_T^q = h_T^q(\cdot | u_{F_1}^q, \dots, u_{F_4}^q), \quad (8)$$

$\forall i \in \mathbb{F}$ are the cooperative q th iteration-updates, see Fig. 6 [22,23].

Between consecutive time steps, the cooperative MPCs perform q iterations of a feasible path algorithm. Let u^* be the overall blended output after the iteration loop, see Fig. 6. u^* is computed such that some cost function, see Eq. (9), is minimized and acceptable for each zone. The cooperation update $u_{F_i}^q = h_{F_i}^q(\cdot | u_T^q)$ denotes the iteration-update for each $FMPC_i$, dependent on the additional disturbance u_T^q . Furthermore, $u_T^q = h_T^q(\cdot | u_{F_1}^q, \dots, u_{F_4}^q)$ is the cooperative iteration-update for the manipulated variable of the coupling zone, dependent on the other 4 manipulated variables from each FMPC within the q th iteration. Note that all other disturbances (ϑ_{amb} , rad , occ) are held constant during the iteration-loop.

The cooperative iteration-updates are calculated in a loop until a maximal number of iteration-steps is reached or if the increment between the $(q-1)$ th and q th manipulated variable (for all five variables) is smaller than a given threshold ε . If one of these

criteria is fulfilled, the algorithm is advancing to time step $k = k + 1$, see Fig. 6.

4.3. CFMPC optimization problem

FMPC are non-linear MPCs, which achieve the global optimum for a given performance criterion. However, for a cooperation between a global MPC with several FMPCs, increased flexibility and a scalable control architecture can be achieved by accepting suboptimal inputs [23,22,25,24]. Hence, a suboptimal FMPC analogous to suboptimal MPC presented in [22,23] is proposed. Note that each FMPC actually acts like a parallel connection of linear MPCs with output-blending, which effectively constitutes a non-linear controller [29,30]. The cost functions for all, the FMPCs and the MPC_T , are equal. For the FMPCs $\#L = 3$ parallel MPCs (for the defined seasons, see Section 3) of each zone are output blended as defined in Section 4.1, Eq. (6), to the overall blended output. In this section, the derivation to the CFMPC optimization problem definition is given and explained. In the following, the variable $\tilde{u} = [u; z]$ describes the stacked variable of manipulated variable and disturbances.

The optimization problem for each MPC can be formulated as:

$$J_j^* = \min_{\Delta u_j} J_j(\tilde{u}_j) \forall j = T, F_i, \forall i \in \mathbb{F} \quad (9)$$

where

$$J_j(\tilde{u}_j^{k, k+n_p-1}) = \sum_{k=0}^{n_p-1} [(Y_j^{\text{ref}, k} - Y_j^{\text{act}, k}) \tilde{Q}_j (Y_j^{\text{ref}, k} - Y_j^{\text{act}, k}) + \tilde{u}_j^{k'} R_j \tilde{u}_j^k] \quad (10)$$

subject to

$$u_{j, \min} \leq u_j \leq u_{j, \max}, \quad (11)$$

$$Y_{j, \min}^{\text{act}} \leq Y_j^{\text{act}} \leq Y_{j, \max}^{\text{act}}, \quad (12)$$

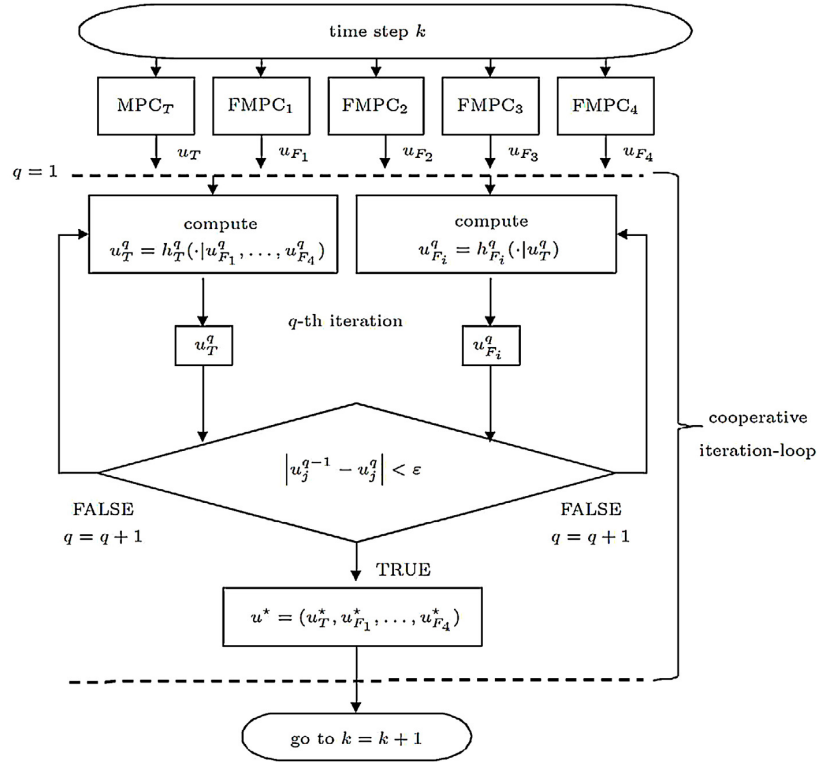


Fig. 6. Schematic flow-chart of cooperative iteration loop of CFMPC. Between consecutive time steps k and $k + 1$, the q th cooperative iteration update $h_i^q(\cdot | \cdot)$ is computed in a loop, $\forall j \in \{T, F_i\}, \forall i \in \mathbb{F} = \{1, 2, 3, 4\}$. The resulting cooperative solution for the manipulated variable is given by u^* . The abort criterion has to be fulfilled for all, the MPC_T and the i FMPCs, in the same iteration-step q to advance to $k = k + 1$, or the maximal number of iterations-steps has to be reached.

$j = \{T, F_i\}, \forall i \in \mathbb{F}$, where n_p denotes the prediction horizon and “ \cdot ” denotes transpose. Note that the $y_i^{\text{ref},k}$ are external reference values and are considered to be known (see Fig. 5). Furthermore, $y_T^{\text{act}} \equiv \bar{y}_T^{\text{act}}$ and $y_T^{\text{ref}} \equiv \bar{y}_T^{\text{ref}}$. Note that the optimization (9)–(12) applies only the u_j , the first part of $\tilde{u}_j = [u_j, z_j]$, $\forall j = T, F_i, \forall i \in \mathbb{F}$. Hence, $\tilde{Q}_j \in \mathbb{R}^{n_{y_j} \times n_{y_j}}$ is a positive semi-definite weighting matrix with dimension n_{y_j} , and $R_j \in \mathbb{R}^{n_{\tilde{u}_j} \times n_{\tilde{u}_j}}$ is a positive definite weighting matrix, with $j = \{T, F_i\}, \forall i \in \mathbb{F}$. Note that $n_{\tilde{u}_j}$ is the dimension of the manipulated variable of u_j including the number of disturbances for the j th MPC, $j = \{T, F_i\}, \forall i \in \mathbb{F}$. The objective function of each FMPC _{i} is also subjected to a LLMN, which consists of L_i LLMs, which are equivalent to r -fuzzy rules.

Now only the i FMPCs are considered. These manipulated variables u_i^{k+t} can be calculated by generating l sets of local linear control inputs in the first step, $u_{i,l}^{k+t}, \forall t \in \{1, 2, \dots, n_c\}, \forall i \in \mathbb{F}, \forall l \in \mathbb{L}$, where n_c denotes the control horizon. In the second step, the weighted sum of the local linear control inputs give the overall output-blended control input as defined in Eq. (6), see Section 4.1. The weight of the l th fuzzy control action $\Phi_{i,l}$ is the same as that for the l th local linear model [12,4,30].

Let u^* be the overall blended output, after the iteration loop, see Section 4.2 Fig. 6, with arbitrary chosen initial condition for the CFMPC algorithm. Then the suboptimal optimization problem is formulated as given in [23] and solved at each iteration $q \geq 0$ for all zones $i \in \mathbb{F}$.

In following equations $\Phi_{i,l}$ are the fuzzy membership functions for output blending for LLM _{l} of LLMN _{i} .

Given the prior feasible iteration $(u_T^q, u_{F_i}^q)$, then the next iteration for the cooperative iteration-loop (for the iteration-update $u_{F_i}^q =$

$h_{F_i}^q(\cdot | u_T^q)$), see Fig. 6, is defined to be

$$\begin{aligned} u^{q+1} &= (u_{F_i}^{q+1}, u_T^{q+1}) \\ &= \Psi_{F_i} \cdot (u_{F_i}^*(u_T^q), u_T^q) + \Psi_T \cdot (u_{F_i}^q, u_T^*(u_{F_i}^q)) \\ &= \Psi_{F_i} \cdot \left(\sum_{l \in \mathbb{L}} \Phi_{F_i,l} u_{F_i,l}^*(u_T^q), u_T^q \right) \\ &\quad + \Psi_T \cdot \left(\sum_{l \in \mathbb{L}} \Phi_{F_i,l} u_{F_i,l}^q, u_T^* \left(\sum_{l \in \mathbb{L}} \Phi_{F_i,l} u_{F_i,l}^q \right) \right) \end{aligned} \quad (13)$$

$$\sum_{j=\{T, F_i\}} \Psi_j = 1 \forall \Psi_j > 0, i \in \mathbb{F}. \quad (14)$$

Here, Ψ_j are arbitrary scalar weighting factors. For $u_T^q = h_T^q(\cdot | u_{F_1}^q, \dots, u_{F_4}^q)$, the calculation is equivalent to Eq. (13) with Eq. (14) with the four FC input as disturbance vector. Stability of the CFMPC concept is proven and discussed in [16].

5. Simulation and validation results

In the following Sections 5.1–5.3, the main simulation results are given and discussed. The CFMPC concept is compared to the FMPC concept, see Fig. 5, without the cooperative iteration-loop, see Fig. 6, is denoted by FMPC_{wo,c}. Furthermore, the CFMPC compared to a global linear MPC concept, denoted as MPC_{lin}, and to the actual implemented rule-based PID-controller strategy from measured data is given.

Unfortunately, a direct comparison between the simulated CFMPC and the historical measured data is not completely fair.

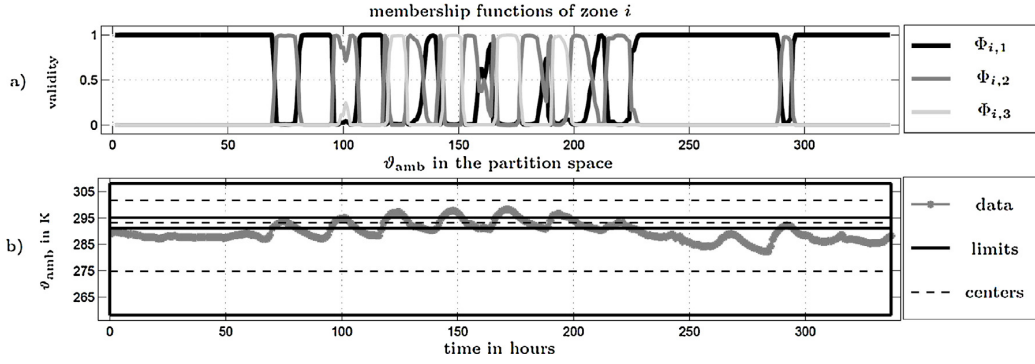


Fig. 7. In (a) the validity of the membership functions is shown during the chosen period. In this sub-figure a, $\Phi_{i,1}$ denotes the winter model, $\Phi_{i,2}$ the transition season model, and $\Phi_{i,3}$ the summer model. Because of the fact that the partition variable is an external input, the validity of the different LLMs is equal for all zones i , $\forall i \in \mathbb{F}$. In (b), the corresponding partition space is given with the partition variable ϑ_{amb} . Furthermore, the limits of the individual models are illustrated with their center points.

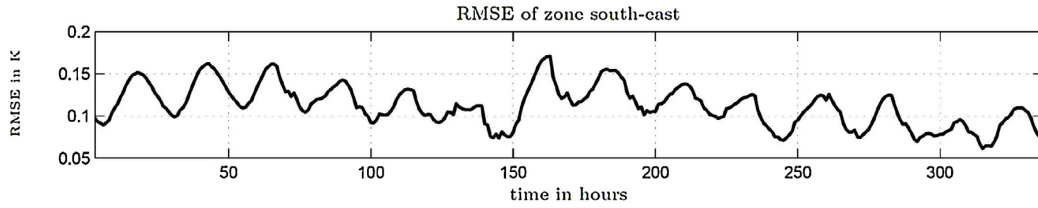


Fig. 8. This figure shows the worst 24-h ahead prediction RMSE of the four zone models in K. The 24-h ahead prediction RMSE values for all zones are given in Table 1.

The actual implemented rule-based PID-controller in the demonstration building is not controlled to one set-point. It is a range [294.15K; 296.15K] where the indoor room temperature is acceptable during working hours. In addition, this range is widened on weekends and during the night. However, for comparison the measured outputs and manipulated variables are shown in the following sections.

5.1. Simulation setup

The setup of four controller schemes is shown for 2 weeks in September 2014. For the CFMPC, the FMPC_{wo,c} and a linear global MPC acting on the office level as a whole, all disturbances are measured from the introduced period. The actual implemented controller is a state-of-the-art rule-based PID-controller, where expert rules in if-then form are combined with PID control for continuous variables. The zoning for the CFMPC is based on the actual supply shafts (which coincide with the cardinal directions) in the demonstration building. Note that the designation of an individual zone is only meaningful if an individual supply (manipulated variable) is available for that zone. If a zone is overlapping with others (as is the case for the TABS), a weighted average of temperature measurements is assigned to that zone, but otherwise the FMPC design is done separately. The cooperative iteration loop then takes care of the proper interaction of the individual FMPC controllers. All results for the rule-based PID-controller are denoted with the suffix "meas", which stands for "measured" and the linear global MPC is given by MPC_{lin}. Furthermore, for the rule-based PID-controller, the reference value is illustrated by the mean of the comfort range [294.15K; 296.15K]. Thus, y_{meas}^{ref} is equal to 295.15K. For the MPC_{lin} one global model for all four zones is considered. Therefore the reference value $y_{MPC_{lin}}^{ref}$ has been defined as the mean of the four zone reference values.

The period of these 2 weeks in September 2014 is chosen, because all possible cases for the fuzzy membership functions are

included: full validity of one LLM, part-validity of 2 LLMs, part-validity of all 3 LLMs, and fast transition between the LLMs. The validation of the zone models is given in Section 5.2, and the comparison of the different controller schemes is described in Section 5.3.

5.2. Model validation

In Fig. 7b, the ambient temperature ϑ_{amb} in the partition space is given for 2 weeks in September 2014. Moreover, the validity of the membership functions is illustrated above in Fig. 7a. It is obvious which function $\Phi_{i,l}$ is valid $\forall i \in \mathbb{F}, \forall l \in \mathbb{L}$, because in Fig. 7b it is well illustrated in the partition space. The steepness k_σ of all LLMs is chosen by $k_\sigma = 1/3$. Therefore, more than 1 LLM is valid in the transitional regions. For instance, 3 LLMs are part-valid at time step $k = 100h$ or 2 LLMs are part-valid at $k = 165h$ ($\Phi_{i,1}$ and $\Phi_{i,2}$).

The model validation is based on a 24-h ahead prediction. The root-mean-square error (RMSE) is computed over 24 values in each time step k for model performance. This statistical value is computed as:

$$RMSE_j = \sqrt{\frac{\sum_{k=1}^N \|\hat{Y}^k - Y_{meas}^k\|_2^2}{N}}, \quad (15)$$

where \hat{Y}^k is value of the 24-h ahead prediction at time step k , Y_{meas}^k gives the output measured from historical data, and N is the number of measurements for $Y, j = \{T, F_i\}, \forall i \in \mathbb{F}$.

The RMSE value is directly interpretable in Kelvin K. In Fig. 8, the RMSE is plotted over the time in hours (226 h = 2 weeks) for the worst model fit.

The model performance shown in the RMSE values in K for all zones $i, i \in \mathbb{F}$, is given in Table 1.

As shown in Table 1, the fit of all models is in the same range, which is in an error rate of about 10% only. Note that a model error of 0.18 K (see Fig. 8) is smaller than the accuracy of measurement. The comparison of these models is presented at the zone

Table 1
RMSE values (model performance) of 24-h ahead prediction of all zones.

Zone ₁ -NE	Zone ₂ -SE	Zone ₃ -SW	Zone ₄ -NW
0.111	0.112	0.106	0.091

level only. The building's system level is discussed separately in [7]. One advantage of the proposed concept is the decoupled controller structure between the comfort and the supply level [24]. Hence, in our manuscript the comfort maximization in the different zones is the optimization goal. Realistic fluctuations in the occupancy profile do not significantly influence the model performance for a 24-h ahead prediction. This is mainly due to the averaging effect of more than 500 users.

5.3. Closed-loop controller simulation

In this Section, the performance of the four introduced controller schemes is compared. Furthermore, the energy consumption of the manipulated variables, calculated in an adapted form (Eq. (16)) as given in Eq. (5), is compared. Occupant thermal comfort is defined as minimal deviation from the indoor-room temperature set-point. Other factors such as radiance, lighting, and humidity [31] are not considered, as they are neither measured nor included in the existing automation system. Therefore, in the comparison before and after the implementation of CFPMC only room temperature deviations are considered. Since all other influencing factors are not significantly changed by the different control schemes, this comparison should be fair. Note that for the measured historical data only an indoor mean room temperature $Y_{\text{meas}}^{\text{act}}$ is given, because the zone splitting is not implemented in the demonstration building yet. In addition, $Y_{\text{meas}}^{\text{ref}}$ is assumed to be equal to 295.15 K. Note that the coupling zone TABS is included in the CFMPC and the MPC_{lin} concepts, in contrast to the FMPC without cooperation, FMPC_{wo,c}, where the information about TABS is not included. In Fig. 9a–c, the

outputs for each zone and their reference values are illustrated. The disturbances are given in Fig. 9d–f. The disturbances are taken from measured historical data. Therefore, the energy consumption of the CFMPC is compared to the energy demand depending on historical measured data, the FMPC_{wo,c}, and the MPC_{lin}. Energy consumption is proportional to the measured temperature difference between feed and return, as the circulation pumps are operating with fixed speed. The heat flow is therefore calculated using this constant mass flow (has been measured during commissioning) and the temperature difference. It is obvious in Fig. 9a–c that the model predictive controllers, which are including the coupling zone TABS, perform better than the state-of-the-art rule-based PID-controller. As the building's rule-based PID-control has been optimized for minimal energy consumption over the last two years, all other control schemes are tuned to the same consumption. The control performance can therefore be seen as main criterion in the comparison. The deviation in the measured data from its assumed set-point is up to 1 K in some regions. Furthermore, a strong time-delayed correlation between the measured indoor room temperature data $Y_{\text{meas}}^{\text{act}}$ and ϑ_{amb} is illustrated in Fig. 9c–d.

With the assumed set-point for the measured indoor temperature, the CFMPC concept is better in performance by 21.86% as compared to the FMPC_{wo,c}. Performance of the presented CFMPC concept provides an improvement of 19.67% over the rule-based PID-controller in the specific demonstration building and 16.17% against the MPC_{lin}.

The corresponding manipulated variables are shown in Figs. 10 and 11. Fig. 10 shows the manipulated variables $u_{T,p}^{\text{CFMPC}}$ and $u_{T,p}$ for the different controllers in kW, and “p” stands for FMPC_{wo,c}, MPC_{lin} or meas. Note that the star-variable results from the cooperative iteration-loop. It demonstrates the different behaviour in this manipulated variable due to different controller schemes. However, the energy cost of TABS is not as high as the cost for FC. Therefore, the different strategies in TABS see Fig. 10, and the higher cost of the fuzzy predictive controllers in TABS, are

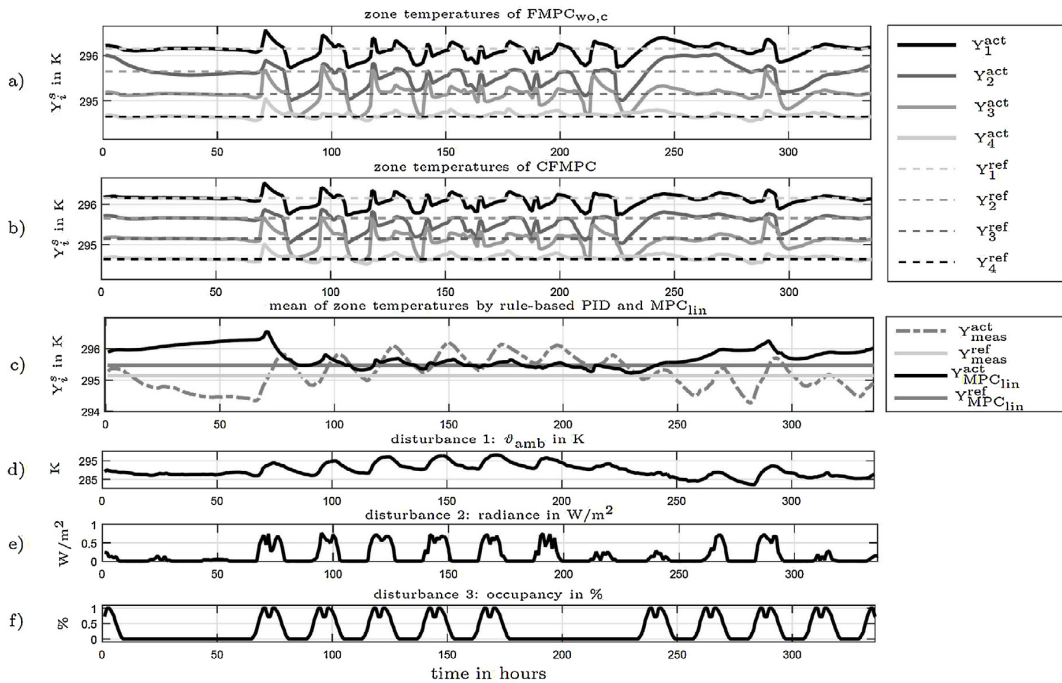


Fig. 9. In subplot (a), the indoor zone temperatures of the FMPC_{wo,c} are given. The same is given for the CFMPC in subplot (b), and the measured output as well as the output of MPC_{lin} is shown in (c). The disturbances are pictured in the subplots (d–f). Note that “s” stands for $s = \{\text{act}, \text{ref}\}$ and $\forall i \in \mathbb{F} \cap \{\text{meas}, \text{MPC}_{\text{lin}}\}$.

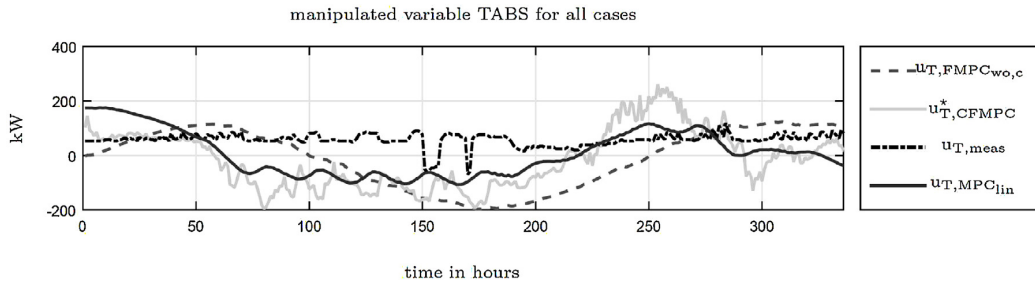


Fig. 10. Manipulated variables $u_{T,CFMPC}^*$ and $u_{T,p}$ for TABS, where “p” stands for FMPC_{wo,c}, MPC_{lin} or meas.

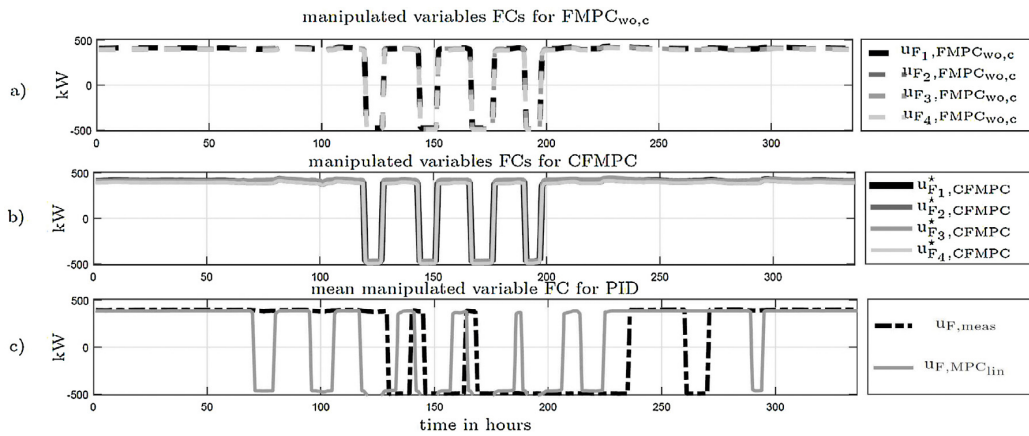


Fig. 11. Manipulated variables $u_{Fi,CFMPC}^*$ and $u_{Fi,p}$ for FC, where “p” stands for the different controllers FMPC_{wo,c}, MPC_{lin} or meas and $i \in \mathbb{F}$, in kW.

Table 2
Comparison of performance and energy supply of four different controller schemes.

Concept	Performance	Energy supply
CFMPC	100%	100%
FMPC _{wo,c}	78.14%	100.21%
MPC _{lin}	83.83%	100.55%
Rule-based PID	80.33%	100.43%

compensated by the predictive use of the FCs, see Fig. 11. The strategies for FMPC_{wo,c} are given in Fig. 11a. They are similar to the FC strategies of the CFMPC, see Fig. 11b. The subplot in the bottom Fig. 11c shows the measured strategy of the manipulated PID variable FC and of the MPC_{lin} during the chosen 2 weeks. It is illustrated that the FCs with PID are in the cooling mode for a longer period of time. Furthermore, it is obvious that the predictive controllers, Fig. 11a and b, are able to cool and heat predictively.

For a comparison of energy costs, Eq. (5) is adapted for each controller concept:

$$\dot{Q}_{\sum,v} = \sum_{i \in \mathbb{F}} |\dot{Q}_{Fi,v}| + |\dot{Q}_{T,v}|, \quad (16)$$

$v = \{\text{FMPC}_{wo,c}, \text{CFMPC}, \text{meas}, \text{MPC}_{lin}\}$. The results of the four mentioned controller schemes in performance and energy demand are summarised in Table 2. Note that all controllers are compared to the CFMPC, for which the reference values in performance as well as in energy supply are assumed to be 100%.

It follows that the energy costs of all controllers is nearly in the same range, see Table 2. Thus, it is noteworthy that the presented CFMPC concept is able to achieve a great performance increase with less energy consumption as compared to all other controllers. It is to

mention that the FMPC_{wo,c} has no information about the coupling zone TABS, and the rule-based PID-controller in the demonstration building has been optimized over the last 2 years.

6. Conclusion

A cooperative FMPC has been proposed for heating and cooling of buildings. It is important to notice that the FMPCs for each zone are designed by input-coupled LLMNs. One coupling variable exists, which influences each building zone. One great advantage of the underlying MPC models is the validity over all seasons – winter, transition season (spring and fall) and summer. Thus, the presented CFMPC concept is able to control both modes, heating and cooling, in contrast to most of the state-of-the-art MPCs in buildings, where just heating or cooling systems are controlled. Another benefit of the CFMPC is the independence of the building and system type. The CFMPC is useful and implementable for all building types with multiple heat/cooling supplies. The data-based model has to be identified for each for specific building, which is standard in process industry. Hence, for each zone a model (suitable for MPC) has to be created which requires availability of suitable input (heat supply and disturbances) and output (temperatures) data. For the demonstration building a model validation of all zones is given, where the fuzzy grey-box model approach is underlined with excellent results.

A cooperative FMPC (CFMPC) is presented to coordinate the different input-coupled manipulated variables. The outstanding performance results are given with a closed-loop simulation. The CFMPC achieves significantly higher control performance with slightly less energy consumption in contrast to two predictive controllers and the rule-based PID-controller which is implemented

in the demonstration building. The simulation examples verify the advantages and effectiveness of the CFMPC for heating and cooling in the field of building control.

Acknowledgements

This work was supported by the project “SMART MSR” (FFG, No. 832103) in cooperation with evon GmbH and Unipark Nonntal, University of Salzburg.

References

- [1] L. Pérez-Lombard, J. Ortiz, C. Pout, A review on buildings energy consumption information, *Energy Build.* 40 (3) (2008) 394–398, <http://dx.doi.org/10.1016/j.enbuild.2007.03.007>.
- [2] S. Privara, J. Cigler, Z. Vána, F. Oldewurtel, C. Sagerschnig, E. Žáčková, Building modeling as a crucial part for building predictive control, *Energy Build.* 56 (0) (2013) 8–22, <http://dx.doi.org/10.1016/j.enbuild.2012.10.024>.
- [3] M. Gwerder, S. Bötschi, D. Gyalistras, C. Sagerschnig, D. Sturzenegger, R. Smith, B. Illi, Integrated predictive rule-based control of a Swiss office building, in: *Clima – RHEVA World Congress*, Prague, Czech Republic, 2013, pp. 1723–1732.
- [4] Y.L. Huang, H. Lou, J.P. Gong, T. Edgar, Fuzzy model predictive control, *IEEE Trans. Fuzzy Syst.* 8 (6) (2000) 665–678, <http://dx.doi.org/10.1109/91.890326>.
- [5] L. Jung, *System Identification: Theory for the User*, Prentice-Hall Information and System Sciences Series, Prentice Hall PTR, 1999.
- [6] O. Nelles, *Nonlinear System Identification: From Classical Approaches to Neural Networks and Fuzzy Models*, Engineering Online Library, Springer, 2001.
- [7] M. Killian, B. Mayer, M. Kozek, Effective fuzzy black-box modeling for building heating dynamics, *Energy Build.* 96 (0) (2015) 175–186, <http://dx.doi.org/10.1016/j.enbuild.2015.02.057>.
- [8] X. Li, J. Wen, Review of building energy modeling for control and operation, *Renew. Sustain. Energy Rev.* 37 (2014) 517–537, <http://dx.doi.org/10.1016/j.rser.2014.05.056>.
- [9] A. Afram, F. Janabi-Sharifi, Black-box modeling of residential (HVAC) system and comparison of gray-box and black-box modeling methods, *Energy Build.* 94 (2015) 121–149, <http://dx.doi.org/10.1016/j.enbuild.2015.02.045>.
- [10] T. Takagi, M. Sugeno, Fuzzy identification of systems and its applications to modeling and control, *IEEE Trans. Syst. Man Cyber.* SMC-15 (1) (1985) 116–132, <http://dx.doi.org/10.1109/TSMC.1985.6313399>.
- [11] S. Mollov, P.V.D. Veen, R. Babuška, J. Abonyi, J.A. Roubos, H. Verbruggen, Extraction of local linear models from Takagi-Sugeno fuzzy model with application to model-based predictive control, in: *Proceedings Seventh European Congress on Intelligent Techniques and Soft Computing EUFIT'99*, 1999, pp. 147–154.
- [12] J. Abonyi, *Fuzzy Model Identification for Control*, Birkhauser, Boston, 2002.
- [13] J. Roubos, S. Mollov, R. Babuska, H. Verbruggen, Fuzzy model-based predictive control using Takagi-Sugeno models, *Int. J. Approx. Reason.* 22 (12) (1999) 3–30, [http://dx.doi.org/10.1016/S0888-613X\(99\)00020-1](http://dx.doi.org/10.1016/S0888-613X(99)00020-1).
- [14] I. Škrjanc, B. Zupančič, B. Furlan, A. Krainer, Theoretical and experimental fuzzy modelling of building thermal dynamic response, *Build. Environ.* 36 (9) (2001) 1023–1038, [http://dx.doi.org/10.1016/S0360-1323\(00\)00053-6](http://dx.doi.org/10.1016/S0360-1323(00)00053-6).
- [15] E. Camacho, C. Bordons, *Model Predictive Control*, Advanced Textbooks in Control and Signal Processing, Springer, London, 2004.
- [16] M. Killian, B. Mayer, A. Schirrer, M. Kozek, Cooperative fuzzy model predictive control, *IEEE Trans. Fuzzy Syst.* (2015), <http://dx.doi.org/10.1109/TFUZZ.2015.2463674> (in press).
- [17] M. Wallace, R. McBride, S. Aumi, P. Mhaskar, J. House, T. Salsbury, Energy efficient model predictive building temperature control, *Chem. Eng. Sci.* 69 (1) (2012) 45–58, <http://dx.doi.org/10.1016/j.ces.2011.07.023>.
- [18] C.-S. Kang, C.-H. Hyun, M. Park, Fuzzy logic-based advanced on-off control for thermal comfort in residential buildings, *Appl. Energy* 155 (2015) 270–283, <http://dx.doi.org/10.1016/j.apenergy.2015.05.119>.
- [19] S. Privara, J. Široký, L. Ferkl, J. Cigler, Model predictive control of a building heating system: the first experience, *Energy Build.* 43 (2–3) (2011) 564–572, <http://dx.doi.org/10.1016/j.enbuild.2010.10.022>.
- [20] Y. Ma, F. Borrelli, B. Hencsey, B. Coffey, S. Benga, P. Haves, Model predictive control for the operation of building cooling systems, *IEEE Trans. Control Syst. Technol.* 20 (3) (2012) 796–803, <http://dx.doi.org/10.1109/TCST.2011.2124461>.
- [21] P.-D. Moroşan, R. Bourdais, D. Dumur, J. Buisson, Building temperature regulation using a distributed model predictive control, *Energy Build.* 42 (9) (2010) 1445–1452, <http://dx.doi.org/10.1016/j.enbuild.2010.03.014>.
- [22] P.O.M. Scolaert, D. Mayne, J. Rawlings, Suboptimal model predictive control (feasibility implies stability), *IEEE Trans. Autom. Control* 44 (3) (1999) 648–654, <http://dx.doi.org/10.1109/9.751369>.
- [23] B.T. Stewart, A.N. Venkat, J.B. Rawlings, S.J. Wright, G. Pannocchia, Cooperative distributed model predictive control, *Syst. Control Lett.* 59 (8) (2010) 460–469, <http://dx.doi.org/10.1016/j.sysconle.2010.06.005>.
- [24] M. Killian, B. Mayer, M. Kozek, Hierarchical Fuzzy MPC Concept for Building Heating Control, in: *Proceedings of the 19th World Congress of the International Federation of Automatic Control (IFAC'14)*, 2014, pp. 12048–12055, <http://dx.doi.org/10.3182/20140824-6-ZA-1003.00772>.
- [25] B. Mayer, M. Killian, M. Kozek, Cooperative and hierarchical fuzzy MPC for building heating control, in: *IEEE International Conference on Fuzzy Systems (FUZZ-IEEE)*, 2014, pp. 1054–1059, <http://dx.doi.org/10.1109/FUZZ-IEEE.2014.6891573>.
- [26] B. Mayer, M. Killian, M. Kozek, Management of hybrid energy supply systems in buildings using mixed-integer model predictive control, *Energy Convers. Manag.* 98 (2015) 470–483, <http://dx.doi.org/10.1016/j.enconman.2015.02.076>.
- [27] R. Babuška, *Fuzzy Modeling for Control*, 1st ed., Kluwer Academic Publishers, Norwell, MA, USA, 1998.
- [28] W.-K. Chang, T. Hong, Statistical analysis and modeling of occupancy patterns in open-plan offices using measured lighting-switch data, *Build. Simul.* 6 (1) (2013) 23–32, <http://dx.doi.org/10.1007/s12273-013-0106-y>.
- [29] K. Tanaka, H. Wang, *Fuzzy Control Systems Design and Analysis: A Linear Matrix Inequality Approach*, Wiley, 2004.
- [30] S. Mollov, R. Babuska, J. Abonyi, H. Verbruggen, Effective optimization for fuzzy model predictive control, *IEEE Trans. Fuzzy Syst.* 12 (5) (2004) 661–675, <http://dx.doi.org/10.1109/TFUZZ.2004.834812>.
- [31] F.R. d'Ambrosio Alfano, B.W. Olesen, B.I. Palella, G. Riccio, Thermal comfort: design and assessment for energy saving, *Energy Build.* 81 (2014) 326–336, <http://dx.doi.org/10.1016/j.enbuild.2014.06.033>.

Curriculum Vitae

Personal Information

Name	Dipl.-Ing. Barbara Mayer, formerly Angermeier
Date of birth	11 th of April, 1980
Place of birth	Graz
Citizenship	Austria
Gender	Female
Address	Schörgelgasse 68F, 8010 Graz



Education

11/2010 -	Vienna University of Technology Doctoral studies in Mechanical Engineering
10/2001 - 07/2002	Universidad de Complutense Madrid Erasmus Exchange
10/1998 - 07/2004	Graz University of Technology Diploma studies in Technical Mathematics
09/1990 - 06/1998	Realgymnasium Hartberg secondary school

Diploma Thesis

Title	Inhomogeneous Markov chains, Monte Carlo simulation, and their Application in Combinatorial Optimization
Supervisor	Univ.-Prof. Dipl.-Ing. Dr.rer.nat. Wolfgang Woess

Professional Work Experience

FH JOANNEUM University of Applied Sciences

Institute of Industrial Management

04/2014 -	Lecturer and Researcher Coordination for Automation and Process Control
02/2010 - 03/2014	Research Assistant

AutomationX GmbH

11/2008 - 06/2009	Deputy Head of Development
10/2006 - 10/2008	Technical assistant of CEO
11/2004 - 09/2006	Software Developer and Designer

Additional Trainings

Systemic Coach, IRWB Vienna

Systemic Developer for Teams and Organizations, IRWB Vienna

IT SKILLS

Office	Microsoft Word/Excel, Latex
Programming	C++, C# .Net, Java, Matlab, SQL
Databases	MSSQL

Languages

German	mother language
English	fluently written and spoken
Spanish	good knowledge written and spoken

Leisure Interests

jogging, skiing, piano-playing, choir-singing

List Of Scientific Publications

International Journals:

1. B. Mayer and M. Killian and M. Kozek. Management of hybrid energy supply systems in buildings using mixed-integer model predictive control. *Energy Conversion and Management*, Volume 98, 2015, pages: 470-483, ISSN 0196-8904.
DOI:10.1016/j.enconman.2015.02.076
2. M. Killian, B. Mayer, A. Schirrer, M. Kozek. Verteilte kooperative modellprädiktive Temperaturregelung für komplexe Gebäude. *e&i Elektrotechnik und Informationstechnik*, Springer Verlag, Volume 132, 2015, pages 474-480, ISSN: 1613-7620.
DOI: 0.1007/s00502-015-0374-6
3. M. Killian, B. Mayer, M. Kozek. Effective fuzzy black-box modeling for building heating dynamics. *Energy and Buildings*, Volume 96, 2015, pages 175-186, ISSN: 0378-7788.
DOI: 10.1016/j.enbuild.2015.02.057
4. M. Killian, B. Mayer, A. Schirrer, M. Kozek. Cooperative Fuzzy Model Predictive Control. *IEEE Transactions on Fuzzy Systems*, Volume 24, 2016, pages 471-482, ISSN: 1063-6706.
DOI: 10.1109/TFUZZ.2015.2463674
5. M. Killian, B. Mayer, M. Kozek. Cooperative Fuzzy Model Predictive Control for Heating and Cooling of Buildings. *Energy and Buildings*, Volume 112, 2016, pages 130-140, ISSN: 0378-7788.
DOI: 10.1016/j.enbuild.2015.12.017
6. B. Mayer and M. Killian and M. Kozek. A branch and bound approach for building cooling supply control with hybrid MPC. *Energy and Buildings*, Volume 128, 2016, pages 553-566, ISSN: 0378-7788.
DOI: 10.1016/j.enbuild.2016.07.027
7. B. Mayer, M. Killian, M. Kozek. Hierarchical model predictive control for sustainable building automation. *Sustainability*, Volume 9, 2017, <http://www.mdpi.com/2071-1050/9/2/264>, ISSN: 2071-1050.
DOI: 10.3390/su9020264

Talks and Poster Presentations on International Conferences (with Proceedings-Entry):

1. M. Killian, S. Grosswindhager, M. Kozek, B. Mayer. Pre-processing of partition data for enhancement of LOLIMOT, in: *Proceedings of 8th EUROSIM Congress on Modelling and Simulation (EUROSIM'13)*, IEEE Computer Society, Washington, DC, USA, 2013, pp.271–275, DOI: 10.1109/EUROSIM.2013.56.
2. B. Mayer, M. Killian, M. Kozek. Modeling workflow for a building model for control purposes. In: *3rd International conference on systems and control (ICSC)*, 2013. IEEE; 2013. pp. 551–556, DOI: 10.1109/ICoSC.2013.6750915.
3. M. Killian, B. Mayer, M. Kozek. Hierarchical fuzzy MPC concept for building heating control, in: *Proceedings of 19th World Congress of the International Federation of Automatic Control (IFAC'14)*, 2014, pp.12048–12055, DOI: 10.3182/20140824-6-ZA-1003.00772.
4. B. Mayer, M. Killian, M. Kozek. Cooperative and hierarchical fuzzy MPC for building heating control, in: *IEEE International Conference on Fuzzy Systems (FUZZ-IEEE)*, 2014, pp.1054–1059, DOI: 10.1109/FUZZ-IEEE.2014.6891573.
5. M. Killian, B. Mayer, M. Mayer, M. Kozek. Eine flexible Methodik für die modellbasierte prädiktive Regelung komplexer Gebäude. In *Proc. of International Congress e-nova: "Nachhaltige Gebäude"*, November 26–27, 2015, Pinkafeld, Austria, invited paper for special session, ISBN: 978-3-7011-0350-8.
6. B. Mayer, M. Killian, M. Kozek. Modular Model Predictive Control Concept for Building Energy Supply Systems: Simulation Results for a Large Office Building, in: *Proceedings of 9th EUROSIM Congress on Modelling and Simulation (EUROSIM'16)*, IEEE Computer Society, Washington, DC, USA, 2016, in press, DOI: 10.1109/EUROSIM.2016.

Talks and Poster Presentations (without Proceedings-Entry):

1. M. Mayer, B. Mayer, M. Killian, M. Kozek. Nichtlineare hierarchische modellprädiktive Klimaregelung für komplexe Gebäude. Vortrag: Mechatroniktag des Instituts für Mechanik und Mechatronik 2015, Wien; 30.09.2015.